



# LUND UNIVERSITY

## Development of an Ultrasensitive Capacitive DNA-sensor: A promising tool towards microbial diagnostics

Mahadhy, Ally

2015

[Link to publication](#)

*Citation for published version (APA):*

Mahadhy, A. (2015). *Development of an Ultrasensitive Capacitive DNA-sensor: A promising tool towards microbial diagnostics*. [Doctoral Thesis (compilation)]. Lund University (Media-Tryck).

*Total number of authors:*

1

### General rights

Unless other specific re-use rights are stated the following general rights apply:

Copyright and moral rights for the publications made accessible in the public portal are retained by the authors and/or other copyright owners and it is a condition of accessing publications that users recognise and abide by the legal requirements associated with these rights.

- Users may download and print one copy of any publication from the public portal for the purpose of private study or research.
- You may not further distribute the material or use it for any profit-making activity or commercial gain
- You may freely distribute the URL identifying the publication in the public portal

Read more about Creative commons licenses: <https://creativecommons.org/licenses/>

### Take down policy

If you believe that this document breaches copyright please contact us providing details, and we will remove access to the work immediately and investigate your claim.

LUND UNIVERSITY

PO Box 117  
221 00 Lund  
+46 46-222 00 00

# Development of an Ultrasensitive Capacitive DNA-Sensor

A promising tool towards microbial diagnostics

Ally Mahadhy



**LUND**  
UNIVERSITY

Department of Biotechnology  
Doctoral Thesis  
February 2015

Academic thesis, which by due permission of Faculty of Engineering at Lund University, will be publicly defended on Wednesday the 25<sup>th</sup> of February, 2015 at 10.15 a.m. in lecture hall B at the Center of Chemistry and Chemical Engineering, Getingevägen 60, Lund, for the degree of Doctor of Philosophy in Engineering.

Faculty opponent: Dr. Jeff Newman, Department of Analytical Biotechnology, Cranfield University, United Kingdom.

Doctoral Thesis, 2015  
Department of Biotechnology  
Lund University  
P.O. Box 124, 22100  
Lund, Sweden

Front cover photo: Electron micrograph of human oral bacterial community by  
Steve Gschmeissner

Back cover photo by Gaurav Dwivedi

Copyright ©Ally Mahadhy

ISBN 978-91-7422-382-8

ISRN LUTKDH/TKBT – 15 / 1160 – SE

Printed in Sweden by Media-Tryck, Lund University  
Lund 2015

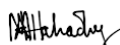


KLIMATKOMPENSERAT  
PAPPER



Organization LUND UNIVERSITY Department of Biotechnology P.O. Box 124, 22100 Lund, Sweden	Document name DOCTORAL DISSERTATION	
	Date of issue 2015-01-30	
Author(s) Ally Mahadhy	Sponsoring organization University of Dar es Salaam - World Bank Project	
Title and subtitle Development of an Ultrasensitive Capacitive DNA-sensor: A promising tool towards microbial diagnostics		
Abstract <p>Fast and sensitive detection of pathogenic microbial cells is a highly important task in medical diagnostics, environmental analysis and evaluation of food safety. Accordingly, the idea of microorganism identification by the recognition of specific DNA sequence using electrochemical technique is one of the leading researches in the development of diagnostic devices. In other words, it should only be a matter of time before a small portable electrochemical device is available at the care centre for quick diagnoses of a patient's infectious disease. However, bottlenecks for such diagnostic systems include selectivity, sensitivity, automation, sample pre-treatment and the architecture of miniaturization.</p> <p>In this thesis, a novel, highly sensitive and automated flow-based DNA-sensor technique for the detection of specific bacterial DNA sequences is introduced. The technique consists of a solid gold electrode that is functionalised using a simple and cheap chemistry to capture desired single stranded DNA in a complex matrix. The technology platform is based on the change in electrical property (capacitance) upon hybridization of the desired ssDNA to a capture probe. The physical and electrochemical properties of the modified electrode surface were studied using atomic force microscopy and cyclic voltammetry in reference to the innovative capacitive DNA-sensor assay. The DNA-sensor was optimized using homo-oligonucleotides with different number of bases (15- to 50 bases in probe length). The signal amplitude was found to increase with increase in oligonucleotide length, from 15- to 25-mer. However, there was no significant difference in signal readout between 25- and 50-mer. When using sandwich hybridization the signal readout for 50-mer oligonucleotides was increased by 46 %, from 78 to 114 nF cm<sup>-2</sup>. In addition, stability and selectivity of the DNA-sensor were investigated at elevated temperatures by applying different types of homo-oligonucleotides on the same capture probe; the sensor proved to be exceedingly stable in wide range of temperatures, from 23 to 50 °C, with selectivity (&gt; 95 %).</p> <p>To demonstrate the capability of the developed capacitive DNA-sensor in a real application, a specific capture probe designed to recognise 16S rDNA of <i>Escherichia coli</i> and other members in the family Enterobacteriaceae was used. This, to explicitly detect certain patches of <i>E. coli</i> 16S rDNA from a laboratory culture. The study showed that unamplified <i>E. coli</i> 16S rDNA could be sensitively detected at very low concentration corresponds to 10 <i>E. coli</i> cells per millilitre with only 15 min hybridization time. The sensor also showed a good selectivity over <i>Lactobacillus reuteri</i> 16S rDNA (Lactobacillaceae) from a laboratory culture. Furthermore, a new approach for pre-treatment of the bacterial DNA-sample prior to flow-based DNA-sensor analysis is demonstrated. The novel pre-treatment method utilizes a commercial single stranded DNA-binding protein to efficiently stabilize the heat-generated single-stranded DNA. Subsequent addition of formamide in the mixture resulted in denaturation of the protein, and hence, hybridization of the heat-generated target ssDNA to capture probe takes place. Another promising application showed for the developed DNA-sensor is the identification of Methicillin-resistant <i>Staphylococcus aureus</i> based on detection of the <i>mecA</i> gene. The study showed that the sensor adequately could detect and recover 95 % of 0.01 nM <i>mecA</i> gene from spiked human saliva, with a detection limit of 0.6 pM</p> <p>In conclusion, the work presented in this thesis demonstrates the development of a sensitive and effective biosensor for bacterial detection based on specific DNA sequence analysis. Compared to the commercially existing techniques for bacterial detection, the developed capacitive DNA-sensor proved to be non-complex, fast and efficient. This thesis work lays the groundwork for the development of a hand-held, field-adopted DNA-sensor for on-site microbial diagnostics, useful in e.g. remote areas.</p>		
Key words Capacitive DNA-sensor, Enterobacteriaceae, <i>mecA</i> gene, Methicillin resistance, automated sequential injection analysis, sandwich hybridization, elevated temperature, polytyramine		
Classification system and/or index terms (if any)		
Supplementary bibliographical information		Language
ISSN and key title		ISBN 978-91-7422-382-8
Recipient's notes	Number of pages 143	Price
	Security classification	

Signature:



Date: 2015-01-16





*To my beloved wife and daughter*  
*Dr. Rahma*  
*&*  
*Princess Amrat*



## Abstract

Fast and sensitive detection of pathogenic microbial cells is a highly important task in medical diagnostics, environmental analysis and evaluation of food safety. Accordingly, the idea of microorganism identification by the recognition of specific DNA sequence using electrochemical technique is one of the leading researches in the development of diagnostic devices. In other words, it should only be a matter of time before a small portable electrochemical device is available at the care centre for quick diagnoses of a patient's infectious disease. However, bottlenecks for such diagnostic systems include selectivity, sensitivity, automation, sample pre-treatment and the architecture of miniaturization.

In this thesis, a novel, highly sensitive and automated flow-based DNA-sensor technique for the detection of specific bacterial DNA sequences is introduced. The technique consists of a solid gold electrode that is functionalised using a simple and cheap chemistry to capture desired single stranded DNA in a complex matrix. The technology platform is based on the change in electrical property (capacitance) upon hybridization of the desired ssDNA to a capture probe. The physical and electrochemical properties of the modified electrode surface were studied using atomic force microscopy and cyclic voltammetry in reference to the innovative capacitive DNA-sensor assay. The DNA-sensor was optimized using homo-oligonucleotides with different number of bases (15- to 50 bases in probe length). The signal amplitude was found to increase with increase in oligonucleotide length, from 15- to 25-mer. However, there was no significant difference in signal readout between 25- and 50-mer. When using sandwich hybridization the signal readout for 50-mer oligonucleotides was increased by 46 %, from 78 to 114 -nF cm<sup>-2</sup>. In addition, stability and selectivity of the DNA-sensor were investigated at elevated temperatures by applying different types of homo-oligonucleotides on the same capture probe; the sensor proved to be exceedingly stable in wide range of temperatures, from 23 to 50 °C, with selectivity (> 95 %).

To demonstrate the capability of the developed capacitive DNA-sensor in a real application, a specific capture probe designed to recognise 16S rDNA of *Escherichia coli* and other members in the family Enterobacteriaceae was used. This, to explicitly detect certain patches of *E. coli* 16S rDNA from a laboratory culture. The study showed that unamplified *E. coli* 16S rDNA could be sensitively detected at very low concentration corresponds to 10 *E. coli* cells *per* millilitre with only 15 min hybridization time. The sensor also showed a good selectivity over *Lactobacillus reuteri* 16S rDNA (Lactobacillaceae) from a laboratory culture. Furthermore, a new approach for pre-treatment of the bacterial DNA-sample prior to flow-based DNA-sensor analysis is demonstrated. The novel pre-treatment method utilizes a commercial single stranded DNA-binding protein to efficiently stabilize the heat-generated single-stranded DNA. Subsequent addition of formamide in the mixture resulted in denaturation of the

protein, and hence, hybridization of the heat-generated target ssDNA to capture probe takes place. Another promising application showed for the developed DNA-sensor is the identification of Methicillin-resistant *Staphylococcus aureus* based on detection of the *mecA* gene. The study showed that the sensor adequately could detect and recover 95 % of 0.01 nM *mecA* gene from spiked human saliva, with a detection limit of 0.6 pM

In conclusion, the work presented in this thesis demonstrates the development of a sensitive and effective biosensor for bacterial detection based on specific DNA sequence analysis. Compared to the commercially existing techniques for bacterial detection, the developed capacitive DNA-sensor proved to be non-complex, fast and efficient. This thesis work lays the groundwork for the development of a hand-held, field-adopted DNA-sensor for on-site microbial diagnostics, useful in e.g. remote areas.

## Popular summary

A handful of diseases-causing pathogenic microorganisms claim millions of lives worldwide each year, mainly due to limited diagnostic capabilities. The lack of simple, cost-effective, sensitive and rapid on-site diagnostic tools lead to delays in the diagnoses with a subsequent lag in treatment, which in turn can result in serious complications or even loss of lives.

Infectious diseases pose a serious threat to human well-being and to the economic development. For instance, the estimate economic burden of the diseases caused by antimicrobial resistant microorganisms within the European Union amounts to € 1.5 billion over all societal costs per year; in Thailand and USA the societal costs totals US\$ 1.3 and 35 billion per year, respectively. Likewise, the economic cost for multi-drug resistance Tuberculosis-related deaths in Sub-Sahara Africa from year 2006 to 2015 is estimated to be US\$ 519 billion.

Most of the current diagnostic tools in our hospitals and clinical laboratories are capable of detecting 'bad bugs' (i.e. pathogenic microorganisms) when their concentration in a patient's clinical sample is reasonably high. However, the pathogens do not reach detectable concentration until the disease has progressed and become significantly inferior. Some of the infectious diseases such as Ebola haemorrhagic fever, which has killed more than 8000 people in West Africa, need an immediate intervention to hinder the exponential spreading and to prevent the situation from becoming an even worse catastrophe than it is today. Currently, the tools for minimizing the spreading of the Ebola virus are few and merely include isolation of infected persons from the rest of the population and thereafter to simply wait out the disease. Hence, many people become infected while encountering patients during their asymptomatic stage of the disease.

Although most of the current diagnostic tools are highly sophisticated, their complexity and expensive operations restricts them to off-site analysis, which additionally serve as an impediment to the efficient pathogen diagnosis in remote areas, especially in developing countries. The limited availability of on-site diagnostic capabilities has significantly increased the need for the development of rapid, cost-effective and portable devices for diagnosis of infectious diseases.

In this work, a novel diagnostic device has been developed, which rapidly can detect small amount of bacteria based on the genetic material (DNA). DNA is the storage house or cellular library that contains all genetic information required in the functioning and growth of every living thing, from humans to single-cell organisms, as well as DNA-viruses.

The developed device, a capacitive DNA-sensor consists of a disposable sensing chip, which is constructed using a simple and cheap manufacturing method. The capacitive DNA-sensor is automated, and it can be miniaturized and adapted for

in-field use including bacterial diagnosis in remote areas under resource-limited settings. The stability and uniqueness of the DNA-material makes the capacitive DNA-sensor highly effective and suitable for the targeting of specific bacteria based on their set of genes. The operational cost for the capacitive sensor is aimed to be very low as a sensing chip can be reused for at least 20 assays before replacement. Furthermore, the developed capacitive DNA-sensor is user-friendly and requires only limited amounts of training to operate.

## List of papers

This thesis is based on the following papers, referred to by their Roman numerals in the text. The papers are appended at the end of the thesis. Reprints are published with kind permission of the respective journals.

- I. Mahadhy, A., StåhlWernersson, E., Mattiasson, B., Hedström, M., 2014. Use of a Capacitive Affinity Biosensor for Sensitive and Selective Detection and Quantification of DNA - A Model Study. *Biotechnology Reports*. 3, 42-48.
- II. Mahadhy, A., Mamo, G., StåhlWernersson, E., Mattiasson, B., Hedström, M., 2014. PCR-Free Ultrasensitive Capacitive Biosensor for Selective Detection and Quantification of Enterobacteriaceae DNA. *Journal of Analytical & Bioanalytical Techniques*. 5, 210.
- III. Mahadhy, A., StåhlWernersson, E., Mattiasson, B., Hedström, M., 2014. Comparison: Polytyramine-Film and 6-Mercaptohexanol-Self-Assembled Monolayers as the Immobilization Layers for a Capacitive DNA-Sensor Chip. Submitted.
- IV. Mahadhy, A., StåhlWernersson, E., Mattiasson, B., Hedström, M., 2014. Rapid Detection of the *mecA* gene for Diagnosis of Methicillin-Resistant *Staphylococcus aureus* by a Novel, Label-free, Real-time Biosensor. Manuscript.



## My contribution to the papers

All the work presented in this thesis was performed under supervision of Professor emeritus Bo Mattiasson, Associate Professor Martin Hedström and Eva Ståhl Wernersson (PhD). For work in **paper II**, Associate Professor Gashaw Mamo was also a supervisor.

**Paper I.** I performed the experimental work and wrote the first draft of the paper. I was responsible for improving it together with the co-authors.

**Paper II.** I planned and executed all the experiments. I wrote the first draft of the manuscript and was responsible for improving it together with the co-authors.

**Paper III.** I planned and performed all the experiments. Maria Wadsäter (PhD) from Department of Physical Chemistry, Lund University, Sweden, assisted me during the atomic force microscopy study. I wrote the first draft of the manuscript and was responsible for improving it together with the co-authors.

**Paper IV.** I planned and performed all the experiments. I wrote the first draft of the manuscript and was responsible for improving it together with the co-authors.

## List of abbreviations

AFM	Atomic force microscopy
ARMs	Antibiotic resistant microorganisms
Cfu	Colony forming unit
CV	Cyclic voltammetry
DNA	Deoxyribonucleic acid
dsDNA	Double stranded DNA
EDC	<i>N</i> -ethylcarbodiimide hydro-chloride
EDL	Electrical double layer
ELISA	Enzyme-linked Immunosorbent assay
ETSSB	Extreme thermostable single stranded DNA binding protein
IUPAC	International Union of Pure and Applied Chemistry
LB	Luria-Bertani
LOD	Limit of detection
MCH	6-mercaptohexanol
MRSA	Methicillin-resistant <i>Staphylococcus aureus</i>
MSSA	Methicillin susceptible <i>Staphylococcus aureus</i>
NCBI	National Centre for Biotechnology Information
NHS	<i>N</i> -hydroxysuccinimide
Oligo	Oligonucleotide
PCR	Polymerase chain reaction
Pty	Polytyramine
QCM	Quartz crystal microbalance
RNA	Ribonucleic acid
RSD	Relative standard deviation
RT	Room temperature
SAM	Self-assembled monolayer
SPR	Surface plasmon resonance



# Table of contents

1.	Introduction	1
1.1	Background	1
1.2	Scope of the thesis	2
1.3	Biosensors	3
1.3.1	Principle of biosensor	4
1.3.2	Classification of biosensors	5
2.	Capacitive DNA-sensor	6
2.1	State of the art	6
2.1.1	Gold electrode	6
2.1.2	Immobilization layers	7
2.1.3	Deoxyribonucleic acid	9
2.2	Characterization of the modified electrode surface	11
2.2.1	Topographical characterization-AFM	11
2.2.2	Electrochemical characterization- CV	13
2.3	Electrical double layer capacitance	15
2.3.1	Electrical double layer theory	15
2.3.2	Behaviour of the electrical double layer capacitance	17
2.4	Capacitance measurements	20
2.4.1	Potential pulse capacitance measurements	20
2.4.2	Current pulse capacitance measurements	24
2.5	Validation of the developed capacitive DNA-sensor	28
3.	Optimization of capacitive DNA-sensor	29
3.1	Oligonucleotide length	29
3.2	Hybridization (working) temperature	31
3.3	Immobilization layer	33
4.	Applications of the capacitive DNA-sensor	36
4.1	Detection and quantification of Enterobacteriaceae	36
4.2	Detection of methicillin-resistant <i>S. aureus-mecA</i> gene	40
4.2.1	Genetic organization and mechanisms of <i>mecA</i> region	40
4.2.2	Laboratory screening for MRSA	41
4.2.3	Capacitive DNA-sensor for MRSA <i>mecA</i> gene	41
5.	Comparison: the capacitive DNA-sensor with other techniques	46
6.	Challenges and limitations in capacitive DNA-sensor development	50
6.1	Conclusion and future perspectives	50
7.	Acknowledgements	52
8.	References	54



# 1. Introduction

## 1.1 Background

Rapid, accurate and sensitive detection with definitive identification of microorganisms, including pathogens, are exceedingly important in many fields including clinical microbiology, microbial forensics, bio-terrorism threats, food analysis and in environmental studies.

Generally, detection and identification of microorganisms rely on phenotypic characterization using traditional methods such as bacterial culturing with subsequent biochemical assaying. Enzyme-linked Immunosorbent assay (ELISA), also known as enzyme immunoassay (EIA), is a biochemical method widely used in medical diagnostics of bacteria and bacterial products (e.g. toxins) [1]; and as quality control measures in various industries such as pharmaceutical production [2] and the food manufacturing sector [3]. In ELISA, the basic immunology concept of an antigen binding to its specific antibody is utilized, which allows detection of very small quantities of antigens such as proteins, peptides, hormones, or antibodies in a fluidic sample. Traditional wet-lab methods such as ELISA that are based on solid-phase interactions are well established and effective but suffer from a number of drawbacks, including a low sensitivity. It should be mentioned that ELISA methods need about 1 million cells to be reliable, and therefore performing such assay on a food sample would require an overnight incubation so that the target organism could reach detectable levels [2]. Also, some strains have > 97 % similarity in biochemical characteristics [4], which might lead to severe cross-reactivity. In addition, antibodies are both expensive and labile and some antigens that they target are equally labile. Moreover, both bacterial culturing and most biochemical methods are laborious and time consuming to execute [5,6]. Phenotypic properties can furthermore be unstable over time and expression can be dependent upon changes in environmental conditions, e.g., cultivation substrate, temperature or pH [7].

One way to overcome the inherent limitations of these conventional methods is the identification of bacteria by their genetic material, i.e. deoxyribonucleic acid (DNA) sequence, linked to pathogenicity/distinctive characteristic of a particular strain [8]. In the past decades, molecular techniques; polymerase chain reaction (PCR) and microarray have proven beneficial in overcoming some limitations of the traditional phenotypic procedures for identification and detection of bacteria.

The shift towards the use of real-time PCR assays has significantly reduced the detection time [9], where PCR also offers remarkable sensitivity and allows the detection of difficult-to-culture microorganisms. Moreover, in multiplex PCR, more than one bacterial target sequences can be amplified in one reaction tube [10]. While PCR can make a significant contribution toward rapid identification of bacteria, including infectious agents, limitations still exist. The PCR method is

costly and its reaction is impaired by the inhibitory substances present in a biological sample. For instance, as low as 0.004 % red blood cells in the sample is enough to completely inhibit the PRC reaction that contains *Taq* DNA polymerase [11]. Additionally, PCR has an inherent bias in the template-to-product ratio. In fact, amplification bias was found to significantly increase with increasing numbers of PCR cycles [12].

The microarray platform is a molecular method that renders it possible to detect and distinguish between different bacteria on a single slide [13-15]. The quick detection of the bacteria in clinical samples is crucial for implementation of antimicrobial treatment and infection control measures. The DNA microarray is employed for the rapid detection and identification of bacteria utilizing species-specific DNA probes crafted for distinctive sequence of different targeted genes. Each oligonucleotide-probe is labelled with a certain fluorescent chemical compound, which fluoresces during hybridization. In spite of its many benefits as mentioned above, microarray has the disadvantage that fluorescent labelling of probes is both expensive, time-consuming as well as laborious [16,14].

Mass spectrometry (MS) has emerged as an efficient tool for the identification of bacteria [17]. Routinely, two different approaches are employed: i) electrospray ionization MS (ESI/MS) [18] and ii) matrix-assisted laser desorption/ionization time of flight MS (MALDI-TOF/MS) [17,19]. Identification is based on determination of base composition of genetic material alone or in combination with the determination of molecular weight of target proteins or peptides [17-19]. However, MS is not very sensitive and the bacterial detection assay requires about  $10^5$  CFU of microbial biomass for analysis [17] or the use of PCR amplification to infer its base composition. The use of MS also carries the difficulty of analysing the target analyte in complex biological matrices, and is severely disturbed by the presence of salts, detergents and some other additives (e.g. minute amounts of polyethylene glycol etc.), which will contribute to reduce the assay sensitivity [17-19]. Even though MS typically is highly automated (in combination with high-performance liquid chromatography, HPLC) and can provide results in less than 1 hour [18], there are major barriers to implement the technology in today's clinical laboratories such as high capital investment and instrument maintenance costs as well as the requirement of special expertise to operate.

The limitations of the currently used diagnostic tools have greatly accentuated the demand for developing fast, sensitive, selective, and cost-effective diagnostic techniques for detection and identification of bacteria from complex matrices such as clinical-, water-, food- and environmental samples.

## 1.2 Scope of the thesis

In view of the outlined background, the work in this thesis is focused on the development of a novel capacitive DNA-sensor for the rapid detection of bacteria from biological samples without the need for amplification or the use of labelling

steps. In **Paper I**, a model study was performed where the development of the capacitive DNA-sensor for detection and quantification of oligonucleotides is in focus. Effect of the length of the target oligonucleotide to the sensor signal amplitude, effect of sensing selectivity by using elevated hybridization temperature, and the possibility of enhancing the sensor signal amplitude by sandwich hybridization were evaluated. The optimum conditions were utilized for detection of real bacterial DNA sample (**paper II and IV**). **Paper II** reports a successful application utilizing the capacitive DNA-sensor that was developed in **paper I** for the selective detection of a DNA-sequence from *E. coli* BL2 (DE3). The results obtained were compared to those obtained from a standard culturing technique. In addition, **paper II** presents an alternative approach to the preparation of bacterial DNA samples for a flow-injection based analysis involving a DNA-sensor. To get insight into the roughness properties of the electrode surface, as well as packing organization of the insulating layer and DNA recognition layer on the electrode surface. The electrode surface was characterized using atomic force microscopy (AFM) and cyclic voltammetry (CV) in reference to the capacitance measurements (**paper III**). **Paper III** reports results from a study related to the effect of insulating layer on sensitivity, selectivity and stability of the DNA-sensor chip. The method used to develop the capacitive DNA-sensor (**paper I**) was employed and integrated into an automated sequential-injection analysis (SIA), for detection of methicillin-resistant *Staphylococcus aureus* (MRSA)-*mecA* gene spiked in a complex matrix (**paper IV**).

### 1.3 Biosensors

Scientists have recognized the power of incorporating biomolecules (e.g. antibody, DNA, RNA, enzyme) or even whole cells and tissue material into the design of devices for detection and quantification of various components including bacteria. Such a concept of combining recognition properties of biomolecules with the sensitivity of a transducer, which converts the recognition event into a readable signal, has led to the emergence of biosensors. The term “biosensor” dates from 1962, when the American scientist; Professor Leland C. Clark argued that, by incorporating an appropriate immobilized enzyme into the electrochemical oxygen electrode, his earlier invention, could lead to the development of various bioanalytical devices [20]. The first model was illustrated by immobilising the enzyme glucose oxidase between two dialysis membranes that were placed over an oxygen probe, which turned a regular platinum electrode into an impressive bioanalytical device for the detection of glucose in clinical samples [21,22]. Since then, we have witnessed a tremendous amount of activity in the area of biosensor development aimed at detection, diagnosis and identification of various analytes of interest.

According to the International Union of Pure and Applied Chemistry (IUPAC), a biosensor is defined as “a self-contained integrated device that is capable of



providing specific quantitative or semi-quantitative analyte information using a biological recognition element, which is retained in direct spatial contact with a transduction element” [23]. In other words, biosensors utilize the inherent specificity and sensitivity of biomolecules as well as physicochemical properties of transducers to perform complex bioanalytical measurements with user-friendly formats [24]. The potential use of biosensors involve essentially every conceivable analytical measurement, varying from clinical and diagnostics applications [24-27], food safety [28], environmental monitoring [29,30], and process control [31,32], forensic [33], to bioterror defence [34], and similar security applications [20,35].

### 1.3.1 Principle of biosensor

The major processes involved in the operation of any biosensor system are: analyte recognition, signal transduction, signal processing and signal readout. As schematically depicted in Fig. 1-1; a target analyte specifically interacts with a biorecognition element, which is attached onto a support that is in close contact with a transducer. The interaction between the biorecognition element and the analyte creates a physico-chemical change that is detected and converted into an electrical signal by the transducer. The signal is processed and sent to a readout device. The displayed signal is typically strictly proportional to the concentration of the target analyte [36].

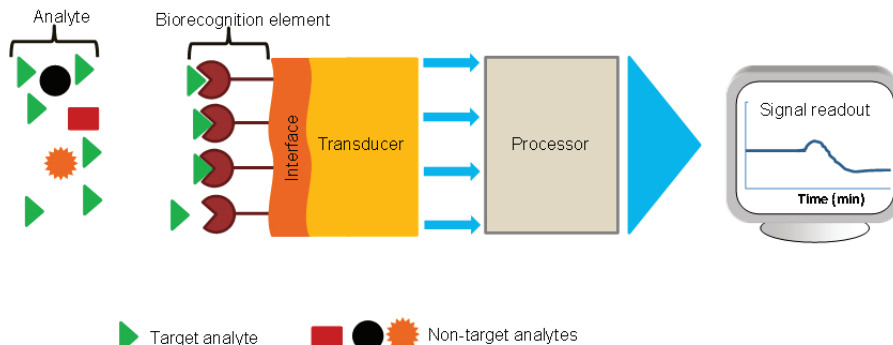


Fig. 1-1: Schematic illustration of a biosensor and its components

Biosensors are clearly distinguished from bioanalytical system due to their ability to be repeatedly calibrated, while bioanalytical devices require additional processing steps, such as reagent addition. However, for a biosensor that is both disposable after one measurement and unable to monitor the analyte concentration continuously or after a rapid and reproducible regeneration step is designated as a ‘single-use biosensor’ [23].

### 1.3.2 Classification of biosensors

The biorecognition elements used in current biosensor platforms include enzymes, antibodies, nucleic acids, microorganisms (cells); animal and plant- and animal tissue slices [37]. Biosensors are mainly classified in two categories based upon the biological specificity-conferring mechanism, namely: i) biocatalytic biosensors and ii) affinity biosensors. Thus, a biocatalytic biosensor consists of biorecognition element (e.g. proteins, cells or tissue), which binds an analyte and catalyse a reaction involving the analyte to produce quantifiable product (s), whereas, an affinity biosensor consists of a biorecognition element (antibody-antigen, DNA-hybridization etc.) which binds specifically to an analyte without a catalytic reaction [23].

Biosensors may be further classified according to the mode of physico-chemical signal transduction [23] as: i) piezoelectric biosensors, commonly known as quartz crystal microbalance (QCM) biosensors, their principle of signal transduction is based on changes in oscillation frequency which is linearly related to the mass changes on the surface of the biosensor [38-39]; ii) Optical biosensors, in which a signal response is obtained by a) determining the changes in light absorption between the reactants and products of a reaction [40] or b) measuring the light output by a luminescent process before and after bioreceptor-analyte interaction [41] or c) measuring the changes in oscillation of electrons stimulated by incident light, which depends linearly on the concentration of an analyte interacted with biorecognition element on the surface, namely, surface plasmon resonance (SPR) [42]; iii) calorimetric biosensors, that are based on the detection of absorbed or generated heat during the interaction between an analyte and a biorecognition element layer [43]; iv) electrochemical biosensors, the largest group of biosensors, that are based on the measuring of changes in electrical properties due to binding event or product formation as a result of bioreceptor-analyte interaction on the surface. A measurable electrical property could be, current (amperometric biosensor) [44,45], conductivity (conductometric biosensor) [46], potential (potentiometric biosensor) [47,48], or capacitance (capacitive biosensor) [25,49,50] changes.

Moreover, other classifications also exist, such as, a classification based on the type of biorecognition layer or target analyte, for examples; immunosensors, where an antibody (or its fragments) is utilized as bioreceptor for the capture of a target antigen [25,51] or vice versa [52]; enzyme biosensors, as the name suggests, these sensors use one or several enzymes to convert a target analyte into a detectable product [53]; aptamer biosensors, using oligonucleotides or peptides as biorecognition elements to detect different molecules *via* affinity binding other than hybridization of complementary bases [54]; and DNA biosensors (DNA-sensors), that use ssDNA as a biorecognition element for detection of other complementary target ssDNA *via* hybridization event [26,28,50].

## 2. Capacitive DNA-sensor

The main components of a biosensor i.e., the biorecognition element, transducer and target analyte are discussed in section 1.3. It should be noted that each component plays a crucial role in the characteristics of a biosensor. Therefore, in constructing a biosensor each component should be carefully chosen in order to meet requirements such as selectivity, sensitivity and stability. In this work, the unique stability and specificity of the interchain DNA base pairing, together with the ability of the capacitive sensor technology to form double layers capacitance and to directly respond to a nanoscale-effect (e.g. size, concentration, or chemical composition) of analyte introduced on the electrode surface, are exploited to construct a sensitive, selective, stable biosensor for detection of a target microorganism based on its genetic material. The biosensor in this work is named *capacitive DNA-sensor*.

The inherent properties of the developed capacitive DNA-sensor suggest the possibility for a paradigm shift within biosensing, including a shift from detection of microorganism using a protein-biorecognition layer (e.g., enzymes and antibodies), which are unstable and expensive to identification of microorganism based on DNA biorecognition layer, which is stable, cheap and possess unique patterns in each individual microorganism. Also, a shift from the identification of microorganism at a specific location and time to the detection of the current and/or past presence of microorganism; as well as from direct detection of microorganism (i.e., collecting whole microbial cells) to indirect detection (i.e., collecting DNA shed from microbial cells).

### 2.1 State of the art

#### 2.1.1 Gold electrode

An electrode is an electrical conductor used to make contact with a non-metallic part of a circuit such as an electrolyte. A great variety of solid electrodes of different materials including platinum, rhodium, nickel, copper, graphite, glassy carbon and gold [55] have been employed in different electrochemical biosensors. Among all, the solid gold electrode offers remarkable electrochemical characteristics, where gold has electrochemical inertness over a broad interval of potentials and good electrical conductivity. In addition, gold offers a relatively large anodic potential range and favourable electron transfer kinetics [56,57]. Moreover, gold electrode surface chemistry can be employed for various sensing and detection application [49-51].

Two types of gold electrodes ( $\varnothing = 3\text{mm}$ , 99.99 % purity) were exclusively used in this work, i.e., durable polished rod-shaped electrodes (**paper I**) and disposable thin film (**papers II, III and IV**) gold electrodes (Fig. 2-1). The former electrode

type requires an extensive cleaning prior to the surface modification steps. The preparation of the rod-shaped electrode involved repeated polishing with alumina slurry of different particle sizes, followed by repeated sonication to remove physically absorbed particles on the surface [58]. For the regeneration of a used electrode, pre-cleaning with Piranha solution (concentrated  $\text{H}_2\text{SO}_4$ :30 %  $\text{H}_2\text{O}_2$ ; 3:1) is required followed by the cleaning steps described previously.

Certainly, the polishing steps involved for the rod-shaped gold electrode are laborious and could lead to irreproducible results per electrode due to inconsistent surface roughness. There are also concerns regarding the potential health effects of long-term exposure to inhaled alumina slurry. For these reasons, a custom-made disposable thin film gold electrode (manufactured by the Academic workshop, Linköping University, Sweden) was used for the work in **papers II, III and IV**.

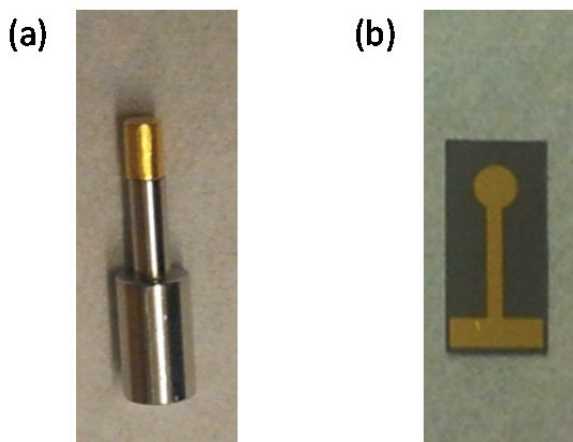


Fig. 2-1: Durable polished rod-shaped (a) and disposable thin film (b) 3 mm diameter gold electrodes used in this work.

### 2.1.2 Immobilization layers

The performance of an electrochemical biosensor greatly depends on the physical and chemical properties of the immobilization layer and hence the chemistry involved in the immobilization steps. Consequently, a variety of different immobilization protocols have been reported for the modification of gold electrode surfaces. The most reported immobilization techniques are based on polymers, both conducting polymer e.g., polypyrrole [59-62] and non-conducting polymer e.g., polytyramine (Pty) [25,51,58,63]. A frequently used technique is based on self-assembled monolayers (SAMs) of both organosulfur compounds [49,64-66] and mercapto-containing organosilanes [67-72]. A major area of interest, valid for all types of electrode immobilization techniques, is related to site-specific orientation of the ligand on the electrode surface interface to provide higher accessibility towards the target molecules. The main benefit is

that steric hindrance between molecules and their binding counterparts can be avoided.

For capacitive biosensors, the insulating property of the interface is an exceedingly important factor. The electrode surface should be sufficiently covered to prevent ions from moving through the interface to the electrode surface, which would cause short-circuit in the system and result in distorted or omitted signals [73].

In this thesis work, polytyramine, a non-conducting polymer (**papers I, II, III and IV**), and self-assembled monolayer of 6-mercaptohexanol (MCH) (**paper III**) were employed as immobilization layers onto the gold electrode surfaces. Stable films of Pty were deposited onto the gold electrode surface via an electropolymerization process through anodic oxidation utilizing CV as shown in Fig. 2-2.

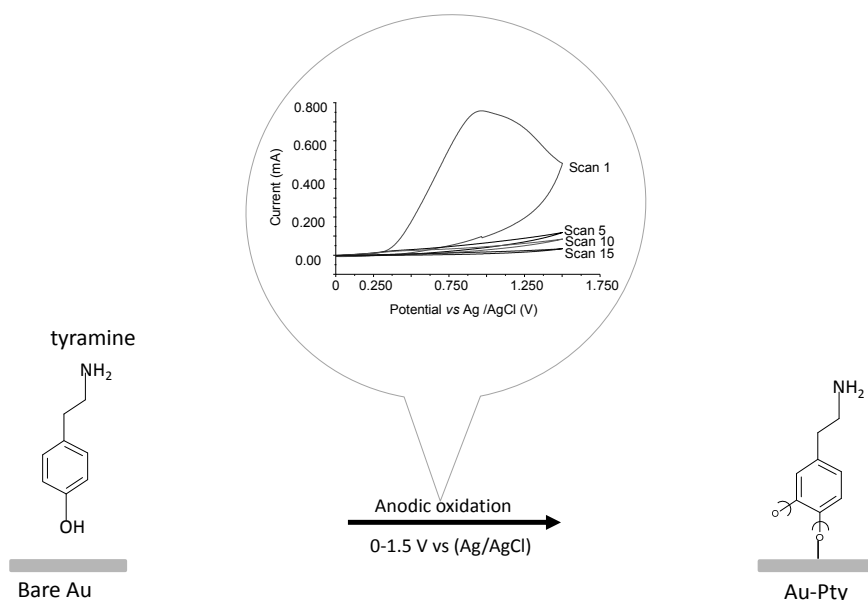


Fig. 2-2: Electropolymerization of tyramine on the surface of a gold electrode.

Polymerization of tyramine onto the electrode surface is relatively non-complex, fast and allows rapid preparations of electrodes [74]. Moreover, the Pty film is stable, and its thickness can be controlled by number of scans applied, thus offering reproducible procedure of DNA-sensor preparation [75]. The electropolymerization was performed in 10 mM potassium phosphate buffer, pH 7.2 mixed with ethanol in the ratio of 3:1, by applying potential sweeps between 0.0 to 1.5 V *vs.* Ag/AgCl, at scan rate of 50 mV s<sup>-1</sup> for 15 cycles. The tyramine oxidation peak of about 0.8 mA at the first cycle was observed to dramatically decrease as the number of scans proceeded. The peak completely disappeared (off scale) during the 15<sup>th</sup> scan. The disappearance of the oxidation peak indicates the

formation of a passivating, non-conductive, insulating layer on the gold electrode surface, which blocks electron transfer between the electrode surface and tyramine monomer in the solution.

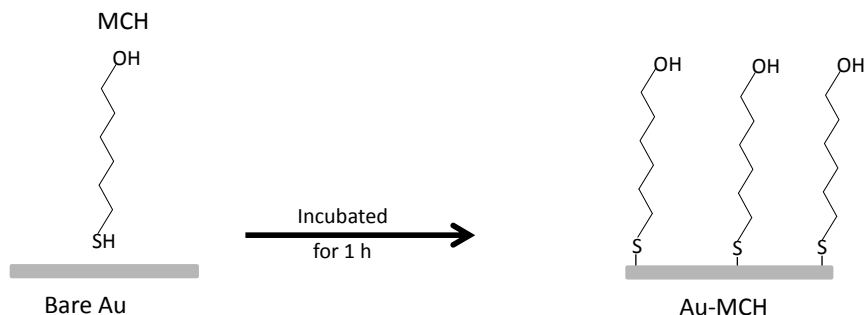


Fig. 2-3: MCH self-assembled monolayer onto the surface of gold electrode.

On the other hand, MCH was attached onto the electrode surface through the self-assembled monolayer (SAM) process. In this case, the high inherent affinity between the gold surface and the sulfhydryl group of the MCH molecule (Fig 2-3) is utilized. The gold electrode was dipped into 3.7 mM 6-MCH ethanolic solution for 1 hour. The adsorption of MCH on the gold surface resulting in the formation of a densely packed SAM. The interaction between the gold electrode surface and MCH is described by the Hard and Soft Acid Base theory, where a soft acid (gold) and a soft base (SH group) said to react very simply to form covalent bonds [76]. The process of depositing the MCH monolayer on the gold electrode is easy and straightforward and the dense coverage of MCH monolayer can quickly be formed in the range from milliseconds to minutes utilizing only minimum amounts of MCH solution [77]. The stability, the uniform surface structure and the relative ease of varying the surface functionalities make the MCH monolayer particularly suitable for the development of the capacitive DNA-sensor [78].

### 2.1.3 Deoxyribonucleic acid

The DNA material carries the hereditary information required for the functioning and growth of every living cell [79] as well as DNA-virus. The information is encrypted in the sequence of nucleotides. A nucleotide consists of pentose sugar (deoxyribose), phosphate group(s) and nitrogenous bases distinguished into purine, namely Adenine (A) and Guanine (G), and pyrimidine, namely Cytosine (C) and Thymine (T). Nucleotides are linked with each other through phosphodiester bond between 5' and 3' carbon atoms of deoxyribose under formation of single-stranded DNA with 5' and 3' ends. According to Crick and Watson's [79] base pairing model, there is a specific base pairing between purine (A or G) and pyrimidine (T or C) as shown in Fig. 2-4.

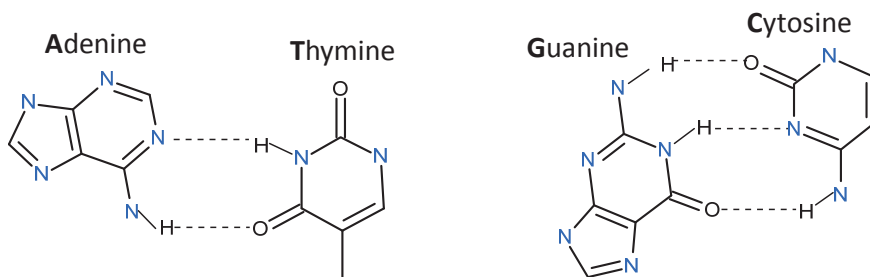


Fig. 2-4: Formation of hydrogen bond (dotted lines) between adenine and thymine and guanine and cytosine according to Crick and Watson base pairing rules.

The pairing of the bases incorporated into DNA forms the double stranded DNA (dsDNA). It should be noted that this pairing of the bases is only possible if the DNA strands are orientated antiparallel with the first having a direction 5' to 3' and the second from the 3' to 5' end. Therefore, only complementary ssDNA strands can specifically interact (hybridize) to form a dsDNA. The capacitive DNA-sensor was utilized to employ the natural phenomenon of hybridization between complementary strands, to capture a target ssDNA strand from a complex pool of DNAs and other biomolecules.

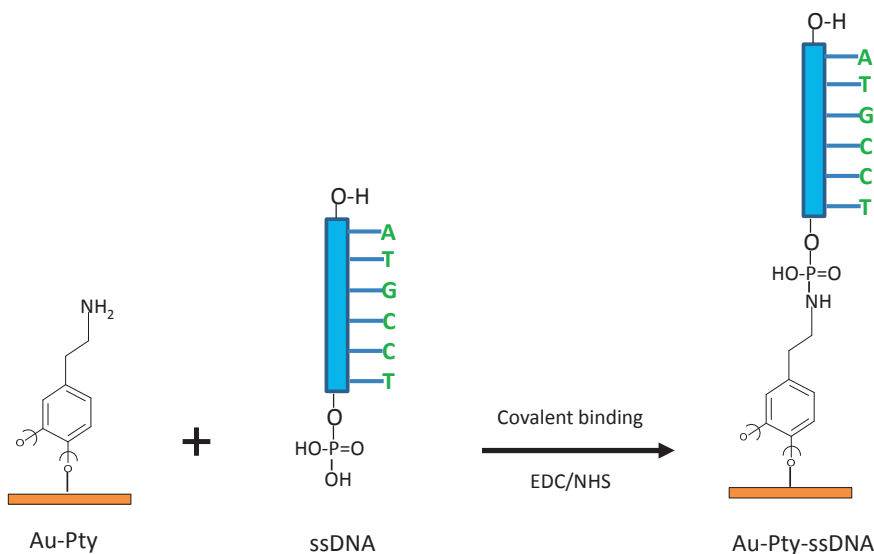
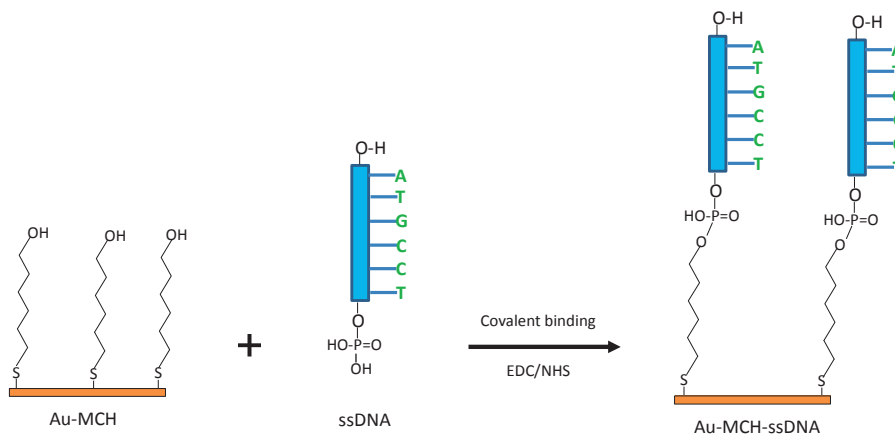


Fig. 2-5: Covalent binding of a capture probe ssDNA phosphate group with reactive amine group of Pty film onto the surface of gold electrode.

As such, one of the complementary strands was attached on the gold electrode via covalent bonding between phosphate group of that capture probe ssDNA and amine group of the polytyramine layer on the electrode surface (**papers I, II, III, and IV**), forming phosphoramidate ester bond [66,75,80] (Fig. 2-5), or between

the phosphate group of the capture probe and the hydroxyl group of MCH in the SAM on the electrode surface (**paper III**), forming a phosphate ester bond [66] (Fig. 2-6).



**Fig. 2-6:** Covalent binding of a capture ssDNA-probe phosphate group with hydroxyl group of MCH self-assembled monolayer onto the surface of gold electrode.

However, the Pty and MCH layers are not free from defects. There are several possible types of defects such as pinholes, sites where the monolayer has collapsed, or monolayer domain boundaries [81,82]. Therefore, the electrode was finally immersed in 10 mM 1-dodecanethiol (in ethanol) for 20 min to fill the pinholes on the electrode surface before use [25,64].

## 2.2 Characterization of the modified electrode surface

There is a wide range of analytical techniques available for electrode surface characterization, all reliant on the type of information needed. The different characteristics regarding the electrode surface that can be obtained are topographical information, chemical compositions and electrochemical properties. Among the techniques used to explore topographical information are scanning electron microscopy (SEM) [83], ellipsometry [84] and AFM [58,84,85]. Fourier transform infrared spectroscopy (FTIR) [86] and X-ray photoelectron spectroscopy (XPS) [84,86] have been widely used to determine the chemical composition on the electrode surface. Electrochemical properties of various electrode surfaces have been intensively studied using CV [25,51,63] and capacitance measurements [50]. In **paper III**, modified electrode surfaces were topographically characterised using AFM. Also, CV was used in this work for studying the electrochemical properties of the electrode surface.



### 2.2.1 Topographical characterization-AFM

AFM is a high-resolution type of scanning probe microscopy, developed for the analysis of surfaces of rigid materials with nanometric resolution. The AFM instrument is equipped with a mechanical probe to magnify surface features up to  $10^8$  times, producing a three-dimensional surface topography at nanometer lateral and sub-angstrom vertical resolution on insulators and conductors [87-89].

In **paper III**, the topography of the electrode surface was mapped by AFM adjusted to contact or non-contact mode in air at room temperature. The roughness parameters were used to evaluate the quality of the surfaces [90]. The electrode surface roughness increased from 2.9 nm for bare electrode (Fig. 2-7a) to 3.60- and 3.10 nm when the Pty film (Fig. 2-7b) and MCH SAM (Fig. 2-7c), were added on the bare electrode surface, respectively.

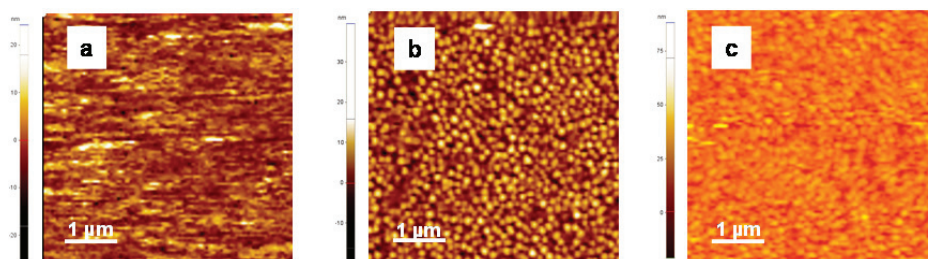
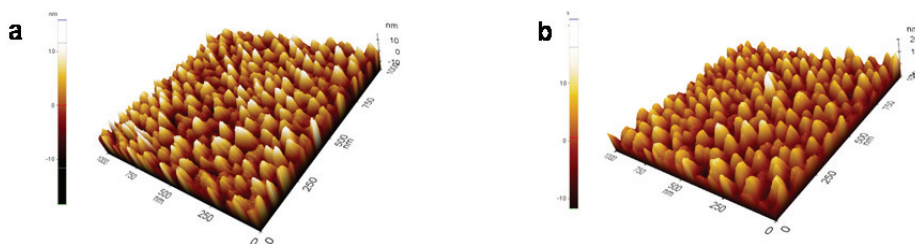


Fig. 2-7: Contact mode AFM ( $5 \mu\text{m} \times 5 \mu\text{m}$ ) images of (a) bare gold electrode surface (b) gold electrode surface after deposited with Pty film (c) gold electrode surface after deposited with MCH. The dark brown colour and white spots represent valley and peaks, respectively.

Unlike MCH SAM, Pty film formed a densely packed and rougher surface, indicating it is not very perfectly self-limiting in growth. The MCH monolayers are able to self-organize on the electrode surface, resulting in a highly ordered smooth surface [78].

The roughness of the Pty modified electrode surface was even further increased, to 3.80 nm after immobilization of ssDNA on the surface (Fig 2-8a). However, immobilization of ssDNA on the MCH SAM modified electrode surface resulted in a decrease of the surface roughness by 0.6 nm (Fig. 2-8b). One possible explanation could be that ssDNA was non-specifically adsorbed onto uncovered spaces on the MCH-modified electrode surface, resulting in a decreased surface roughness. Usually a dense coverage of MCH monolayers could be obtained in short time, however a slow reorganization process requires some hours so as to maximize the density of molecules and to minimize defects on the SAM [77]. The Pty modified electrode observed to host a higher number of dense peaks, most likely ssDNA molecules, than the MCH modified electrode. Theoretically, the Pty film presents one reactive amine group per moiety, which is most likely exists as a positively charged ion ( $-\text{NH}_3^+$ ). Thus, the capture ssDNA probe having a phosphate terminal functional group (negatively charged), is easily attracted and

immobilized on the Pty film, yielding a higher concentration of surface bond capture probe ssDNA [66,75].



**Fig. 2-8:** Three dimensions ( $1\ \mu\text{m} \times 1\ \mu\text{m}$ ) AFM images of (a) gold electrode surface modified with Pty subsequently coupled with ssDNA (b) gold electrode surface modified with MCH and thereafter coupled with ssDNA. The images were mapped by non-contact mode AFM. The dark brown and white colours represent valley and peak, respectively.

Conclusively, well-covered electrode surface with a high surface concentration of capture ssDNA probe is achieved with the Pty film (**paper III**).

### 2.2.2 Electrochemical characterization- CV

CV is the most widely used technique for acquiring qualitative information about the electrochemical reactions of the electrode surface or/and the electrolyte solution [91]. In **paper III**, the electrode surfaces before and after modifications were electrochemically characterized by CV.

The efficiency of the formation of immobilization layers on the electrode surfaces is described in terms of surface coverage. It is qualitatively determined by either comparing the redox peaks or the areas of the gold oxide (AuO)-reduction peaks for the bare and modified gold electrode surfaces. In the former case, the CV is performed in  $\text{Fe}(\text{CN})_6^{3-/4-}$  (redox couple) solution, where electron exchange between the electrode surface and redox couple for each surface is followed [25,74], (**papers I, II, III and IV**). However, when the area of AuO-reduction peaks are compared, the CV is performed in  $0.1\ \text{M}\ \text{H}_2\text{SO}_4$  [93], (**paper III**) as represented in Fig. 2-9. A CV for a bare electrode surface exhibited a high AuO-reduction peak (a), indicating large electrode surface was available for Au oxidation. However, the AuO-reduction peaks were found to decrease after electrode surface modifications. Curves (b) and (c), where the Pty-ssDNA and MCH-ssDNA were used to cover and functionalize the surfaces, indicates a prevented AuO formation on the gold electrodes.

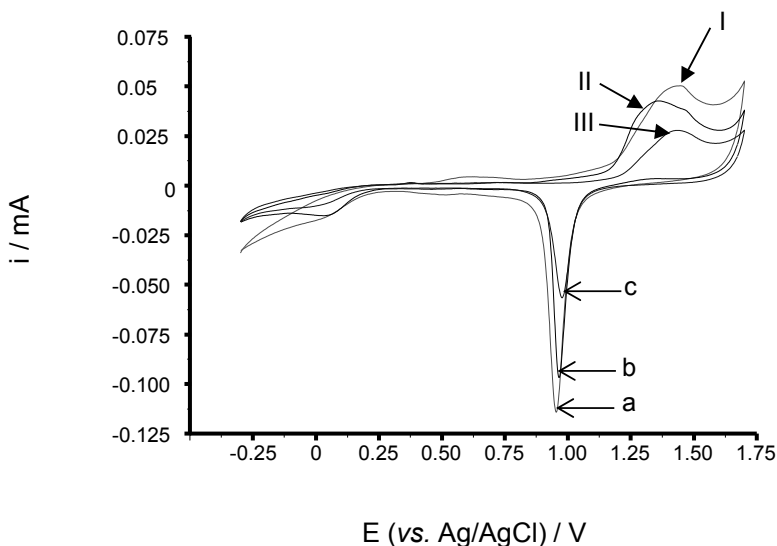


**Fig. 2-9:** The AuO reduction peaks for (a) a bare electrode surface (b) an electrode surface modified with MCH-ssDNA and (c) an electrode surface modified with Pty-ssDNA, with their Au oxidation peaks: I, II and III, respectively. Cyclic voltammograms were recorded in 0.1 M  $H_2SO_4$  at the sweep rate of  $0.1 \text{ V s}^{-1}$  and the potential range between, -0.3 to 1.7 V (*vs.* Ag/ AgCl)

The decrease in AuO-reduction peak for Pty-ssDNA modified electrode (curve (c)) was more pronounced compared to the MCH-ssDNA modified electrode (curve (b)), indicating that Pty-ssDNA has better insulating properties than MCH-ssDNA. The Pty is a non-conducting polymer with high resistivity that forms a passivating film when deposited on the electrode surface [92,93,94]. Such a layer on the surface contributes to the better displayed surface coverage.

Moreover, the surface coverage could be quantitatively determined by comparing the electric charges exchanged during the reduction of AuO for the bare and the modified gold electrode surfaces (**paper III**). It is calculated according to Eq.1 and expressed in % as shown Table 1.

$$\% \text{ Surface coverage} = \frac{Q_{Bare} - Q_{Mod}}{Q_{Bare}} \times 100 \quad (1)$$

where  $Q_{Bare}$  and  $Q_{Mod}$  ( $C \text{ cm}^{-2}$ ) are amounts of electric charges exchanged during AuO reduction for bare and modified gold electrode surfaces, respectively.

Moreover, the surface of the electrodes, before and after consecutive modifications with immobilization layers and capture probes ssDNA, were electrochemically characterized through capacitive (baselines) measurements (**paper III**). See the capacitance measurements in *section 2.4*.

**Table 1:** Percentage (%) coverage and capacitances of Pty- and MCH- modified electrode surfaces

Parameter (s)	Pty only	MCH only	Pty-ssDNA	MCH-ssDNA
% surface coverage	65 ± 2	26 ± 2	75 ± 3	30 ± 2
Capacitance/ baseline (nF cm <sup>-2</sup> )	10790	8510	11040	9140

The registered capacitance for bare gold electrode surface was 10420 nF cm<sup>-2</sup>. Upon coating with Pty, the capacitance slightly increased as shown in Table 1. The deposition of Pty on the surface made the surface more hydrophilic due to the primary amino groups present in the Pty layer. Hence, the presence of these amines attracted the electrical double layer closer to the electrode surface with an increase in capacitance as consequence [95]. In addition, the presence of the active amino groups on the surface increased the dielectric properties on the electrode surface, which also could have contributed to an increase in capacitance.

Conversely, deposition of alkanethiol (MCH) monolayers on the electrode surface resulted in a decrease in capacitance (Table 1). MCH has a low dielectric constant [96], forming a hydrophobic monolayer on the electrode surface [97]. The hydrophobic nature of the modified surface derives from the presence of the long hydrocarbon chains that displace the electrical double layer further away from the electrode surface, resulting in a decrease in capacitance. However, immobilization of the capture ssDNA probe in both immobilization layers resulted in increase in their capacitances. As the ssDNA is very hydrophilic [97], it attracts the electrical double layer closer to the electrode surface, resulting in an increase in capacitance.

## 2.3 Electrical double layer capacitance

A double layer capacitance is an electric charge stored at the electrode/electrolyte solution interface when a potential or current is applied to the electrode [98,99]. The interface region is called electrical double layer (EDL). The capacitive measurements employed in this thesis are based on the EDL theory (Fig. 2-11).

### 2.3.1 Electrical double layer theory

The first theoretical model of the existence of an EDL at a metal/electrolyte solution interface was introduced by von Helmholtz in year 1879 [100]. In this model, it was proposed that both excess charges on the metallic phase and counter ions (EDL) in the solution phase, reside at the metal surface, separated by a fixed distance. This structure is equivalent to parallel-plate capacitor. The weakness of this model was proposed to be the prediction of the constant capacitance across the EDL. Therefore, later on Gouy [101] and Chapman [102] extended the concept of the EDL by involving the diffuse layer, hydrated ions in the solution. The maximum concentration of excess hydrated ions would be adjacent to the

electrode surface where electrostatic forces are most able to overcome the thermal processes, while progressively lower concentrations would be found at greater distances as those forces become weaker. This model predicts that the average distance of the charge separation is dependent on potential and concentration of electrolyte. Thus, as the electrode becomes more charged, the diffuse layer would become more compact and the amount of charges stored should rise. As the electrolyte concentration increases, there should be a similar compression of the diffuse layer and a consequent rise in capacitance. However, the model did not consider the fact that the ions have a finite size, so some entities cannot approach the surface any closer than the ionic radius. If they remain solvated, the thickness of the primary solution sheath would have to be added to that radius. In the further development in 1924, Stern combined the Helmholtz and Gouy/Chapman models [103]. In this interfacial model, Stern suggested the existence of both a fixed layer (Helmholtz layer) and a mobile diffuse layer (Gouy and Chapman layer). Since, this interfacial model only considered the long-range electrostatic effects as a basis for creating the excess of hydrated ions found in the solution phase, later on Grahame in 1947 proposed the existence of specifically adsorbed ions at the metal surface due to other forces apart from electrostatic interaction [104].

A simplified model of the electrical double layer that has been widely used is presented in Fig. 2-11 [100].

When a positively charged electrode is immersed in the electrolyte solution, the charges will attract or repel the polarised molecules in the medium such as water, based on their polarity and the specific EDL region is formed (Fig. 2-10). Two theoretical layers involved in the EDL concept can be distinguished, closest to the electrode surface is the Stern layer, consisting of solvent molecules e.g., water molecules, which are polarized, and hence oriented (Fig. 2-10). These are specifically adsorbed ions, which possess a chemical affinity (e.g., van der Waals, hydrophobic bond, pi-electron exchange and complex formation) for the surface in addition to the Coulomb interactions. The locus of the electrical centers of the specifically adsorbed ions is called inner Helmholtz plane (IHP). Adjacent to IHP is a layer of solvated ions.

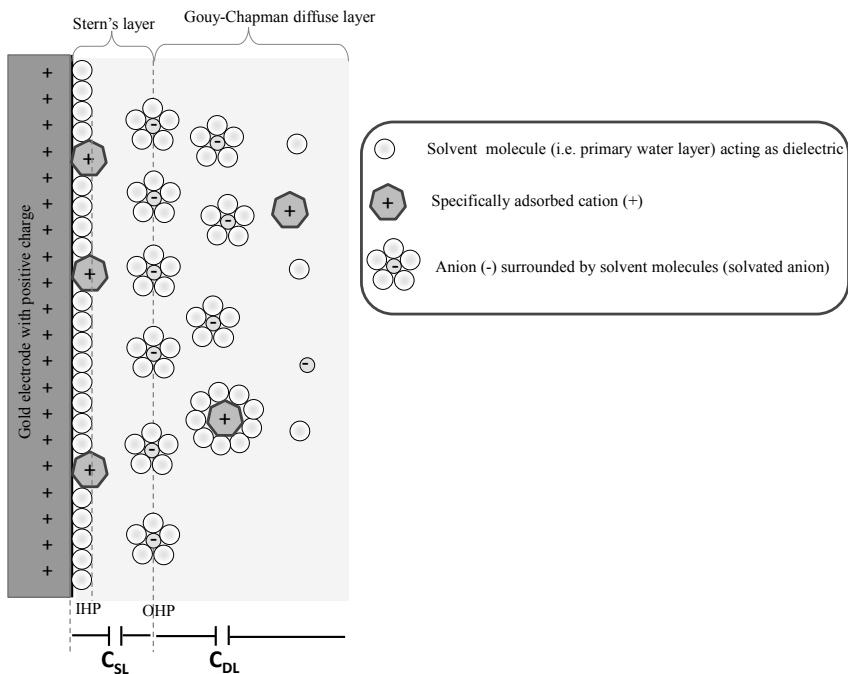


Fig. 2-10: Schematic representation of electrical double layer regions and differential capacitances in series on the gold electrode interface.

The interaction of the electrode with solvated ions is independent from chemical properties of the ions and is governed by a long-range electrostatic force. The locus of these nearest solvated ions is called the outer Helmholtz plane (OHP). The solvated ions are distributed in the diffuse layer. The layer extends to the bulk solution and the region from OHP to bulk solution is called Gouy-Chapman diffuse layer [100] see Fig. 2-10.

### 2.3.2 Behaviour of the electrical double layer capacitance

An electrode at which no charge transfer can occur across the electrode-solution interface, regardless of the potential imposed by an external source of potential, is called an *ideal polarized electrode* (IPE). Although, no electrode can behave as IPE over the whole potential range available in the electrolyte solution, a gold surface that hosts a non-conducting polymer or an adsorbed SAM of alkanethiol approaches the behaviour of IPE [100]. For the capacitive DNA-sensor the gold electrode surfaces were modified with a non-conducting polymer (Pty) (papers I, II, III, and IV) and a SAM of a functionalized alkanethiol (MCH) (paper III) as described in section 2.12. Thus the modified gold electrodes used in the capacitive DNA-sensor were regarded as IPEs. When the potential is changed at IPE, the corresponding charge accumulates on the solution phase until the potential difference across the EDL matches with the applied potential, since the charge

cannot cross the IPE interface. Thus, the behaviour of the EDL capacitance is governed by a non-Faradaic process according to Eq. 2 [100].

$$C = \frac{Q}{V} \quad (2)$$

where  $C$  is the EDL capacitance,  $Q$  is the charge stored across the EDL, and  $V$  is the potential across the EDL.

The EDL capacitance is directly related to the electrode-surface area, but inversely related to the distance between the electrode surface and EDL according to Eq. 3.

$$C = \epsilon_0 \epsilon \frac{A}{d} \quad (3)$$

where  $C$  is the EDL capacitance,  $\epsilon_0$  is the permittivity of free space (vacuum),  $\epsilon$  is dielectric constant of the material between surface of electrode and EDL,  $A$  is the surface area of electrode, and  $d$  is the separation distance between the surface of electrode and EDL.

In the electrode/solution interface, Stern's (adsorbed) and Gouy-Chapman (diffuse) layers, behave like two capacitors connected in series (see Fig. 2-11). Therefore, EDL capacitance is expressed as a total capacitance,  $C_{TOT}$ , and calculated as follows (Eq. 4).

$$\frac{1}{C_{TOT}} = \frac{1}{C_{SL}} + \frac{1}{C_{DL}} \quad (4)$$

where  $C_{TOT}$  is the total capacitance,  $C_{SL}$  is the capacitance of Stern's layer, and  $C_{DL}$  is the capacitance of the Gouy-Chapman diffuse layer.

Typically for the capacitive DNA-sensor, the capacitance at electrode/solution interface is built up of several layers, which act like several capacitors connected in series, i.e., i) the immobilization layer, ii) capture probe plus any contribution from adsorbed (Stern) layer, and iii) diffuse (Gouy-Chapman) layer (Fig. 2-11).

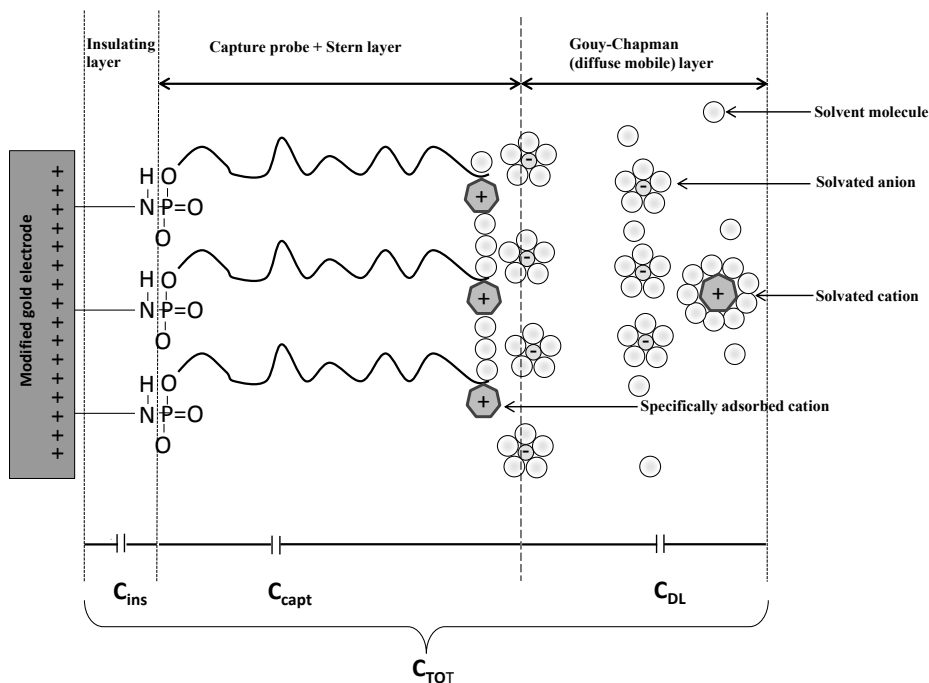


Fig. 2-11: Schematic representation of differential capacitances in series at the modified electrode/solution interface.

The total capacitance ( $C_{TOT}$ ) for the modified electrode/solution interface can be calculated as follows (Eq.5).

$$\frac{1}{C_{TOT}} = \frac{1}{C_{INS}} + \frac{1}{C_{CP}} + \frac{1}{C_{DL}} \quad (5)$$

where  $C_{TOT}$  is the total capacitance,  $C_{INS}$  is the capacitance of the insulating layers, Pty (**papers I, II, III and IV**) or 6-MCH (**paper III**),  $C_{CP}$  is the capacitance of the capture probe (ssDNA) with any contribution from Stern's layer, and  $C_{DL}$  is the capacitance of the Gouy-Chapman diffuse layer.

Since, the Stern's layer consists of a fixed layer that is adsorbed to the surface of the capture probe interface, the changes in total capacitance is mainly attributed to the Gouy-Chapman diffuse layer. As such, the thickness of the EDL depends on total ionic concentration in the electrolyte solution. The thinner the EDL the closer the counter ions to the surface of the electrode; which results in a more sensitive capacitive system towards changes on the electrode surface (e.g. a binding event). For the 10 mM potassium phosphate buffer used in this work, the thickness of the EDL was less than 10 nm or 0.01  $\mu\text{m}$  [100]. This means, that the counter ions are very close to the electrode surface, and that the capacitive DNA-sensor is sensitive even to nanoscale size effects introduce on the electrode surface.



## 2.4 Capacitance measurements

Several different methods have been reported for the measuring of EDL capacitance; impedance spectroscopy [105], CV (potential sweep) [106], potential pulse [64,25] and current pulse [51]. In this work, the capacitances were measured by the potential pulse (**papers I and II**) and current pulse (**papers III and IV**) methods. The detection principle is based on the response of the double layer capacitance upon hybridization of a target ssDNA to the capture probe (Fig. 2-12).

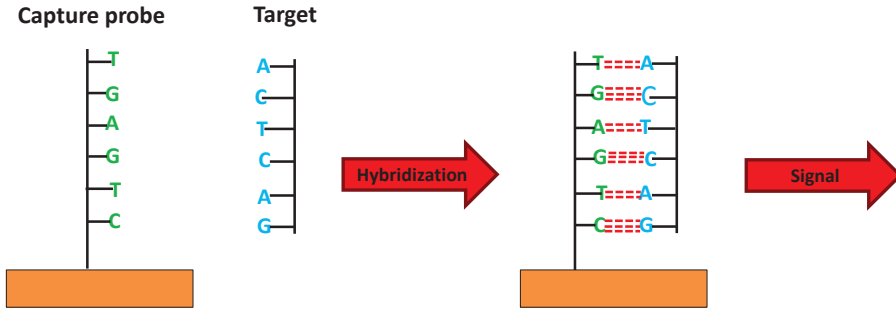


Fig. 2-12: Detection of a target ssDNA using a capacitive DNA-sensor.

### 2.4.1 Potential pulse capacitance measurements

The methodology of potential pulsing for capacitance measurements (**papers I and II**) was based on an assumption that the system (Fig. 2-11) could be described as a simple RC-circuit [107, 108] as represented in Fig. 2-13a.

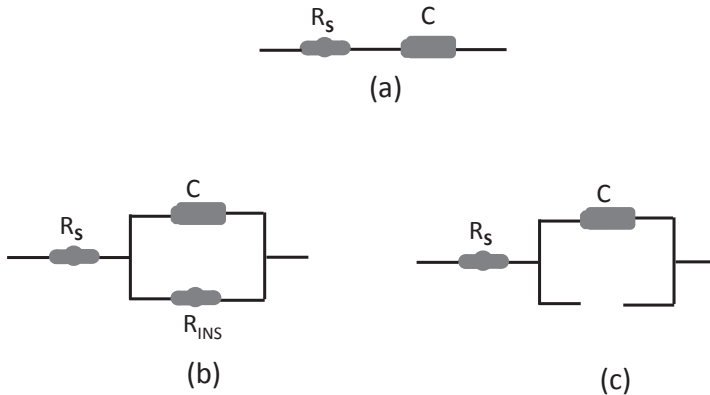


Fig. 2-13: Different model of circuits: a) RC b) R(RC), with very high resistance at  $R_{INS}$  the circuit behaves like open circuit c), very similar to RC model, since extremely large current will flow through  $R_s$  and  $C$ , which are serially connected.

A solution-resistor,  $R_s$ , and EDL-capacitor,  $C$ , are serially connected. However, for the capacitive biosensor, the electrode is typically modified with a highly insulating layer, which behaves like a resistor that is in parallel connected to  $R_s$  and  $C$ . As such, a better description of reality for the system should be represented as  $R(RC)$  circuit model [107] as shown in Fig. 2-13b. Yet, the electrode surface is designed to be highly insulated, meaning that resistance at  $R_{INS}$ , is made to be much greater than that of  $R_s$ . Thus, extremely small currents will flow to  $R_{INS}$ , and therefore the system could be simplified as  $(RC)$  circuit [73] as shown in Fig. 2-13c.

For the potential pulse method, the measurements were executed with an interval of 60 s, by applying 50 mV potential pulse of 20 ms *vs.* Ag/AgCl, followed by a relaxation as show in Fig. 2-14a.

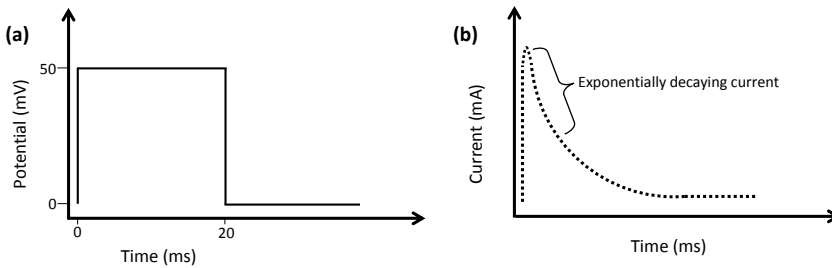


Fig. 2-14: Potential step: (a) applied potential pulse and (b) resulting exponentially decaying current.

The behaviour of the current,  $i$ , with time,  $t$ , when applying a potential ( $V$ ) (Fig. 2-14 b, is expressed by Eq. 6.

$$i(t) = \frac{V}{R_s} e^{-\frac{t}{R_s C_{TOT}}} \quad (6)$$

Taking the natural logarithm of Eq. 6, a linear relationship exists between  $(\ln) i(t)$  and  $t$ , (see Eq. 7), the values of  $C_{TOT}$  and  $R_s$  was calculated by the in-house made computer software (PotStat, Pascal 7.0).

$$\ln i(t) = \ln\left(\frac{V}{R_s}\right) - \left(\frac{t}{R_s C_{TOT}}\right) \quad (7)$$

In **papers I and II**, the potential pulse capacitive measurements were performed in a manual flow injection system (Fig. 2-15).

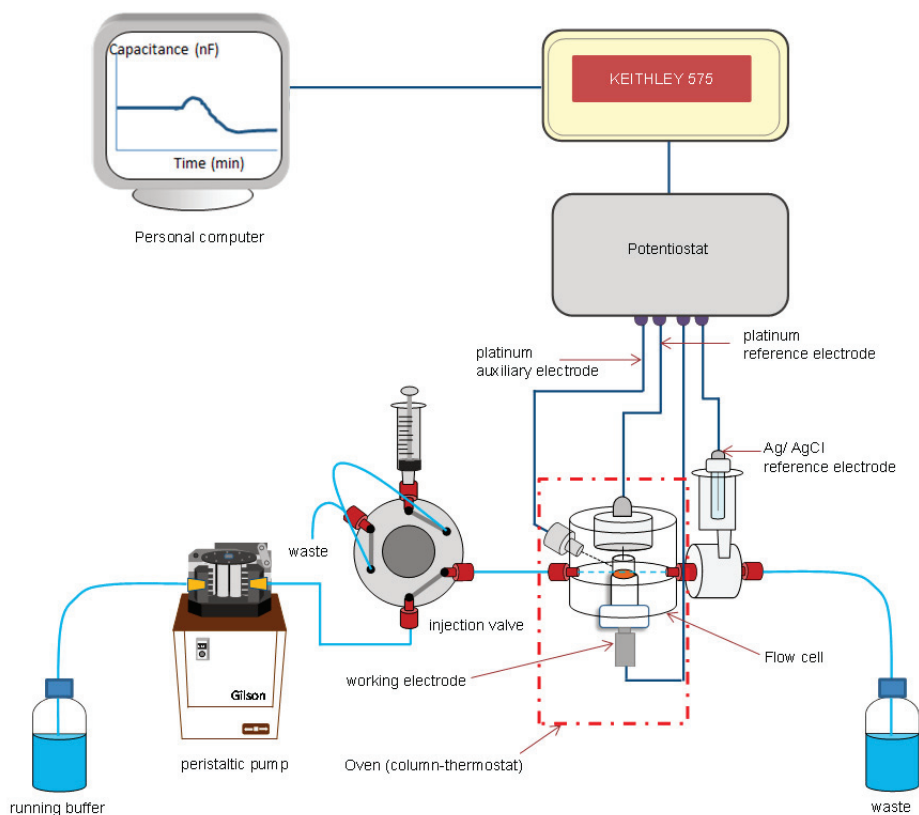


Fig. 2-15: Experimental set up of flow-injection capacitive DNA-sensor system using potential pulse for capacitance measurements

The modified electrode hosting the capture probe ssDNA was placed in a 10  $\mu\text{L}$ -dead volume four-electrode flow cell, which consists of the platinum-wire counter electrode, Ag/AgCl- and platinum-wire reference electrodes [107]. The flow cell was connected to potentiostat and kept in the column-thermostat and all tubes were insulated with aluminium foil for temperature control. The potentiostat was connected to a data acquisition unit which, in turn was connected to personal computer. As such, the potentiostat was powered from the data acquisition unit. The latter was powered from the personal computer *via* a galvanometric insulated power supply in order to moderate the background noise during the capacitance measurements. Running buffer (10 mM potassium phosphate buffer, pH 7.2) was continuously pumped through the flow-cell with a peristaltic pump at flow rate of 100  $\mu\text{L min}^{-1}$ . Since, the area of the electrode and concentration of the buffer are constants, the system registered a constant  $C_{TOT}$ , which in Fig. 2-16 is indicated as  $C_{\text{before analyte}}$  and  $C_{\text{after analyte}}$  (baselines).

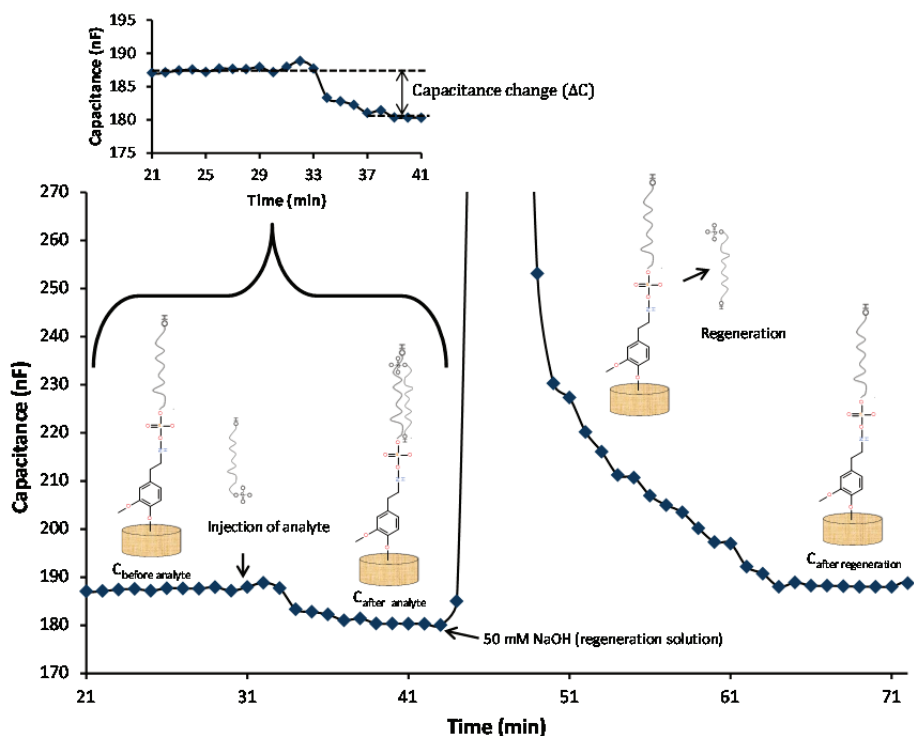


Fig. 2-16: Registered capacitance upon injection of the target ssDNA and regeneration solution. Inset showing the capacitance change ( $\Delta C$ ).

However, upon injection of a target complementary ssDNA sample to the flow system via a 250  $\mu\text{L}$  sample loop, the hybridization between capture probe and target ssDNA took place. The hybridization leads to a displacement of the EDL away from the electrode surface, and a decrease in the dielectric constant of the capture probe, resulting in a decrease in the registered capacitance,  $C_{TOT}$  as demonstrated in Fig. 2-16.

Subsequent to the hybridization step a regeneration solution (50 mM NaOH) was injected in order to disrupt hydrogen bonds between the paired capture probe and target ssDNA. The capacitance then returned to the original baseline with the continued flow of running buffer, ready for next measurements (Fig. 2-16). The overall analysis cycle took 45 min (papers I and II).

The capacitance change ( $\Delta C$ ) was calculated as difference of the baseline levels, before and after injection of the sample (Fig. 2-16 *inset*). The  $\Delta C$  proved linearly related to the logarithmic concentrations of a target ssDNA injected into the system as depicted in Fig. 2-17. In order to obtain a reliable analytical signal, an average of the last five capacitance readings for each base line was used in the calculation. The necessity of evaluating an average of at least five capacitance readings was previously mathematically proved [109].

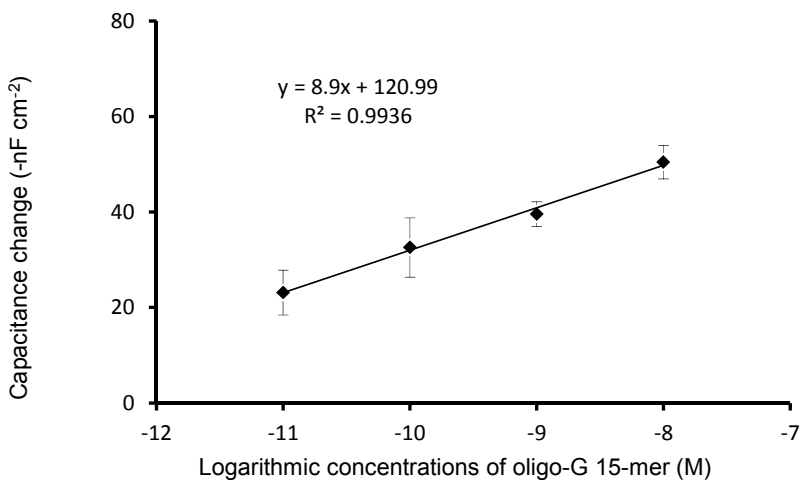


Fig. 2-17: A linear relationship between the capacitance change and logarithmic concentrations of 15-mer oligo-G applied to the sensor system containing an electrode surface with 25-mer oligo-Cs as capture probe (paper I).

#### 2.4.2 Current pulse capacitance measurements

The principal theory of the current pulse technology is similar to the previously described potential pulse method, where both applications are based on the electrical double layer theory, considering the system as a simple circuit  $R_S C_{TOT}$  model. In papers III and IV a pulse of constant current (10 mA) was applied to the working electrode every 60 s by the measurement unit integrated in the capacitance biosensor, as represented in Fig. 2-18a. When the electrode in the electrolyte solution was charged with a constant current ( $i$ ), a potential ( $V$ ) was linearly built-up across the electrode/solution interface (EDL) with time ( $t$ ), resistance of the solution ( $R_S$ ) as represented in Fig. 2-18b and expressed in Eq. 8.

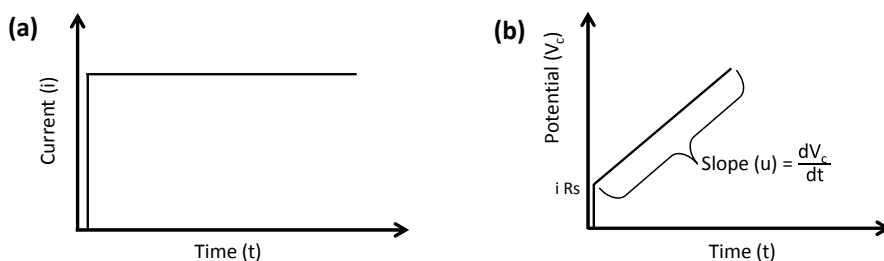


Fig. 2-18: Current pulse: (a) applied potential pulse, and (b) a resulting built-up potential across the EDL.

$$V = i(R_s + \frac{t}{C_{TOT}}) \quad (8)$$

$$\text{Since, } V = V_o + V_c \quad (9)$$

where  $V$  is the total potential in the system,  $V_o$  is the jump in potential after application of the current  $i$  at time zero,  $R_s$  is the resistance of the solution and  $V_c$  is the built-in potential across the EDL capacitance after applying the current  $i$  at time  $t$ .

When time  $t$  is zero, the potential in the system is described by Ohm's law (Eq. 10).

$$V_o = i \times R_s \quad (10)$$

However, during the charging of EDL, a transient external capacitive current flows, considering Eq.2 above, and can be re-written as Eq. 11.

$$C_{TOT} = \frac{dQ}{dV_c} = \frac{idt}{dV_c} \quad (11)$$

where  $C_{TOT}$  is the capacitance across the EDL,  $Q$  is the charge accumulated in the EDL,  $i$  is the applied current to the electrode,  $t$  is the time of current flow, and  $V_c$  is the potential built across the EDL capacitance at time  $t$ . Therefore, the capacitance across the EDL was calculated from the slope of the potential curve ( $V$  vs.  $t$ ) as shown in Eq. 12.

$$C_{TOT} = \frac{i}{u} \quad (12)$$

where  $C_{TOT}$  is the capacitance across the EDL,  $i$  is the applied current to the electrode, and  $u$  is the slope of the graph ( $V$  vs.  $t$ ).

In order to meet biosensor requirements such as convenience and user-friendliness, the current pulse-capacitance measurements (**paper III** and **IV**) were performed in automated sequential injection flow system with software control. The schematic diagram of the automated sequential-injection flow system is represented in Fig. 2-19.

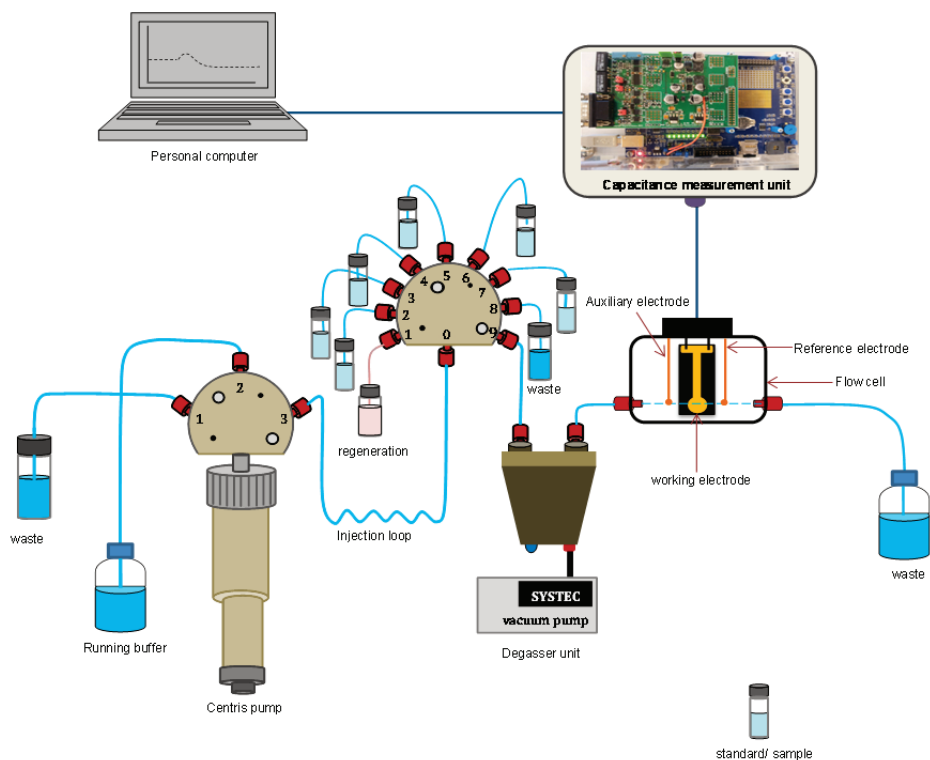


Fig. 2-19: Schematic diagram of the automated sequential-injection flow system used in this work.

The automated sequential-injection flow system comprises a centris pump, two separate valves i.e., 3- and 9-port valves, a degasser unit, a three-electrode flow-cell, and a CapSense-capacitance measurement unit [73]. The 3- port valve is connected to the centris pump; port #1 is employed to drain the waste during the initialization. Port #2 is extended into the running buffer vessel, in which the syringe plunger will withdraw the buffer solution. The injection loop is fitted between port #3 and the inlet of the 9-port valve. A volume of 250  $\mu\text{L}$  of either a standard, sample- or regeneration solution is automatically and sequentially injected into the flow cell by the injection valve *via* the degassing unit by using the 9-port valve. The centris pump continuously pushes the running buffer to the flow cell. The CapSense-capacitance measurement unit is controlled by the software, and equipped with resistometer, connected between the potentiostat and flow cell to supply an interrupted current pulse. In addition, the measuring unit consists of an analogue-to digital converter (ADC) unit. Thus, the system automatically applies a constant current to the working electrode and calculates the capacitance change.

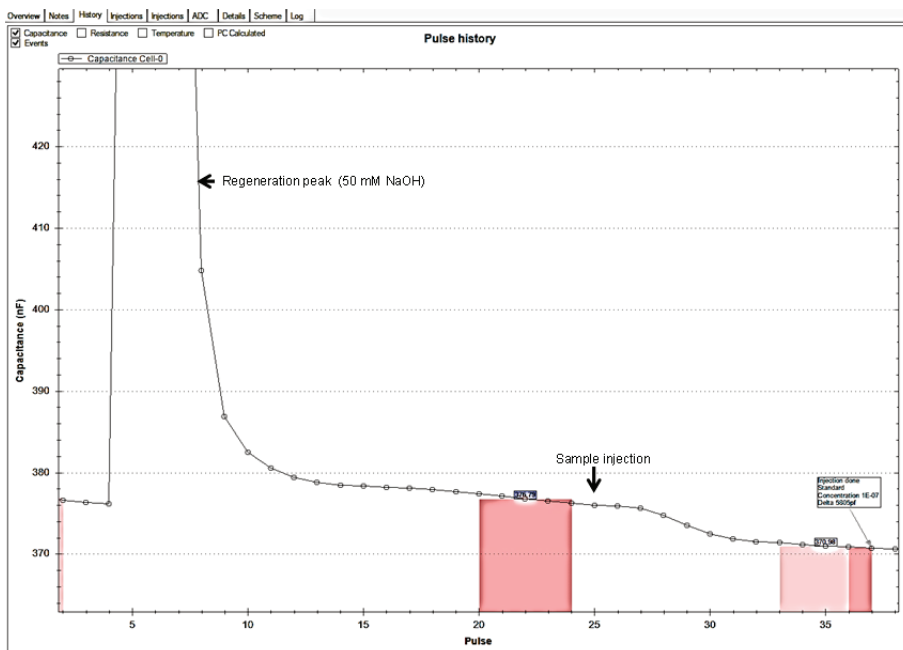


Fig. 2-20: Time course graph showing decrease of capacitance upon injection of a target analyte (25-mer *mecA* gene) in the automated flow sequential injection system (CapSense™ Biosystem) with 10 min analysis time.

The automated sequential-injection flow system has improved sample handling and reduced turn-around time. In comparison to the manual flow injection system (papers I and II), the overall analysis cycle was 35 min (compared to 45 min for the manual system) of which 25 min are related to the regeneration step (Fig. 2-20). In addition, the automated sequential-injection flow system has simplified the process of determining the linearity range between the different analyte concentrations and their individual signal amplitudes. In addition, as data evaluation strictly is performed *in silico*, the bias related to operator involvement is reduced. In fact, the sensor system automatically plots the calibration curve for injected sample concentrations *vs.* capacitance change (signal) as represented in Fig. 2-21.



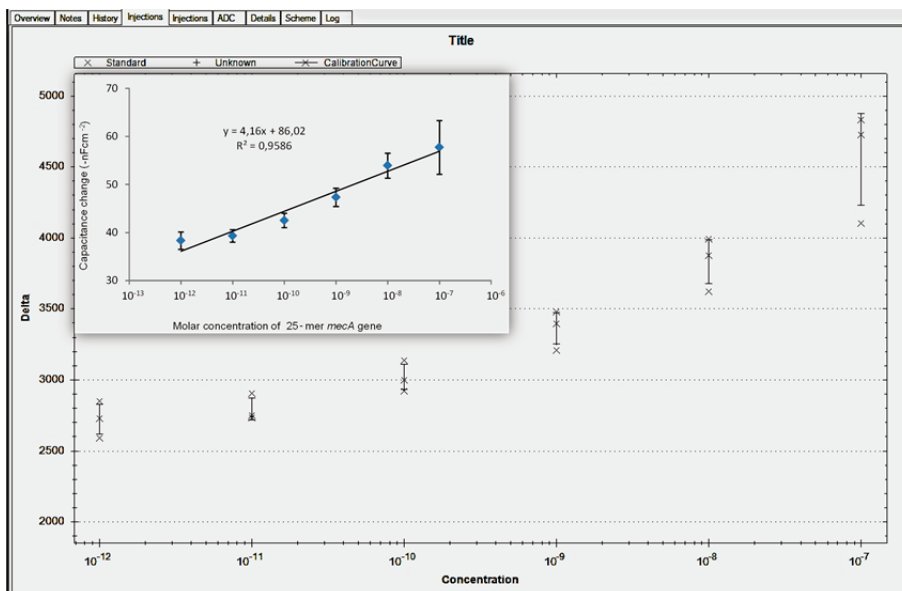


Fig. 2-21: The automatically plotted calibration curve for capacitance change vs. concentrations of injected sample (25-mer *mecA* gene). The inset shows linearity of the molar concentrations of sample (25-mer *mecA* gene) vs. capacitance change. The mean of three signal values for each concentration with its standard deviation was manually calculated from same data of the automated plotted curve

## 2.5 Validation of the developed capacitive DNA-sensor

The capacitive DNA-sensor developed in this work was evaluated in accordance with standard criteria, as recommended in the IUPAC protocols for biosensor assays [110,111]. The capacitive DNA-sensor was validated for analytical and performance characteristics, including calibration characteristics (sensitivity, linear concentration range and detection limit), selectivity, reproducibility/reusability, stability and lifetime. In addition, the developed capacitive DNA-sensor was compared diligently to an established and accepted 'gold standard' methodology, i.e., the plate counting technique (paper II).

### 3. Optimization of capacitive DNA-sensor

To accelerate the development of the capacitive DNA-sensor, the signal amplitude, sensitivity, specificity and reusability of the sensor were optimized (papers I and III).

#### 3.1 Oligonucleotide length

The signal amplitude of the capacitive DNA-sensor is dependent primarily on the distance of which the EDL is being displaced from the electrode surface during the hybridization of the target ssDNA to the capture probe [50]. In **paper I** the effect of the length of the target oligonucleotide was investigated to optimize the signal amplitude of the developed capacitive DNA-sensor, which could in turn lead to an optimized analytical sensitive. The registered signal was found to some extent to be dependent on the length of the applied oligo-G, where applying a 25-mer oligo-G resulted in a capacitance change which was approximately twice higher than that registered by the same concentration of 15-mer oligo-G (Table 2).

Table 2: Calculated capacitance change upon applying of oligo-G of different lengths on the electrode surface coupled with capture probe

Oligo-G length (-mer)	Capacitance change: Average $\pm$ SD (-nFcm <sup>-2</sup> )		
	at $10^{-8}$ M	at $10^{-9}$ M	at $10^{-11}$ M
15	51 $\pm$ 4	40 $\pm$ 3	23 $\pm$ 5
25	89 $\pm$ 5	76 $\pm$ 5	40 $\pm$ 2
50	78 $\pm$ 4	61 $\pm$ 3	40 $\pm$ 2

SD standard deviation

A longer oligonucleotide molecule that is allowed to hybridize onto the capture surface, would theoretically result in that the EDL will be displaced furtherout from the surface interface. This would hence result in a larger capacitance decrease (a higher signal amplitude). However, there was no significant difference in the signal amplitude between 25- and 50-mer oligo-Gs at the same concentration. In fact, linear DNA-molecules over a certain treshold length have a high intrinsic tendency to adopt a bent conformation [112,113]. The persistence lengths (maximum inflexible lengths) for ssDNA and dsDNA are 2 and 50 nm, respectively [113]. Thus, the unhybridized portion of the 50-mer oligo-G (about 25-mer), which is about 10 nm contour length, behaves as a flexible ssDNA chain. Whereas, the fully hybridized 25-mer oligo-G, assumes the conformation of a rigid dsDNA chain. The increased rigidity of dsDNA obviously results from

base-pair stacking which tends to compress the DNA-strands and hence decrease the interphosphate repulsion, which strongly contributes to DNA stretching [112]. Moreover, when an electrode surface is positively charged (by applying a positive potential pulse), the negatively charged DNA is pulled towards the electrode and hence adopts a tilted orientation [114]. Since, the longer the DNA-molecule the more negative charges it possesses, a 50-mer would be pulled towards the electrode surface even more (more tilted) than 25-mer oligo-G, resulting in a smaller signal amplitude than expected (Fig. 3-1 b).

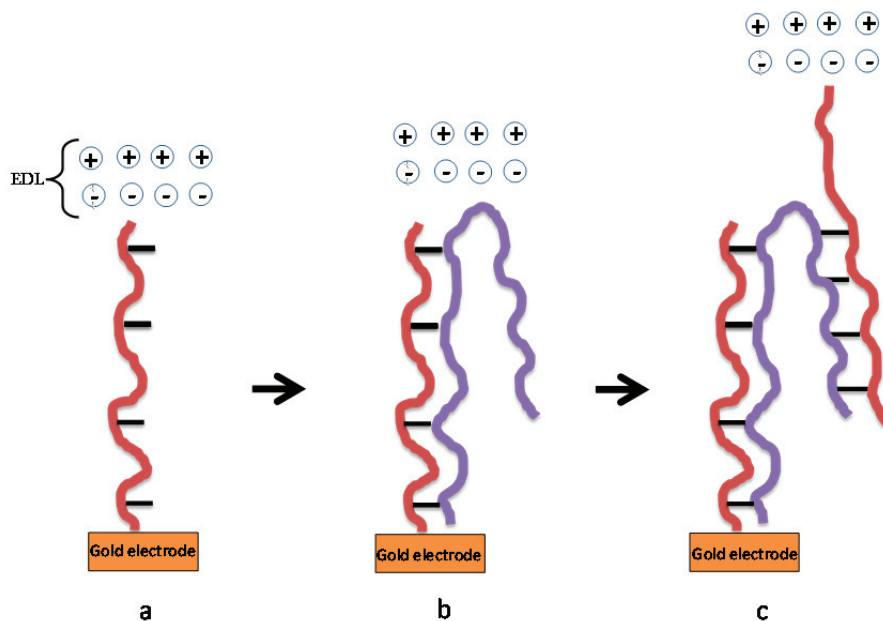


Fig. 3-1: Schematic representation of sandwich hybridization approach. (a) 25-mer oligo-C capture probe (b) hybridization of a target 50-mer oligo-G to the capture probe, (c) hybridization of 25-mer oligo-C after (b).

However, by introducing a sandwich hybridization approach for the target 50-mer oligo-G (Fig. 3-1c), as schemetically represented in Fig. 3-1, it was possible to increase the signal amplitude, which was almost twice as high as the that of 50-mer oligo-G alone (Fig. 3-2).

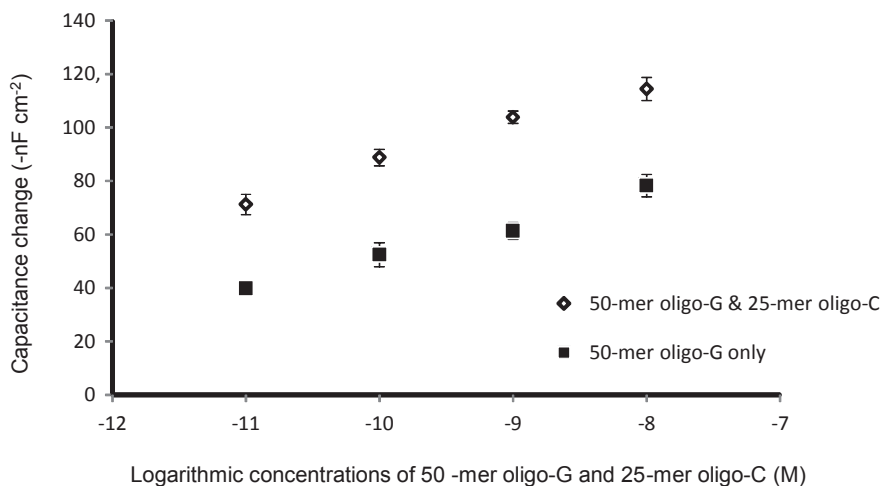


Fig. 3-2: Sandwich hybridization 50-mer oligo-G followed by 25-mer oligo-C, compared with 50-mer oligo-G alone.

These results imply that the subsequently injected 25-mer complementary oligonucleotide hybridized with bases from a partially bent long oligonucleotide molecule, and resulted in an amplification of the signal, which indicates that the EDL was even further displaced from the surface of the gold electrode due to hybridization of the second oligonucleotide molecules. Consequently, when executing the capacitive DNA-sensor assay, it seems relevant to treat long DNA-molecules differently from short ones.

### 3.2 Hybridization (working) temperature

When the temperature of a solution containing dsDNA is raised sufficiently, strand separation or ‘melting’ occurs due to an increase in molecular motion where breaking of the weak interactions is induced. The melting temperature ( $T_m$ ) of a dsDNA is defined as the temperature at which half of the nucleic acid exist in the double-stranded state and the other half in the single stranded state with the two molecular forms in equilibrium [115]. The strand separation involves disruption both of the hydrogen bonds between the paired bases and the hydrophobic interaction between the stacked bases. The  $T_m$  value can vary in the range from 0 to 100 °C, depending on the ionic strength of the solution [116], possible denaturing agents present [117], the size and base composition of the DNA-molecule [118, 119]. After breaking the bonds, two separate single ssDNA are formed, which can re-associate with decreasing temperature into the dsDNA conformation.

For analytical purposes it is indispensable to consider high specificity of the sensor. For the DNA-sensor, the analytical step is the hybridization between a target ssDNA in solution and a capture probe on the electrode surface. In order to

increase the selectivity of the hybridization, i.e. discriminate non-target (mismatch) DNA molecules from hybridization to the capture probe, it is conceivable to increase the hybridization temperature to at least 25 °C below the theoretical value of  $T_m$  of the complementary strands [120]. The  $T_m$  decreases by about 1 °C for every 1 % of mismatched base pairs [121]. However, for DNA-molecules tethered to a positively polarized metallic transducer, and for short and very closely related DNA sequences, an even higher temperature up to 5 °C below the theoretical  $T_m$  may be required to achieve the desirable selectivity [50, 117, 122].

The highest hybridization temperature reported for a flow system-DNA-based biosensor is 45 °C, which resulted in high selectivity for a short capture probe ssDNA (8-mer). However, this temperature did not improve the selectivity for a 26-mer capture probe ssDNA [50].

In **paper I**, hybridisation of a 25-mer oligo-C capture probe to complementary and non-complementary 25-mer probes, and for oligo-G and oligo-T, respectively, were performed at the different temperatures; 23, 45 and 50 °C. However, it was necessary to first understand the influence of temperature on the modified electrode surface in order to decide whether a measured capacitance change is caused by changes in temperature or by the actual hybridization event on the electrode surface. It was also important to determining the intrinsic stability of the electrode surface on the different temperatures. Hence, the modified (Pty-oligo-C) electrode surface was subjected to different temperatures; 23, 30, 40, 50 and 60 °C for 30 min each and the corresponding capacitive baselines were determined. Raising the temperature of the electrolyte, increases the mobility of ions in the EDL, resulting in an increased electrical conductivity of the electrolyte, and hence an increase in registered capacitance-baseline [123]. The modified electrode surface seemed to withstand temperatures up to 50 °C. Since the hybridization of DNA is often carried out in even lower temperature, this temperature range is sufficient for most application of DNA-sensors.

Working at 50 °C could efficiently reduce non-specific interactions by more than 90 % without significantly altering the specific interactions between oligo-C and oligo-G (Fig. 3-3). However, there must be a trade-off between raising the temperature to eliminate non-specific interactions and the temperature effect on the specific interactions. This is an aspect that needs to be kept under control, though it does not seem to be a problem at temperatures below 50 °C as was shown in this study.

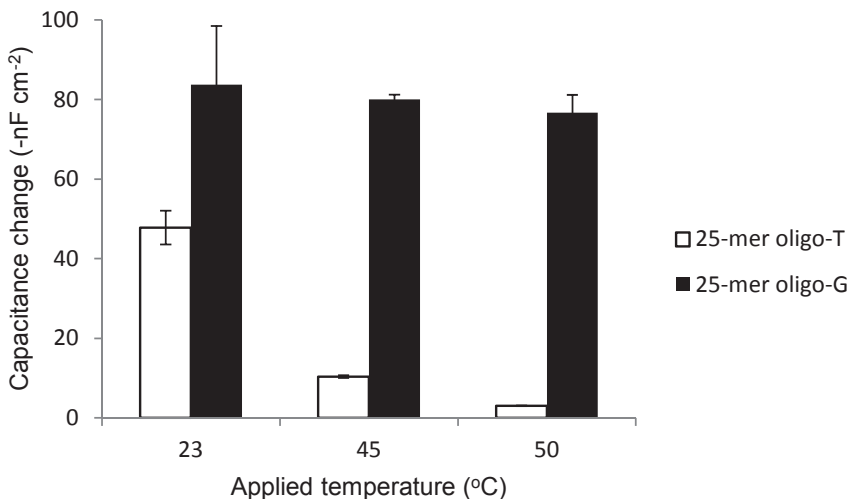


Fig. 3-3: Capacitance change from an electrode immobilized with 25-mer oligo-C (capture probe), for injections with  $10^{-8}$  M complementary 25-mer oligo-G and non-complementary 25-mer oligo-T.

### 3.3 Immobilization layer

The ssDNA strands immobilized on the capture probe are often nonspecifically adsorbed on the bare electrode surface. This may result in multi-point tethering of the capture probe ssDNA and hence an impaired hybridization [124,125]. Consequently, the capture strands have to be immobilized in such a way that their stability, optimal orientation and reactivity to target ssDNA are retained. A suitable immobilization layer enhances the one-point grafting that defines the conformational freedom of the capture probe, which is essential for hybridization [126]. The hybridization is generally enhanced for capture probe DNA that extend away from a surface, since the steric hinderance is lower for such brushlike probes than for the DNA directly adsorbed on the surface of the gold electrode [127]. Furthermore, the sensitivity and signal amplitude of the capacitive DNA-sensor depend directly on the surface density of the immobilized capture DNA-probes [66] and to the vicinity of the EDL to the electrode surface [98], respectively.

However, increasing the capture probe ssDNA density on the surface may lead to intermolecular interactions, which might result in a decrease of the probe fraction that actually is available for hybridization [126]. For instance, at surface densities  $\leq 5 \times 10^{12}$  cm<sup>-2</sup>, a typical probe sequences (15 - 30 mer) can hybridize with efficiencies  $> 60$  %, but at probe densities  $> 1 \times 10^{13}$  cm<sup>-1</sup> hybridization efficiency is often reduced due to increased steric constraints and electrostatic repulsion [127].

In **paper III**, two different types of immobilization layers, i.e., non-conducting polymer film (Pty) and self-assembled monolayer of a functionalized alkane thiol (MCH) were investigated for the analytical performance of the capacitive DNA-sensor. The capacitive DNA-sensor based on Pty-modified electrode surfaces displayed better performance than those manufactured with MCH-SAM (Fig. 3-4).

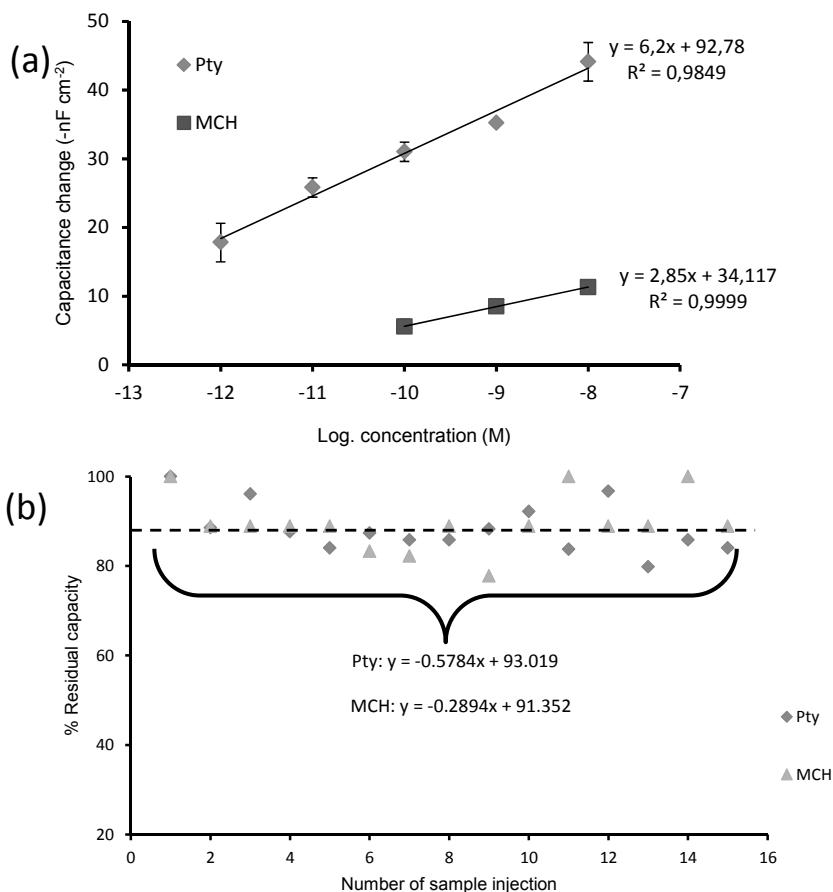


**Fig. 3-4:** (a) Calibration curves showing linear responses at log molar concentration ranges of applied target ssDNA onto the Pty- and MCH-ssDNA modified electrodes; (b) re-usability of the Pty-ssDNA and MCH-ssDNA modified electrodes.

The electrodes modified with Pty and MCH showed linearity responses at concentrations ranging from 0.001 to 10 nM (Pty) and from 0.1 to 10 nM (MCH), with LODs of 0.4 pM and 70 pM, respectively (Fig. 3-4a). Both electrodes could be reused for more than 15 cycles with residual hybridization capacity of more than 90 % relative to the original signal (Fig. 3-4b).

The qualitative data (**paper III**) suggest that, one of the reasons for the better analytical performance of the Pty modified electrode could be its capacity to host more capture probes than for the MCH modified electrode. However, further studies regarding the surface capture probe density, the use of radiolabeling or other electrochemical methods [113] should be conducted in order to obtain conclusive quantitative information. Such study could make it possible to further control the capture probe ssDNA density on the surface since density and the overall design of the capture probe are key components, determining both, selectivity and sensitivity as well as reproducibility of the DNA assay.



## 4. Applications of the capacitive DNA-sensor

Diseases caused by microorganisms are responsible for more human deaths than any other single cause [5]. In an era of vaccine, antibiotics and dramatic scientific progress, it is conceivable that these diseases should have been brought under control. Yet, they continue to kill at an alarming rate, mainly due to limited diagnostic capabilities. Millions of persons die on a yearly basis, particularly in developing countries, from microbial diseases such as tuberculosis, cholera, pneumonia, respiratory diseases and diarrheal syndromes [5]. Additionally, humans worldwide are under the threat of diseases that could emerge suddenly such as Ebola haemorrhagic fever, Marburg haemorrhagic fever and Enterohemorrhagic *E. coli* (EHEC) infection, as well as emergence of antibiotic resistant bacteria, e.g., methicillin-resistant *S. aureus* (MRSA). Moreover, there is also a worldwide threat from those who might employ microorganisms as a bioterror agent. Under certain circumstance infectious diseases can be transmitted and spread sporadically throughout a population [5]. Clearly microorganisms are a serious health threat to humans and animals in all parts of the world. There is hence an urgent need for the development of novel, fast on-site solutions for the detection of bacteria, viruses and prions.

In **papers II and IV**, the developed capacitive DNA-sensor was employed for DNA-based detection of life-threatening bacteria i.e., Enterobacteriaceae and Methicillin-resistant *S. aureus*, respectively.

### 4.1 Detection and quantification of Enterobacteriaceae

Intestinal infectious diseases are common global health threats, as such more than 4.5 billion cases are reported yearly. This group of diseases is in the third-place among the most deadly human diseases, claiming the lives of more than 1.9 million people each year [128]. The rod-shaped Enterobacteriaceae such as, *Salmonella*, *Shigella*, and *E. coli* are the causative agents of severe bacillary dysentery, typhoid, diarrhoea and other intestinal diseases.

Immunoassays, especially ELISA have been widely used for detection of different members of Enterobacteriaceae [1-3]. Moreover, the presence of virulent genes such as *eaeA* gene of *EHEC* O157:H7 or DNA-markers like hyper-viable regions of 16S rDNA, which are present in all bacteria [129], has led to the development of several molecular techniques with different detection principles, including microarray [16], PCR [17], QCM [38,39] and SPR [42] for the detection of various members of the family Enterobacteriaceae.

In **paper II** *E. coli* BL21 (DE3), a member of the family Enterobacteriaceae was employed as an example for the study. The detection and quantification of *E. coli* was based on the 16S rDNA. The detection of target 16S rDNA involved sample preparation steps, including ssDNA generation. The most efficient, reliable and

widely used methods for ssDNA generation from dsDNA are heat denaturation with subsequent chilling on regular water ice [26] and asymmetric PCR [130]. However, the former approach poses a challenge to the flow-based hybridization assays. The heat-denatured ssDNA might re-associate to form dsDNA prior to analysis. Otherwise, a further purification step is required to remove one of the complementary strands from the sample. The latter approach, PCR, is a complex and expensive technique with a usage that is limited to centralized hospitals and research laboratories [11].

In **paper II**, a new, simple, cheap and effective approach to bacterial genomic DNA-sample preparation was demonstrated (Fig. 4-1).

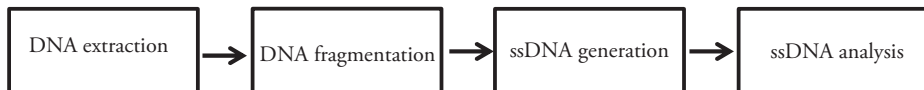


**Fig. 4-1:** Schematic diagram of genomic DNA sample preparation for capacitive DNA-sensor analysis.

The complete sample preparation procedure was acceptably short; less than 90 min and the hybridization time was 15 min. The preparation protocol was initiated by (1) extraction of genomic DNA (2) DNA-fragmentation by the use of restriction enzyme (*AciI*), generating right size of targeted complementary DNA sequence with reference to capture DNA-probe on the sensor-chip(3) DNA heat-denaturation to produce ssDNA, with subsequent addition of *extreme thermostable ssDNA binding protein* (ET SSB) to block re-association of the produced ssDNA and (4) Denaturation of ET SSB by adding formamide into the sample up to 30 % (v/v). It is then directly injected into the flow based DNA-sensor for analysis.

The application of ET SSB exhibited improved efficiency relative to traditional cooling approach in preventing the heat-generated ssDNAs from re-annealing prior to analysis. In principle, instant hasty cooling of heat-generated ssDNAs prevents them from re-association by causing a prompt aggregation to the individual strands [26]. However, this approach is not effective for low concentration and/or short sequence of ssDNAs [131]. Fig. 4-2, lanes #: 2, 3, 4, and 5 shows the DNA bands of the heat-denatured cool-treated samples. They migrated to the position between 25- and 35 bp ladder DNA (approximately 30 bp in size). This implies that, most of the heat-generated ssDNAs reannealed during the cooling step, resulting in the formation of dsDNA bands.



Fig. 4-2: Electrophoresis gel profile (3 % agarose, 80 V, 2 h 45 min) presenting the effect of different conditions of denaturation in the stability of ssDNA. L: DNA ladder. 1: Single stranded 30-mer 16S rDNA. 2: Double stranded 16S rDNA sample (30 bp). For lane 3 to 7: Heat denaturation (95 °C) of the 16S rDNA (30 bp) was the first step of the treatment for all samples. The second step was different for each lane as follows; 3: Chilling in the ice water (0.6 °C). 4: Placing in the ethanol cryostat (-12 °C). 5: Chilling in the dry ice (-78 °C). 6: Presence of ET SSB during the first step. 7: Like lane 6 but additional ET SSB denaturation with formamide 30 % (v/v).

However, ET SSB binds specifically and firmly to heat-produced ssDNAs, hence preventing them from re-annealing, leading to stable ssDNA molecules [132]. The hydrogen-bonding, electrostatic and stacking interactions form the basis for ET SSB specificity to ssDNAs. Moreover, due to hydrophobic nature of ET SSB-ssDNA stacking interactions, the binding of ET SSB to ssDNA does not require distinctive surface of ssDNA. This makes ET SSB adaptable to assays that employing DNA of different types and/or sequences [133]. Fig. 4-2, lane #6, shows a DNA band of a heat-generated-ET SSB treated-ssDNAs sample. It migrated to the same position as that of a 25 bp band of the DNA ladder and 30-mer ssDNA-band of control sample (lane #1). Consequently, addition of formamide to the ET SSB-ssDNA complex generated ET SSB-free ssDNA, which freely re-associated to form dsDNA (Fig. 4-2, lane #7). In theory formamide competes with ET SSB for backbone hydrogen bonds, resulting in unfolding of ET SSB [134].

The calibration curve was established by applying different concentrations of a standard complementary single stranded 30-mer 16S rDNA onto the capacitive sensor chip hosting the 30-mer capture 16S rDNA probe. The linearity response was obtained at log concentration ranging from  $10^{-12}$  to  $10^{-7}$  M, with a LOD of  $6.5 \times 10^{-13}$  M, and a slope of  $13.6 \text{ -nF cm}^{-2} \text{ M}^{-1}$ .

The infective dose of *E. coli* is 10 cells for *E. coli* 0157:H7 or 4 cells per 100 ml for *E. coli* (coliform standard) in water [135]. However, the developed capacitive DNA sensor could detect the concentration of target 44-mer 16S rDNA from the pre-treated *E. coli* genomic DNA that corresponds to 10 cells  $\text{mL}^{-1}$ . It is 10 times lower than that detected by the plate counting technique (Table 3).

Table 3: Comparison: Detection of *E. coli* cells at concentration range 1 to  $10^5$  cells  $\text{mL}^{-1}$  using plate counting method and capacitive DNA-sensor.

Applied no. of cells $\text{mL}^{-1}$	Plate counting (CFU $\text{mL}^{-1}$ )	DNA sensor (-nF $\text{cm}^{-2}$ )
$10^5$	$(9.5 \pm 0.5) \times 10^4$	$84 \pm 9$
$10^4$	$(7.8 \pm 0.3) \times 10^3$	$57 \pm 5$
$10^3$	$(8.8 \pm 0.2) \times 10^2$	$40 \pm 4$
$10^2$	$(9.2 \pm 0.2) \times 10^1$	$27 \pm 4$
$10^1$	ND	$21 \pm 3$
$10^0$	ND	$10 \pm 1^*$

\* Below Limit of Detection. ND = Not Detected

The capacitive DNA-sensor should in many aspects be regarded as more advantageous over plate counting as it could detect viable and dead cells, as well as free DNA in a complex sample. For many cases such as foodborne intoxication, the toxic-producing bacteria cells (e.g. *Clostridium botulinum* and *S. aureus*) [136] might already be dead when a food sample is collected for analysis. Yet, its DNA, one of the most stable biomolecules [137], is most likely available, thus the pathogen could be indirectly detected by using the capacitive DNA sensor. However, unlike the capacitive DNA-sensor, the plate counting technique can only detect viable and cultivable cells.

The developed capacitive DNA-sensor was highly specific for *E. coli* BL21 (DE3)16S rDNA over *L. reuteri* DSM 20016 16S rDNA when the hybridization temperature was changed from 30 to 40 °C while keeping 30 % formamide in the

working buffer (Fig. 4-3). Either, a sensor-chip utilized for the capacitive DNA-sensor is efficient of performing up to 20 samples.

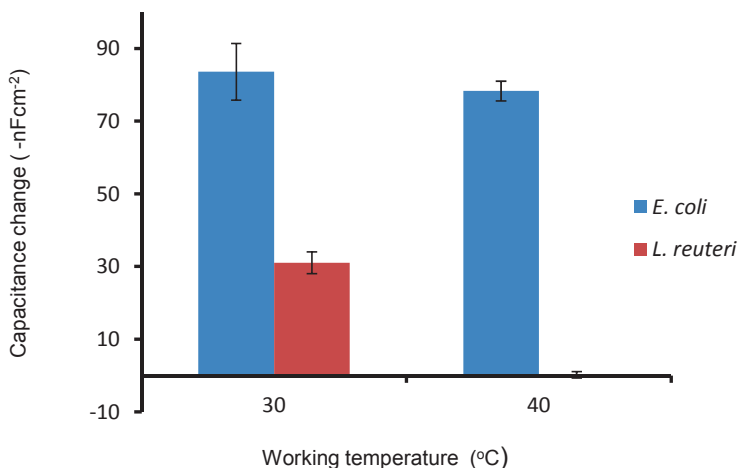


Fig. 4-3: Selectivity study without DNA amplification: capacitive responses from DNA-sensor chip immobilized with 30-mer *E. coli* 16S rDNA following injection of unamplified whole genomic DNA samples at concentration corresponding to  $10^5$  cell  $\text{ml}^{-1}$  of *E. coli* and *L. reuteri* samples. Working (hybridization) temperatures were 30 and 40 °C, and constant concentration of 30 % formamide in the mobile phase.

## 4.2 Detection of methicillin-resistant *S. aureus-mecA* gene

Antibiotic resistance is the proficiency of a microorganism to counterattack the effect of an antibiotic (e.g., methicillin) that was originally effective against it [138]. It is steadily rising among bacterial pathogens associated with both community and nosocomial infections [139,140] and thus, threatens the effective prevention and treatment of bacterial infections. Most of the patients infected with antibiotic resistant microorganisms (ARMs) do not respond to standard therapies. As such, ARMs pose serious problems to human health and well-being, including persistent sickness with a greater risk of complications or fatality, as well as high health-care costs. For instance, MRSA infection is estimated to be 64 % more lethal than the non-resistant form of the infection [138]. MRSA is the etiologic agent for a wide range of clinical illness, ranging from common skin infections such as impetigo and cellulitis to the more serious manifestations of necrotizing fasciitis, abscess, osteomyelitis, pneumonia and sepsis [141]. Moreover, today MRSA is ubiquitous in both the community and hospital settings [142-146]. MRSA is resistant to all  $\beta$ -lactam antibiotics such as methicillin, penicillin, cloxacillin, cephalosporins and carbapenems. The  $\beta$ -lactam

resistance of MRSA is determined by the production of a novel penicillin-binding protein 2a (PBP2a) that has a low binding affinity for  $\beta$ -lactam antibiotics [147].

#### 4.2.1 Genetic organization and mechanisms of *mecA* region

Fig. 4-4 represents genetic organisation in MRSA and MSSA staphylococcal chromosomal cassettes (SCCs). The genes are marked in the direction of transcription as arrows. Conserved regions in the SCC elements are shaded light blue and the genes are represented with the same colour. The genes with no similarity, as well as are not *mecA*, *mecR1* or *mecI* are represented with the white colour. The green arrow shows the direction of the sequence with the locations of *mecA*, *mecR1* and *mecI* gene.

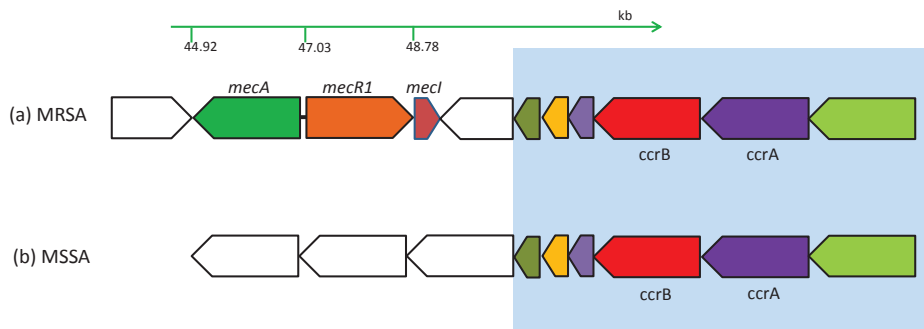


**Fig. 4-4:** Genetic organisation of *mecA* gene and comparison of SCC elements: (a) MRSA-SSC and (b) MSSA-SSC. The figure is redrawn with modification from Holden et al., [146].

The *mecA* gene encodes PBP2a and is located on a *SCC<sub>mec</sub>*, which is horizontally transferable among staphylococcal species [148]. The *SCC<sub>mec</sub>* in MRSA has two other essential regulatory genes, *mecI* and *mecR1* that encodes for a repressor- and an inducer protein that are active in the *mecA* expression [145]. The two regulatory genes are located upstream on the DNA-stretch from the *mecA* as represented in Fig. 4-4 (a).

The presence of *mecA*, *mecI* and *mecR1* genes in staphylococcal chromosomal cassette (SSC) makes a fundamental difference between MRSA and Methicillin susceptible *Staphylococcus aureus* (MSSA) (Fig. 4-4 (b)). The *mecA* gene is transcribed in the opposite direction (downstream) from its regulatory genes (*mecR1* and *mecI*), encoding for PBP2a, which displays a low affinity to  $\beta$ -lactams. PBP2a takes over the functions of high-binding-affinity proteins (PBPs) normally present and hence, permitting the cell to grow in the presence of  $\beta$ -lactams [149].

#### 4.2.2 Laboratory screening for MRSA

Laboratory screening for MRSA is a complex balance between speed of analysis, sensitivity, specificity and cost. The current methods for detecting MRSA can be

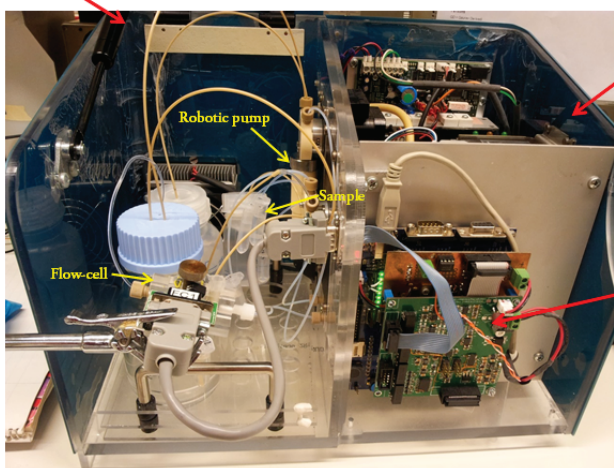
divided into culture based methods for phenotypic test, and molecular based methods for genotypic test [150,151]. The culture methods, including plate, broth and chromogenic media tests, measure the bacteriostatic or bacteriocidal effect of  $\beta$ -lactam antibiotics to *S. aureus* [150]. Such methods typically require long incubation periods up to 72 h, due to the slow growth of the *S. aureus* [152]. Molecular methods including microarray and polymerase chain reaction (PCR) techniques are widely used for the *mecA* gene determination. The PCR technique has been successfully utilized to detect the MRSA *mecA* gene of *S. aureus* isolated from municipal wastewater treatment plants [144] and from metro stations [146]. These molecular techniques are rapid and sensitive [153] but also rather expensive. Consequently, they are not appropriate for usage in developing countries at resource-limited settings. Therefore, more rapid and cheap diagnostic tools must be a priority for the clinical research. Hence, field-adopted assays of MRSA will allow patients with MRSA to be isolated and correct therapy can be initiated with minimal delay. This strategy will not only improve treatment outcomes, but will also reduce the risk of transmission of MRSA.

In **paper IV**, the capacitive DNA-sensor was used for detection of the *mecA* gene from the complex biological matrix (human saliva).

#### 4.2.3 Capacitive DNA-sensor for MRSA *mecA* gene

The detection of *mecA* gene was performed in an automated sequential-injection flow system (Fig. 4-5).

Robotic-pump, 3- and 9-port valves and flow-cell section



Degasser unit, robotic-pump and temperature controllers section

CapSense-Capacitance measurement unit

Fig. 4-5: CapSense™ Biosystem: automated sequential injection flow system used for detection of MRSA *mecA* gene (for more details about the CapSense™ Biosystem see section 2.4.2) .

The sensing platform is based on the immobilization of a single stranded 25-mer *mecA* gene onto an electropolymerized Pty layer created on the gold electrode

surface. The 25-mer *mecA* gene probe was designed from *S. aureus* subsp. aureus MRSA252 *mecA* gene sequence, retrieved from the National Centre for Biotechnology Information (NCBI) database [145]. The capacitive DNA-sensor was calibrated by injecting a complementary single stranded (ss) 25-mer *mecA* gene dissolved in potassium phosphate buffer (PB) *via* a sample loop to the system. The curve of capacitance change *vs.* applied concentrations is represented in Fig. 4-6.

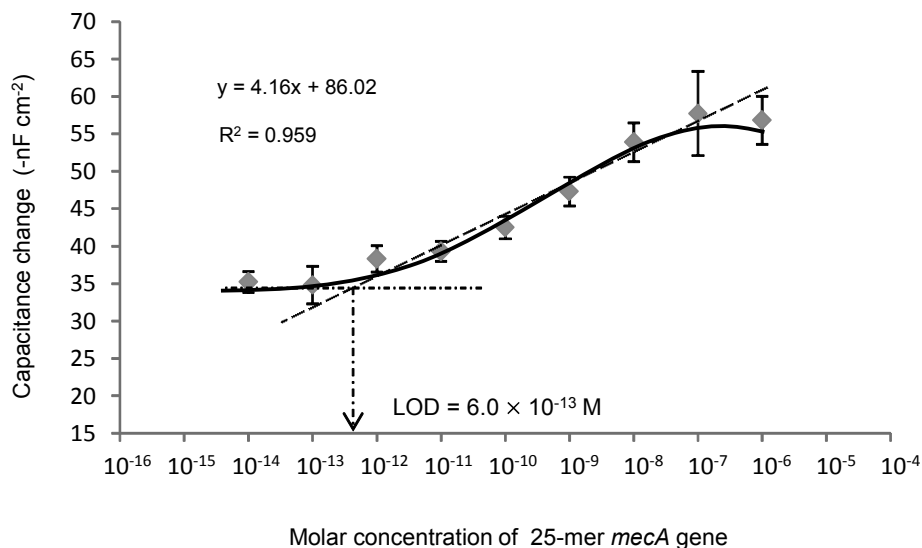


**Fig 4-6:** The capacitive DNA-sensor calibration curve, presenting LOD and linearity range for the detection of 25-mer *mecA* gene, prepared in PB.

The calibration curve obtained with the capacitive DNA-sensor showed a linear behaviour at concentration range of 0.001 to 100 nM, with a LOD of 0.6 pM. The LOD for the detection of MRSA obtained by the capacitive DNA-sensor was seventeen times lower than a recently reported electrochemical DNA sensing system based on the chronoamperometric detection of ferrocene-labeled probes that were conjugated to gold nanoparticles (AuNPs) [154]. Either, it was 20 times faster than a novel culture-based assay, Bactile Rapid MRSA test, which was used to detect ciprofloxacin-resistant bacteria with a total time assay of 5 h [151].

Moreover, the capacitive DNA-sensor showed a clear discrimination between the complementary target probe and single-base-mismatch, two-base-mismatch and twelve-base-mismatch *mecA* gene probes at their equimolar concentrations. The presence of single-base, two-base, and twelve-base mismatches in the *mecA* gene sequence decreased the signal amplitude by 13 %, 26 %, and 89 %, respectively, relative to the signal amplitude of complementary target probe. Reduction of the signal amplitude observed with different mismatches is a result of the base-pair



disruptions, and proving the ability of the sensor to discriminate between the complementary target probe and target probes possessing mismatches as well as for non-target DNA-material.

The developed capacitive DNA-sensor was subsequently applied for the detection of the *mecA* gene in complex matrices (in this work saliva was chosen). Human saliva was spiked with 25-mer *mecA* gene standards in final concentrations of 1000, 10, and 1.0 nmolL<sup>-1</sup>. They were then diluted by a factor of 10<sup>5</sup>, 10<sup>3</sup> and 10<sup>2</sup> in PB, respectively so as to attain the same *mecA* gene concentration in the final volume for analytical reasons and comparative ground. Also, the effect of the matrix on the capacitive DNA-sensor signal was determined by injecting different diluted un-spiked samples of saliva into the capacitive DNA-sensor.

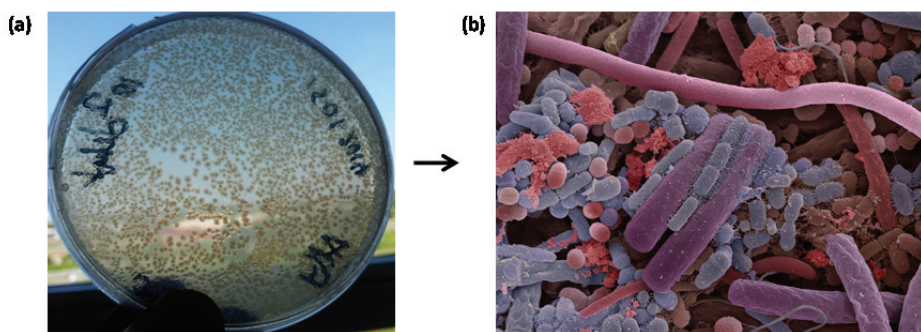


Fig. 4-7: Showing the complexity of the matrix. (a) Various bacteria grown from 100 times diluted human saliva (b) Human oral bacterial community: The oral cavity of human contains high number of various bacteria as shown in this electron micrograph. The image was reproduced with permission of the copyright owner (Steve Gschmeissner).

A non-specific signal was observed upon injection of non-spiked undiluted human saliva samples. However, the signal was observed to decrease with an increase in dilution factor. In fact, human saliva typically contains high number of various bacteria [5], thus the observed non-specific signal could be due to non-specific interaction between the hydrophobic-bacterial cell surfaces present in the human-saliva with hydrophobic-single-stranded capture probe on the electrode surface. Hence, in order to visualise the microbiological complexity of the human saliva, diluted non-spiked human saliva samples were cultured and results for 1.1 × 10<sup>2</sup> diluted sample are shown in Fig. 4-7.

The percentage (%) recovery was calculated from the average signal of the triplicate analyses of *mecA* gene in the human saliva, as shown in Eq. 13. Results were summarized and are presented in Table 4.

$$\% \text{ Recovery} = \frac{\Delta C_1 - \Delta C_2}{\Delta C_3} \times 100 \quad (13)$$

where  $\Delta C_1$  and  $\Delta C_2$  are the signal of the *mecA*-spiked saliva sample and non-spiked saliva sample at the same dilution factor, respectively.  $\Delta C_3$  is the signal of 0.01 nmol L<sup>-1</sup> *mecA* gene in 10 mM potassium phosphate buffer (pH 7.2), read-off from the calibration curve.

Table 4: Determination of the *mecA* gene in spiked saliva sample by the capacitive DNA-sensor

Sample dilution	Final concentration (nmol L <sup>-1</sup> )	Calculated concentration (nmol L <sup>-1</sup> )	% Recovery	% RSD (n = 3)
10 <sup>2</sup>	0.01	0.0071	71	9.0
10 <sup>3</sup>	0.01	0.0076	76	6.5
10 <sup>5</sup>	0.01	0.0095	95	3.5

The capacitive DNA-sensor showed a promising performance for the analysis of MRSA based on the *mecA* gene present in a complex biological matrix. The higher recovery and lower variation (% RSD) obtained in the highly diluted sample imply a reduced matrix effect due to the increased dilution (Table 4). However, further studies and more validation tests involving clinical samples are required for the capacitive DNA-sensor before it can be considered for clinical use.

## 5. Comparison: the developed capacitive DNA-sensor with other techniques for detection of bacteria

The full potential of the presented technology with regard to microbial detection will only be recognized when the sensitivity and speed of analysis can compete with the established techniques, the gold standards. A novel technology platform also needs to be cost-competitive compared to the current techniques. Hence, in this chapter the developed capacitive DNA-sensor is comprehensively compared with different techniques reported in the literature as summarized in Table 5.

**Table 5:** Comparison of the capacitive DNA-sensor with other reported techniques.

Technique	Analyte	LOD (Cells mL <sup>-1</sup> )	Time	Cost/test (US\$)	Reference
Chromogenic culture	<i>EHEC</i> cells	10 <sup>2</sup>	18-48 h	3	[155,156]
ELISA assay	<i>E. coli</i> O157:H7 cells	10 <sup>5</sup> -10 <sup>3</sup>	3 h	10-30	[157,158]
DNA-Microarray	<i>E. coli</i> O157:H7- <i>eaeA</i> gene	55	17 h	100-200	[159-161]
PCR	* <i>EHEC</i> O157- <i>HlyA</i> gene	10 <sup>0</sup>	2-3 h	50-100	[161,162]
CV-immunosensor	<i>E. coli</i> O157:H7 cells	6	1 h	≥ 1.2	[163]
QCM DNA-sensor	<i>E. coli</i> O157:H7- <i>eaeA</i> gene	10 <sup>3</sup> -10 <sup>2</sup>	2-4 h	≥ 6	[34,159,164,165]
SPR immunosensor	<i>E. coli</i> O157:H7 cells	10 <sup>2</sup>	15 min	≤ 16	[166,167]
Capacitive DNA-sensor	<i>E. coli</i> BL21(DE3) 16S rDNA	10 <sup>1</sup>	15 min	2-7	[pp. II]

\*Enterohemorrhagic *Escherichia coli* O157- *Haemolyticum A* gene

In Table 5 it can be observed that there is an imbalance between the speed of analysis, sensitivity and cost for the existing published techniques. For instance,

the chromogenic culture assay is cheaper and more sensitive [155,156] than the capacitive DNA-sensor. However, it is a laborious assay [155] and less selective [156] compared to the capacitive DNA-sensor. Additionally, for the chromogenic culture assay it takes up to two days to obtain the initial results, which in turn needs to be confirmed using other techniques such as biochemical and molecular techniques [156].

Compared to the reported ELISA techniques [157,158], the capacitive DNA-sensor is at least 100-fold more sensitive and 12 times faster. However, ELISA is much less expensive if few samples are to be analysed. The ELISA kit (with reagents) is available for US\$ 270-700 [158]. The ELISAs are typically performed in a 96-well plate, which can be used for 25 samples, one blank and 6 standards, in triplicate. However, if many samples are analysed, e.g. screening or routine analysis, the capacitive DNA-sensor will be significantly more cost-effective over time. The capacitive DNA-sensor (CapSenze™ Biosystem) is priced at US\$ 62,000, and it would require about US\$ 7 for sensor-chip and reagents to run a one first test, and down to US\$ 2 for the next 19 consecutive tests, with one sensor-chip capable of performing up to 20 analyses of un-amplified DNA samples.

For the CV-biosensor reported by Settingington and Alocilja [163], the detection of *E. coli* O157:H7 cells equivalent to 6 cells ml<sup>-1</sup> was performed in just 60 minutes. The specificity of the method was however not fully clarified. Since the technique relies on the inhibition of current response in CV due to binding of the target cells onto the immuno-functionalized electrode surface, everything else present in the sample that would result in a decrease in current response will also be registered as a positive signal. In addition, during the CV-biosensor measurements, the double-layer charging current ( $I_c$ ) is generated as the background current at the working electrode [100]. The generated  $I_c$  interferes with the measured redox-current, hence resulting in an inaccurate estimation of bacterial cells. Moreover, the pH and ionic strength of biofluids (e.g. blood, urine) can differ significantly, which adversely can affect the interaction of the antibody with target cells in the biofluidic sample [168]. This implies that this technique is better suited for screening purposes. Although, a sensor chip used in the CV-biosensor is 5 times cheaper (US\$ 1 per chip) than the one used in the capacitive DNA-sensor (US\$ 5 per chip), it is disposed of after a single use [163]. The sensor-chip used in the capacitive DNA-sensor technique can be used multiple times (up to 20 times), bringing the consumable costs down compared to the CV-biosensor.

Compared to the established microarray technology, the capacitive DNA-sensor is significantly faster (refer to Table 5). However, the DNA-microarray has the clear advantage of being adapted for multiplex analysis. More than 1,000 different genes can be analysed simultaneously by using the microarray technique [169]. Thus, it can be used to screen unknown pathogenesis-related genes, which for the

capacitive DNA-sensor would be impractical or even not possible. Moreover, introduction of an automated microarray [170] makes the procedure even easier. However, such automation comes with a rather high price; the microarray facility costs up to US\$ 1 million [160] that is 16 times more expensive than the CapSense™ Biosystem instrument (US\$ 62,000). Moreover, a typical basic experiment involving, e.g., 50 pairwise hybridizations in the microarray technique would cost between US\$ 5000 and US\$ 10,000 in reagents [160]. The capacitive DNA-sensor would require US\$ 5 for sensor-chip and about US\$ 40 in reagents to analyse more than 20 samples. Even though, both techniques require sample pre-treatment steps prior to analysis, the microarray involves more steps, including probes labelling, which is an exceedingly time- and labour-intensive procedure [169].

The capacitive DNA-sensor is 10-fold less sensitive than the monoplex PCR [162] as shown in Table 5. The detection of bacteria with extreme sensitivity as shown in PCR is important since some bacteria manifest infectivity at extremely low levels. More recently, the use of multiplex PCR has facilitated the detection of more than one type of bacteria at once [171]. However, sensitivity of multiplex PCR is comparable to the capacitive DNA-sensor. Fan et al., [162] detected *EHEC* down to 10 cells ml<sup>-1</sup> by using multiplex PCR. Yet, the applicability of the PCR technique is somewhat hindered by the cost associated with operation and the PCR-system. For instance, a PCR-machine (thermocycler) only costs between US\$ 5000 and US\$ 20,000 [172], and operational cost is about US\$ 100 per assay, rendering it inaccessible for many regular users like primary health centre and school laboratories. On the other hand, when the PCR-machine is compared to the CapSense™ Biosystem instrument, the latter is more expensive by at least 3 times than PCR-machine, however its operational cost *per* test is at least 10 times less costly than PCR assay. Yet, unlike CapSense™ Biosystem, PCR-instrumentation usually includes various separate, large and complex units, which could make it more expensive and not suitable for field adopted measurements.

The developed capacitive DNA-sensor showed to be at least 10-fold more sensitive than the reported QCM [39,163,164] and SPR [166,173] techniques. Oh *et al.*, have reported to develop an SPR immunosensor that could detect as low as 10<sup>2</sup> cells mL<sup>-1</sup> of whole target cells without sample pre-treatment steps [173]. That makes SPR a simpler and less time demanding technique compared to the capacitive DNA-sensor. However, the SPR-instrument is almost twice as expensive as the CapSense™ Biosystem instrument. It is priced at US\$ 112,000. The sensor-chip employed for SPR analysis costs about US\$ 200, which is capable of perming up to 100 samples [160]. The QCM-instrument is the cheapest of these three techniques, averaging about US\$ 13,000 and its sensing-chip costs approximately US\$ 25, allowing analysis up for 25 samples [160]; however, the QCM is several orders of magnitude less sensitive compared to the

capacitive sensor. In addition, the assay takes several hours to reach the result as shown in Table 5.

## 6. Challenges and limitations in capacitive DNA-sensor development

- Application of the developed capacitive DNA-sensor to a real biological sample is limited to the sample pre-treatment steps: cell lysis, purification to get rid of RNAs and proteins, and generation of ssDNA. Therefore its sensitivity and selectivity are partly dependent on the sensitivity and efficiency of the methods used for pre-treatment steps. Integration of all pretreatment steps to reduce sample handlings and entire time to a few minutes has so far been unreachable.
- The capacitive DNA-sensor response signal is limited to short oligos of less than 50-mer. Therefore designing a capture probe for recognition of such short specific oligo is a big challenge.
- There are limitations with using the developed capacitive DNA-sensor in real environmental samples: i) DNA hybridization capacity is in part dependent on assay conditions, e.g. pH and ionic strength ii) capacitance measurement can be interfered by the electroactive molecules from the complex matrix, which interact with the electrode surface.
- Specificity of the developed capacitive DNA-sensor is temperature-dependent, hence posing a challenge when it comes to construction of a hand-held version.

### 6.1 Conclusion and future perspectives

The gap between functional biosensor models that operates in research laboratories and the concept of commercial biosensors that can be adopted in real-world environments continues to be sizeable. However in recent years, the growth within the field of biosensor development is phenomenal with emerging applications in a wide range of disciplines, including medical analysis, food, defence and the environment. Yet, most of these applications are at a phase where it is not obvious which bioreceptor would be most suitable. However, the field will keep on evolving in different directions as technologies such as capacitive DNA-based sensors (**papers I, II, III, and IV**) and molecular imprinted polymers (MIPs) [174] become more established.

The results from this thesis work verify a promising ultrasensitive, automated flow-based and portable gene-sensor, which was developed by combining the inherent stability and uniqueness of the DNA molecule with a low-cost, sensitive, portable and simple detection platform (i.e., capacitive sensing). The developed PCR-free biosensor has proved the possibility for powerful detection of foodborne pathogens in diagnostic situations as well as multidrug-resistant bacteria such as MRSA in the near future. Rapid detection of foodborne outbreak is critical since

immediate intervention can be made before many people are infected. Similarly, early detection of MRSA will lead to earlier isolation of infected patients, and hence reducing the risk of MRSA spreading.

Further development and optimization are however required to explore the performance of the developed capacitive DNA-sensor in real clinical samples such as tissue culture media or plasma, and in the presence of other potential interferents. Where, various issues (challenges) with regard to the capacitive detection system should be very well addressed. Among these are an increased selectivity and higher sensitivity. The latter can be achieved by combining the developed capacitive DNA-sensor with nanotechnology and more specifically the use of nanoparticles such as gold-nanoparticles. Nanoparticles have the inherent property of increasing the surface area for immobilization of the capture probe, as well as improving the surface chemistry. There is also a need to configure a detection scheme from a single to multiplex detection mode for the simultaneous detection of different target DNA molecules. Such a device will remarkably reduce 'turnaround time' as it would have the ability to assay large number of samples in a couple of minutes, and hence would be practically possible to screen the unknown gene sequence related to pathogenicity. In addition, a handheld battery-operated diagnostic tool is of great interest especially in developing countries, as most populations living in rural/remote areas do not have access to relevant medical- and social services.

In all, this thesis work lays the groundwork for further development of a new 'handheld' diagnostic platform for a rapid, selective and sensitive detection of microorganisms from food/environmental and clinical samples.



## 7. Acknowledgements

*First and foremost, I thank Allah (S.W), the Almighty, the most Beneficent, and the most Merciful, for having made everything possible by giving me strength, knowledge and courage to do this work.*

This thesis terminates my four-year journey to earn Ph.D. degree at Lund University, department of Biotechnology, which commenced on February 14, 2011. Since then my experience at the department of Biotechnology has been nothing short of amazing. I have been given unique opportunities...and taken advantage of them. These include instructing practical classes in Bioanalysis course and giving a lecture in Electrochemical Biosensors to MSc students in 2011 and 2014, respectively.

The work presented in this thesis is the outcome of great ideas, hard-work, enthusiasm, guidance and inspiration of dozens of people, who I wish to acknowledge.

Special thanks to Professor emeritus Bo Mattiasson; first he welcomed me as master's student, introducing to the world of Bioseparation and Bioanalysis, and in later time, accepted me back for the PhD studies and giving me opportunity to delve deeper into Bioanalysis field, specifically-Biosensing techniques. He has always been providing me with his guidance and support. His great ideas, knowledge and experiences have been the fuel for this work.

Lot of thanks to Associate Professor Martin Hedström. His superior scientific guidance, diligence and invaluable knowledge in biotechnology have made this work to move swiftly and successfully.

I am extremely indebt to Dr. Eva StåhlWernersson who had patiently taken pains to peruse carefully and review the early drafts of manuscripts. Her experience and great knowledge in microbiology, as well as limitless devotion to research have greatly made this work possible.

I am much thankful to Associate Professor Gashaw Mamo. His comprehensive and intimate knowledge in Biotechnology made him to be a potential co-author in **paper II**. He is always personable, easy to communicate with and always ready to share his knowledge and skill.

Thanks to Professor Tommy Nylander and Dr. Maria Wadsäter from department of physical chemistry, Lund University. The AFM work was only possible with the assistance and support from them.

I am much thankful to Professor Rajni Hatti-Kaul, the ex-head of the department of Biotechnology, without her support I would not have undertaken this work. She accepted me as a Ph.D. student in her department and 'at one time' acted as my main supervisor.

My deep and strong appreciation goes to the past and present members of Bioanalysis/Biosensor group; Kosin, Dmitri, Alvaro, Lesedi, Jit, Gaurav, Kumar and Muhammad for your sisterly and brotherly atmosphere.

Special thanks to all former and present members of Biotechnology department, for creating high quality social-academic atmosphere. I am particularly grateful to the head of department, Professor Olle Holst; the deputy head of department, Maria Anderson (Mia); as well as past and present secretaries Siv and Emma, respectively, for their administrative and logistical supports.

To my lovely wife Rahma, and our princess Amrat, thanks for the love, understanding, support, incessant encouragement, prayers and sacrifices. You are my truly inspiration and my daily motivation.

In a very special way, lot of thanks to my mother (Salma) and father (Mr. Mahadhy), for all the support and encouragement that they have given me all the times. My heartfelt thanks go to my sisters, brothers, and the rest of the family, as well as comrades and friends. You have made this journey so enriching.

Last but most important, I am grateful to acknowledge, this PhD thesis work was financially supported by World Bank Project implemented at University of Dar es Salaam, Tanzania.

## 8. References

1. Karu, A., Belk, E., 1982. Induction of *E. coli* recA protein via recBC and alternate pathways: Quantitation by enzyme-linked immunosorbent assay (ELISA). *Molecular and General Genetics*. 185, 275-282.
2. Findlay, J., Smith, W., Lee, J., Nordblom, G., Das, I., de-Silva, B., Khan, M., Bowsher, R., 2000. Validation of immunoassays for bioanalysis: a pharmaceutical industry perspective, *Journal of Pharmaceutical and Biomedical Analysis* 21, 1249-1273.
3. Fung, D.Y., 2002. Rapid methods and automation in microbiology. *Comprehensive Reviews in Food Science and Food Safety*. 1, 3-22.
4. Janda, J.M., Abbott, S.L., 2002. Bacterial identification for publication: when is enough enough? *Clinical Microbiology*. 40, 1891-1887.
5. Madigan, M.T., Martinko, M.J., Stahl, D.A., Clark, D.P., 2012. *Brock, Biology of microorganisms*. Pearson Education, Inc, San Francisco.
6. Weenk, G.H., 1992. Microbiological assessment of culture media - comparison and statistical evaluation of methods. *International Journal of Food Microbiology*. 17, 159-181.
7. Rosselló-Mora, R., Amann, R., 2001. The species concept for prokaryotes. *Federation of European Microbiological Societies Microbiology Reviews*. 25, 39-67.
8. Naravaneni, R., Jamil, K., 2005. Rapid detection of food-borne pathogens by using molecular techniques. *Journal of Medical Microbiology*. 54, 51-54.
9. Ye, Y.K., Ju, H.X., 2003. DNA electrochemical behaviours, recognition and sensing by combining with PCR technique. *Sensors*. 3, 128-145.
10. Elnifro, E.M., Ashshi, A.M., Cooper, R.J., Klapper, P.E., 2000. Multiplex PCR: optimization and application in diagnostic virology. *Clinical Microbiology Reviews*. 13, 559-570.
11. Radstrom, P., Knutsson, R., Wolffs, P., Lovenklev, M., Lofstrom, C., 2004. Pre-PCR processing - Strategies to generate PCR-compatible samples. *Molecular Biotechnology*. 26,133-146.
12. Smith, C.J., Osborn, A.M., 2009. Advantages and limitations of quantitative PCR (QPCR)-based approaches in microbial ecology. *Federation of European Microbiological Societies Microbiology Ecology*. 67, 6-20.
13. Maity, B., Trivedi, R., Kashyap, V.K., 2008. Development of a microarray based on 16S-23S rDNA probe hybridization for rapid diagnosis of human pathogenic bacteria. *Indian Journal of Biotechnology*. 5, 448-455.
14. Vora, G.J., Meador, C. E., Stenger, D. A., Andreadis, J. D., 2004. Nucleic acid amplification strategies for DNA microarray-based pathogen detection. *Applied and Environmental Microbiology*. 70, 3047-3054.
15. Zhou, J., 2003. Microarrays for bacterial detection and microbial community analysis. *Current Opinion in Microbiology*. 6, 288-294.
16. Jin, H-Y., Tao, K-H., Li, Y-X., Li, F-Q., Li, S-Q., 2005. Microarray analysis of *Escherichia coli* O157: H7. *World Journal of Gastroenterology*. 11, 5811-5815.
17. Wieser, A., Schneider, L., Jung, J., Schubert, S., 2012. MALDI-TOF MS in microbiological diagnostics-identification of microorganisms and beyond (mini review). *Applied Microbiology and Biotechnology*. 93, 965-974.
18. Chingin, K., Liang, J., Chen, H., 2014. Direct analysis of in vitro grown microorganisms and mammalian cells by ambient mass spectrometry. *Royal Society of Chemistry Advances*. 4, 5768-5781.
19. Seng, P., Drancourt, M., Gouriet, F., Scola, B., Fournier, P-E., Rolain, J.M., Raoult, D., 2009. Ongoing Revolution in Bacteriology: routine identification of bacteria by matrix-assisted laser desorption ionization time-of-flight mass spectrometry. *Clinical Infectious Diseases*. 49, 543-551.

20. Turner, A.P., 2013. Biosensors: sense and sensibility. *Chemical Society Reviews*. 42, 3184-3196.
21. Palchetti, I., Mascini, M., 2009. Biosensor technology: a brief history. In: 14th Italian conference on sensors and microsystems, AISEM 2009, February 24, 2009 - February 26, 2009, Pavia, Italy, 2010. *Lecture notes in electrical engineering*. Springer Verlag. pp 15-23.
22. Clark, L.C., Lyons, C., 1962. Electrode systems for continuous monitoring in cardiovascular surgery. *Annals of the New York Academy of Sciences*. 102, 29-45.
23. Thévenot, D.R., Toth, K., Durst, R.A., Wilson, G.S., 2001. Electrochemical biosensors: recommended definitions and classification. *Biosensors and Bioelectronics*. 16, 121-131.
24. Newman, J.D., Turner, A.P.F., 2005. Home blood glucose biosensors: a commercial perspective. *Biosensors and Bioelectronics*. 20, 2435-2453.
25. Teeparuksapun, K., Hedstrom, M., Wong, E.Y., Tang, S.X., Hewlett, I.K., Mattiasson, B., 2010. Ultrasensitive detection of HIV-1 p24 antigen using nanofunctionalized surfaces in a capacitive immunosensor. *Analytical Chemistry*. 82, 8406-8411.
26. Patel, M.K., Solanki, P.R., Kumar, A., Khare, S., Gupta, S., Malhotra, B.D., 2010. Electrochemical DNA sensor for *Neisseria meningitidis* detection. *Biosensors and Bioelectronics*. 25, 2586-2591.
27. Arora, K., Prabhakar, N., Chand, S., Malhotra, B.D., 2007. *Escherichia coli* genosensor based on polyaniline. *Analytical Chemistry*. 79, 6152-6158.
28. Nica, A., Mascini, M., Ciucu, A., 2004. DNA-based biosensor for detection of genetically-modified organisms. *Chimie Annual*. 23, 84-94.
29. Mulchandani, A., Mulchandani, P., Kaneva, I., Chen, W., 1998. Biosensor for direct determination of organophosphate nerve agents using recombinant *Escherichia coli* with surface-expressed organophosphorus hydrolase. 1. Potentiometric microbial electrode. *Analytical chemistry*. 70, 4140-4145.
30. Mascini, M., 2001. Affinity electrochemical biosensors for pollution control. *Pure Applied Chemistry*. 73, 23-30.
31. Brooks, S.L., Ashby, R.E., Turner, A.P.F., Calder, M.R., Clarke, D.J., 1987. Development of an on-line glucose sensor for fermentation monitoring. *Biosensors*. 3, 45-56.
32. Kole, M.M., Ward, D., Gerson, D.F., 1986. Simultaneous control of ammonium and glucose concentrations in *Escherichia coli* fermentations. *Journal of Fermentation Technology*. 64, 233-238.
33. Redshaw, N., Dickson, S.J., Ambrose, V., Horswell, J., 2007. A preliminary investigation into the use of biosensors to screen stomach contents for selected poisons and drugs. *Forensic Science International*. 172, 106-111.
34. Petrosova, A., Konry T., Cosnier, S., Trakht, I., Lutwama, J., Rwaguma, E., Chepurnov, A., Mühlberger, E., Lobel, L., Marks, R.S., 2007. Development of a highly sensitive, field operable biosensor for serological studies of Ebola virus in central Africa. *Sensors and Actuators B-Chemical*. 122, 578-586.
35. Narayanaswamy, R., 2006. Optical chemical sensors and biosensors for food safety and security applications. *Acta Biologica Szegediensis*. 50, 105-108.
36. Eggins, B.R., 1996. *Biosensors: an introduction*. Wiley, Chichester. pp 16-19.
37. Chambers, J.P., Arulanandam, B.P., Matta, L.L., Weis, A., Valdes, J.J., 2008. Biosensor recognition elements. Texas univ at san antonio dept of biology.
38. Rijal, K., Mutharasan, R., 2013. A method for DNA-based detection of *E. coli* O157:H7 in a proteinous background using piezoelectric-excited cantilever sensors. *Analyst*. 138, 2943-2950.
39. Wang, L.J., Wei, Q.S., Wu, C.S., Hu, Z.Y., Ji, J., Wang, P., 2008. The *Escherichia coli* O157 : H7 DNA detection on a gold nanoparticle-enhanced piezoelectric biosensor. *Chinese Science Bulletin*. 53,1175-1184.

40. Bharadwaj, R., Sai, V.V.R., Thakare, K., Dhawangale, A., Kundu, T., Titus, S., Verma, P.K., Mukherji, S., 2011. Evanescent wave absorbance based fiber optic biosensor for label-free detection of *E. coli* at 280 nm wavelength. *Biosensors and Bioelectronics*. 26, 3367-3370.
41. Binkowski, B.F., Butler, B.L., Stecha, P.F., Eggers, C.T., Otto, P., Zimmerman, K., Vidugiris, G., Wood, M.G., Encell, L.P., Fan, F., Wood, K.V., 2011. A luminescent biosensor with increased dynamic range for intracellular cAMP. *American Chemical Society Chemical Biology*. 6, 1193-1197.
42. Tanious, F.A., Nguyen, B., Wilson, W.D. Biosensor-surface plasmon resonance methods for quantitative analysis of biomolecular interactions. In: John, J.C., Detrich, W.H., 2008. *Methods in cell biology*, 3rd edition. Academic Press, New York. pp 53-77.
43. Zhang, Y., Tadigadapa, S., 2004. Calorimetric biosensors with integrated microfluidic channels. *Biosensors and Bioelectronics*. 19, 1733-1743.
44. Jiang, D.N., Liu, F., Liu, C., Liu, L.L., Pu, X.Y., 2013. An electrochemical sensor based on allosteric molecular beacons for DNA detection of *Escherichia coli* O157:H7. *International Journal of Electrochemical Science*. 8, 9390-9398.
45. Palchetti, I., Mascini, M. Amperometric biosensor for pathogenic bacteria detection. In: Zourob, M., Elwary, S., Turner, A., 2008. *Principles of bacterial detection: Biosensors, recognition receptors and microsystems*. Springer, New York. pp 299-312.
46. Muhammad-Tahir, Z., Alocilja, E.C., 2003. Fabrication of a disposable biosensor for *Escherichia coli* O157:H7 detection. *The Institute of Electrical and Electronics Engineers Sensors Journal*. 3, 345-351.
47. Hernández, R., Vallés, C., Benito, A.M., Maser, W.K., Rius, F., Riu, J., 2014. Graphene-based potentiometric biosensor for the immediate detection of living bacteria. *Biosensors and Bioelectronics*. 54, 553-557.
48. Zelada-Guillen, G.A., Bhosale, S.V., Riu, J., Rius, F.X., 2010. Real-time potentiometric detection of bacteria in complex samples. *Analytical Chemistry*. 82, 9254-9260.
49. Limbut, W., Kanatharana, P., Mattiasson, B., Asawatreratanakul, P., Thavarungkul, P., 2006. A comparative study of capacitive immunosensors based on self-assembled monolayers formed from thiourea, thioctic acid, and 3-mercaptopropionic acid. *Biosensors and Bioelectronics*. 22, 233-240.
50. Berggren, C., Stålhandske, P., Brundell, J., Johansson, G., 1999. A feasibility study of a capacitive biosensor for direct detection of DNA hybridization. *Electroanalysis*. 11, 156-160.
51. Lebogang, L., Hedström, M., Mattiasson, B., 2014. Development of a real-time capacitive biosensor for cyclic cyanotoxic peptides based on Adda-specific antibodies. *Analytica Chimica Acta*. 826, 69-76.
52. Drouvalakis, K.A., Bangsaruntip, S., Hueber, W., Kozar, L.G., Utz, P.J., Dai, H., 2008. Peptide-coated nanotube-based biosensor for the detection of disease-specific autoantibodies in human serum. *Biosensors and Bioelectronics*. 23, 1413-1421.
53. Mulchandani, A., Pan, S., Chen, W., 1999. Fiber-optic enzyme biosensor for direct determination of organophosphate nerve agents. *Biotechnology Progress*. 15, 130-134.
54. Wang, W., Chen, C., Qian, M., Zhao, X.S., 2008. Aptamer biosensor for protein detection using gold nanoparticles. *Analytical Biochemistry*. 373, 213-219.
55. Schneider, E., Clark, D.S., 2013. Cytochrome P450 (CYP) enzymes and the development of CYP biosensors. *Biosensors and Bioelectronics*. 39, 1-13.
56. Uslu, B., Ozkan, S.A., 2007. Solid electrodes in *Journal of Electroanalytical Chemistry: present applications and prospects for high throughput screening*

- of drug compounds. *Combinatorial Chemistry and High Throughput Screening*. 10, 495-513.
57. Chen, D., Li, J., 2006. Interfacial design and functionization on metal electrodes through self-assembled monolayers. *Surface Science Reports*. 61, 445-463.
  58. Sankoh, S., Samanman, S., Thipmanee, O., Numnuam, A., Limbut, W., Kanatharana, P., Vilaivan, T., Thavarungkul, P., 2013. A comparative study of a label-free DNA capacitive sensor using a pyrrolidinyll peptide nucleic acid probe immobilized through polyphenylenediamine and polytyramine non-conducting polymers. *Sensors and Actuators B- Chemical*. 177, 543-554.
  59. Ates, M., 2013. A review study of (bio)sensor systems based on conducting polymers. *Materials Science and Engineering C-Materials for Biological Applications*. 33, 1853-1859.
  60. Malhotra, B.D., Chaubey, A., Singh, S.P., 2006. Prospects of conducting polymers in biosensors. *Analytica Chimica Acta*. 578, 59-74.
  61. Kros, A., Sommerdijk, N.A.J.M., Nolte, R.J.M., 2005. Poly(pyrrole) versus poly (3,4-ethylenedioxythiophene): implications for biosensor applications. *Sensors and Actuators B-Chemical*. 106, 289-295.
  62. Peng, H., Soeller, C., Vigar, N., Kilmartin, P.A., Cannell, M.B., Bowmaker, G.A., Cooney, R.P., Travas-Sejdic, J., 2005. Label-free electrochemical DNA sensor based on functionalised conducting copolymer. *Biosensors and Bioelectronics*. 20, 1821-1828.
  63. Labib, M., Hedstrom, M., Amin, M., Mattiasson, B., 2010. A novel competitive capacitive glucose biosensor based on concanavalin A-labeled nanogold colloids assembled on a polytyramine-modified gold electrode. *Analytica Chimica Acta*. 659, 194-200.
  64. Labib, M., Hedstrom, M., Amin, M., Mattiasson, B., 2009. A capacitive immunosensor for detection of cholera toxin. *Analytica Chimica Acta*. 634, 255-261.
  65. Teeparuksapun, K., Hedstrom, M., Kanatharana, P., Thavarungkul, P., Mattiasson, B., 2012. Capacitive immunosensor for the detection of host cell proteins. *Journal of Biotechnology*. 157, 207-213.
  66. Zhao, Y.D., Pang, D.W., Hu, S., Wang, Z.L., Cheng, J.K., Dai, H.P., 1999. DNA-modified electrodes; part 4: optimization of covalent immobilization of DNA on self-assembled monolayers. *Talanta*. 49, 751-756.
  67. Campuzano, S., Pedrero, M., Montemayor, C., Fatas, E., Pingarron, J.M., 2006. Characterization of alkanethiol-self-assembled monolayers-modified gold electrodes by electrochemical impedance spectroscopy. *Journal of Electroanalytical Chemistry*. 586, 112-121.
  68. Fu, Y.Z., Yuan, R., Xu, L., Chai, Y.Q., Zhong, X., Tang, D.P., 2005. Indicator free DNA hybridization detection via EIS based on self-assembled gold nanoparticles and bilayer two-dimensional 3-mercaptopropyltrimethoxysilane onto a gold substrate. *Biochemical Engineering Journal*. 23, 37-44.
  69. Piwonski, I., Grobelny, J., Cichomski, M., Celichowski, G., Rogowski, J., 2005. Investigation of 3-mercaptopropyltrimethoxysilane self-assembled monolayers on Au(111) surface. *Applied Surface Science*. 242, 147-153.
  70. Choi, J.W., Park, K.S., Lee, W.C., Oh, B.K., Chun, B.S., Paek, S.H., 2004. Regulation of anti-LDL immobilization on self-assembled protein G layer using CHAPS and its application to immunosensor. *Materials Science and Engineering C-Biomimetic and Supramolecular Systems*. 24, 241-245.
  71. Blasini, D.R., Tremont, R.J., Batina, N., Gonzalez, I., Cabrera, C.R., 2003. Self-assembly of (3-mercaptopropyl)trimethoxysilane on iodine coated gold electrodes. *Journal of Electroanalytical Chemistry*. 540, 45-52.



72. Park, S., Weaver, M.J., 2002. A versatile surface modification scheme for attaching metal nanoparticles onto gold: characterization by electrochemical infrared spectroscopy. *Journal of Physical Chemistry B*. 106, 8667-8670.
73. Erlandsson, D., Teepruksapun, K., Mattiasson, B., Hedstrom, M., 2014. Automated flow-injection immunosensor based on current pulse capacitive measurements. *Sensors and Actuators B-Chemical*. 190, 295-304.
74. Lebogang, L., Mattiasson, B., Hedström, M., 2014. Capacitive sensing of microcystin variants of *Microcystis aeruginosa* using a gold immunoelectrode modified with antibodies, gold nanoparticles and polytyramine. *Microchimica Acta*. 1-9.
75. Tran, L.D., Piro, B.T., Pham, M.C., Ledoan, T., Angiari, C., Dao, L.H., Teston, F., 2003. A polytyramine film for covalent immobilization of oligonucleotides and hybridization. *Synthetic Metals*. 139, 251-262.
76. Nath, S., Ghosh, S.K., Kundu, S., Praharaj, S., Panigrahi, S., Pal, T., 2006. Is gold really softer than silver? HSAB principle revisited. *Journal of Nanoparticle Research*. 8, 111-116.
77. Vericat, C., Vela, M., Benitez, G., Carro, P., Salvarezza, R., 2010. Self-assembled monolayers of thiols and dithiols on gold: new challenges for a well-known system. *Chemical Society Reviews*. 39, 1805-1834.
78. Chaki, N.K., Vijayamohan, K., 2002. Self-assembled monolayers as a tunable platform for biosensor applications. *Biosensors and Bioelectronics*. 17, 1-12.
79. Cohen, B., 1965. *The biological role of the nucleic acids*. Edward Arnold, London.
80. Tenreiro, A., Cordas, C.M., Abrantes, L.M., 2003. Oligonucleotide immobilisation on Polytyramine-Modified Electrodes Suitable for Electrochemical DNA Biosensors. *Portugaliae Electrochimica Acta*. 21, 361-370.
81. Diao, P., Guo, M., Jiang, D., Jia, Z., Cui, X., Gu, D., Tong, R., Zhong, B., 2000. Fractional coverage of defects in self-assembled thiol monolayers on gold. *Journal of Electroanalytical Chemistry*. 480, 59-63.
82. Loyprasert, S., Hedström, M., Thavarungkul, P., Kanatharana, P., Mattiasson, B., 2010. Sub-attomolar detection of cholera toxin using a label-free capacitive immunosensor. *Biosensors and Bioelectronics*. 25, 1977-1983.
83. Tenreiro, A., Cordas, C., Abrantes, L., 2003. Oligonucleotide immobilisation on polytyramine-modified electrodes suitable for electrochemical DNA biosensors. *Portugaliae Electrochimica Acta*. 21, 361-370.
84. Losic, D., Cole, M., Thissen, H., Voelcker, N.H., 2005. Ultrathin polytyramine films by electropolymerisation on highly doped p-type silicon electrodes. *Surface Science*, 584, 245-257.
85. Zhu, N., Gao, H., Gu, Y., Xu, Q., He, P., Fang, Y., 2009. PAMAM dendrimer-enhanced DNA biosensors based on electrochemical impedance spectroscopy. *Analyst*. 134, 860-866.
86. Xia, B., Xiao, S-J., Guo, D-J., Wang, J., Chao, J., Liu, H-B., Pei, J., Chen, Y-Q., Tang, Y-C., Liu, J-N., 2006. Biofunctionalisation of porous silicon (PS) surfaces by using homobifunctional cross-linkers. *Journal of Materials Chemistry*. 16, 570-578.
87. Binnig, G., Quate, C.F., Gerber, C., 1986. Atomic force microscope. *Physical Review Letters*. 56, 930-933.
88. Meyer, E., 1992. Atomic force microscopy. *Progress in Surface Science*. 41, 3-49.
89. Braga, P., Ricci, D. Atomic force microscopy. In: Gillespie, S., 2001. *Antibiotic resistance, methods in molecular medicine*. Humana Press, New York. pp 199-207.

90. Raposo, M.F., Ribeiro, P. A. A Guide for Atomic Force microscopy analysis of soft-condensed matter In: Méndez-Vilas A.D., 2007. Modern research and educational topics in microscopy. Formatex, Badajoz. pp 758-769.
91. Vielstich, W., 2010. Cyclic voltammetry. John Wiley & Sons, Ltd, New Jersey.
92. Chung, T.D., Jeong, R-A., Kang, S.K., Kim, H.C., 2001. Reproducible fabrication of miniaturized glucose sensors: preparation of sensing membranes for continuous monitoring. *Biosensors and Bioelectronics*. 16, 1079-1087.
93. Sabatani, E., Rubinstein, I., Maoz, R., Sagiv, J., 1987. Organized self-assembling monolayers on electrodes .1. octadecyl derivatives on gold. *Journal of Electroanalytical Chemistry*. 219, 365-371.
94. Yuqing, M., Jianrong, C., Xiaohua, W., 2004. Using electropolymerized non-conducting polymers to develop enzyme amperometric biosensors. *Trends in Biotechnology*. 22, 227-231.
95. Zhou, L., Shang, F., Pravda, M., Glennon, J.D., Luong, J.H., 2009. Selective detection of dopamine using glassy carbon electrode modified by a combined electropolymerized permselective film of polytyramine and polypyrrole-1-propionic acid. *Electroanalysis*. 21, 797-803.
96. Rivera-Gandia, J., Cabrera, C.R., 2007. Self-assembled monolayers of 6-mercapto-1-hexanol and mercapto-n-hexyl-poly(dT) 18-fluorescein on polycrystalline gold surfaces: an electrochemical impedance spectroscopy study. *Journal of Electroanalytical Chemistry*. 605, 145-150.
97. Ladik, A.V., Geiger, F.M., Walter, S.R., 2001. Immobilization of DNA onto gold and dehybridization of Surface-bound DNA on glass. *Nanoscope*. 7, 23.
98. Gebbert, A., Alvarez-Icaza, M., Stoecklein, W., Schmid, R.D., 1992. Real-time monitoring of immunochemical interactions with a tantalum capacitance flow-through cell. *Analytical Chemistry*. 64, 997-1003.
99. Yoshida, A., Imoto, K., Yoneda, H., Nishimo, A., 1992. An electric double-layer capacitor with high capacitance and low resistance. *Components, Hybrids, and Manufacturing Technology*. The Institute of Electrical and Electronics Engineers Transactions. 15, 133-138.
100. Bard, A.J., Faulkner, L.R., 2001. *Electrochemical Methods: fundamentals and applications*, 2nd edition. John Willey and Sons, Inc., New York
101. Gouy, M., 1910. Sur la constitution de la charge électrique a la surface d'un électrolyte. *Journal of Theoretical and Applied Physics*. 9, 457-468.
102. Chapman, D.L., 1913. A contribution to the theory of electrocapillarity. *The London, Edinburgh, and Dublin Philosophical Magazine and Journal of Science*. 25, 475-481.
103. Stern, O., 1924. The theory of the electrolytic double-layer. *Zeit Elektrochemical*. 30, 508-516.
104. Grahame, D.C., 1947. The electrical double layer and the theory of electrocapillarity. *Chemical Reviews*. 41, 441-501.
105. McNeil, C.J., Athey, D., Ball, M., Ho, W.O., Krause, S., Armstrong, R.D., Des-Wright, J., Rawson, K., 1995. Electrochemical sensors based on impedance measurement of enzyme-catalyzed polymer dissolution: theory and applications. *Analytical Chemistry*. 67, 3928-3935.
106. Ding, S-J., Chang, B-W., Wu, C-C., Lai M-F., Chang, H-C., 2005. Electrochemical evaluation of avidin-biotin interaction on self-assembled gold electrodes. *Electrochimica Acta*. 50, 3660-3666.
107. Berggren, C., Johansson, G., 1997. Capacitance Measurements of antibody-antigen interactions in a flow system. *Analytical Chemistry*. 69, 3651-3657.
108. Berggren, C., Bjarnason, B., Johansson, G., 1999. Instrumentation for direct capacitive biosensors. *Instrumentation Science and Technology*. 27, 131-139.



109. Ramanaviciene, A., Ramanavicius, A., 2004. Pulsed amperometric detection of DNA with an ssDNA/polypyrrole-modified electrode. *Analytical and Bioanalytical Chemistry*. 379, 287-293.
110. Jacobson, R., 1998. Principle of Validation of diagnostic assays for infectious diseases. *Diagnosis and Epidemiology of Animal Diseases in Latin America*. 10-25.
111. Thevenot, D.R., Toth, K., Durst, R.A., Wilson, G.S., 1999. Electrochemical biosensors: recommended definitions and classification. *Pure and Applied Chemistry*. 71, 2333-2348.
112. Williams, L. D., Maher III, L. J., 2000. Electrostatic mechanisms of DNA deformation. *Annual Review of Biophysics and Biomolecular Structure*. 29, 497-521.
113. Steel, A., Levicky, R., Herne, T., Tarlov, M.J., 2000. Immobilization of nucleic acids at solid surfaces: effect of oligonucleotide length on layer assembly. *Biophysical Journal*. 79, 975-981.
114. Kelley, S.O., Barton, J.K., Jackson, N.M., McPherson, L.D., Potter, A.B., Spain, E.M., Allen, M.J., Hill, M.G., 1998. Orienting DNA helices on gold using applied electric fields. *Langmuir*. 14, 6781-6784.
115. Wilson, W.D., Tanious, F.A., Fernandez-Saiz, M., Rigl, C.T., 1997. Drug-DNA interaction protocols. Springer, New York. pp 219-240.
116. Schildkraut, C., Lifson, S., 1965. Dependence of the melting temperature of DNA on salt concentration. *Biopolymers*. 3, 195-208.
117. McConaughy, B.L., Laird, C.D., McCarthy, B.J., 1969. Nucleic acid reassociation in formamide. *Biochemistry*. 8, 3289-3295.
118. Lehninger, A., Nelson, D., Cox, M., 1993. Principles of biochemistry, Worth, New York. pp 631-632.
119. Bonner, T.I., Brenner, D.J., Neufeld, B.R., Britten, R.J., 1973. Reduction in the rate of DNA reassociation by sequence divergence. *Journal of Molecular Biology*. 81, 123-135.
120. Sambrook, J., Fritsch, E.F., Maniatis, T., 1989. Molecular cloning. Cold Spring Harbor Laboratory Press, New York.
121. Stachan, T., Rea, A.P., 1999. Human molecular genetics, 2 nd edition. Willy-Liss, New York.
122. Peterson, A. W., Heaton, R. J., Georgiadis, R. M., 2001. The effect of surface probe density on DNA hybridization. *Nucleic Acids Research*. 29, 5163-5168.
123. Hong, J., Yoon, D.S., Park, M-I., Choi, J., Kim, T.S., Im, G., Kim, S., Pak, Y.E., No, K., 2004. A dielectric biosensor using the capacitance change with AC frequency integrated on glass substrates. *Japanese Journal of Applied Physics*. 43, 5639.
124. Lee, C.-Y., Gong, P., Harbers, G. M., Grainger, D. W., Castner, D. G., Gamble, L. J., 2006. Surface coverage and structure of mixed DNA/alkylthiol monolayers on gold: characterization by XPS, NEXAFS, and fluorescence intensity measurements. *Analytical Chemistry*, 78, 3316-3325.
125. Herne, T. M., Tarlov, M. J., 1997. Characterization of DNA probes immobilized on gold surfaces. *Journal of the American Chemical Society*. 119, 8916-8920.
126. Gebala, M., Schuhmann, W., 2012. Understanding properties of electrified interfaces as a prerequisite for label-free DNA hybridization detection. *Physical Chemistry Chemical Physics*. 14, 14933-14942.
127. Schreiner, S. M., Shudy, D. F., Hatch, A. L., Opdahl, A., Whitman, L. J., Petrovykh, D. Y., 2010. Controlled and efficient hybridization achieved with DNA probes immobilized solely through preferential DNA-substrate interactions. *Analytical chemistry*. 82, 2803-2810.

128. Jarzab, A., Górska-Frączek, S., Rybka, J., Witkowska, D., 2010. Enterobacteriaceae infection-diagnosis, antibiotic resistance and prevention. *Postepy Higieny i Medycyny Doswiadczalnej*. 65, 55-72.
129. Chakravorty, S., Helb, D., Burday, M., Connell, N., Alland, D., 2007. A detailed analysis of 16S ribosomal RNA gene segments for the diagnosis of pathogenic bacteria. *Journal of Microbiological Methods*. 69, 330-339.
130. Bermingham, N., K, Luettich., 2003. Polymerase chain reaction and its applications. *Current Diagnostic Pathology*. 9, 159-164.
131. Thompson, W.F., 1976. Aggregate formation from short fragments of plant DNA. *Plant Physiology* 57, 617-622.
132. Jain, S., Zweig, M., Peeters, E., Siewering, K., Hackett, K. T., Dillard, J. P., Van Der Does, C., 2012. Characterization of the single stranded DNA binding protein SsbB encoded in the gonococcal genetic island. *PLoS One*. 7, e35285.
133. Shamo, Y., 2002. Single-stranded DNA-binding proteins. Macmillan Publishers Ltd, Nature Publishing Group/www.els.net/ November 15, 2013.
134. Knubovets, T., Osterhout, J.J., Klibanov, A.M., 1999. Structure of lysozyme dissolved in neat organic solvents as assessed by NMR and CD spectroscopies. *Biotechnology and Bioengineering*. 63, 242-248.
135. Stratis-Cullum, D., Sumner, J. Biosensors and bioelectronics. In: Armstrong, R.E., Drapeau, M.D., Loec, C.A., Valdes, J.J., 2010. Bio-inspired innovation and national security. Smashbooks, New York, pp 77-103.
136. Adams, M.R., Moss, M.O., 2010. Food microbiology. The Royal Society of Chemistry, Cambridge.
137. Thiel, C. S., Tauber, S., Schütte, A., Schmitz, B., Nuesse, H., Moeller, R., Ullrich, O., 2014. Functional activity of plasmid DNA after entry into the atmosphere of earth investigated by a new biomarker stability assay for ballistic spaceflight experiments. *PLoS One*. 9, e112979.
138. World Health Organization., 2014. Antimicrobial resistance: global report on surveillance. Geneva.
139. Goldmann, D.A., Weinstein, R.A., Wenzel, R.P., Tablan, O.C., Duma, R.J., Gaynes, R.P., Schlosser, J., Martone, W.J., Acar, J., Avorn, J., 1996. Strategies to prevent and control the emergence and spread of antimicrobial-resistant microorganisms in hospitals: a challenge to hospital leadership. *The Journal of the American Medical Association*. 275, 234-240.
140. Shlaes, D.M., Gerding, D.N., John, J.F., Craig, W.A., Bornstein, D.L., Duncan, R.A., Eckman, M.R., Farrer, W.E., Greene, W.H., Lorian, V., 1997. Society for healthcare epidemiology of America and infectious diseases society of America joint committee on the prevention of antimicrobial resistance: guidelines for the prevention of antimicrobial resistance in hospitals. *Clinical Infectious Diseases*. 25, 584-599.
141. Long, C.B., Madan, R.P., Herold, B.C., 2010. Diagnosis and management of community-associated MRSA infections in children. *Expert Review of Anti-Infective Therapy*. 8, 183-195.
142. Ma, X.X., Ito, T., Tiensasitorn, C., Jamklang, M., Chongtrakool, P., Boyle-Vavra, S., Daum, R.S., Hiramatsu, K., 2002. Novel type of staphylococcal cassette chromosome mec identified in community-acquired methicillin-resistant *Staphylococcus aureus* strains. *Antimicrobial Agents and Chemotherapy*. 46, 1147-1152.
143. Jemili-Ben, J.M., Boutiba-Ben, B.I., Ben, R.S., 2006. Identification of staphylococcal cassette chromosome mec encoding methicillin resistance in *Staphylococcus aureus* isolates at Charles Nicolle Hospital of Tunis. *Pathologie Biologie*. 54, 453-455.
144. Börjesson, S., Melin, S., Matussek, A., Lindgren, P-E., 2009. A seasonal study of the *mecA* gene and *Staphylococcus aureus* including methicillin-

- resistant *S. aureus* in a municipal wastewater treatment plant. *Water Research*. 43, 925-932.
145. Holden, M.T., Feil, E.J., Lindsay, J.A., Peacock, S.J., Day, N.P., Enright, M.C., Foster, T.J., Moore, C.E., Hurst, L., Atkin, R., 2004. Complete genomes of two clinical *Staphylococcus aureus* strains: evidence for the rapid evolution of virulence and drug resistance. *Proceedings of the National Academy of Sciences of the United States of America*. 101, 9786-9791.
  146. Zhou, F., Wang, Y., 2013. Characteristics of antibiotic resistance of airborne *Staphylococcus* isolated from metro stations. *International Journal of Environmental Research and Public Health*. 10, 2412-2426.
  147. Lim, D., Strynadka, N.C., 2002. Structural basis for the  $\beta$ -lactam resistance of PBP2a from methicillin-resistant *Staphylococcus aureus*. *Nature Structural and Molecular Biology*. 9, 870-876.
  148. Severin, A., Tabei, K., Tenover, F., Chung, M., Clarke, N., Tomasz, A., 2004. High level oxacillin and vancomycin resistance and altered cell wall composition in *Staphylococcus aureus* carrying the staphylococcal *mecA* and the enterococcal *vanA* gene complex. *Journal of Biological Chemistry*. 279, 3398-3407.
  149. Chambers, H., 2001. Methicillin-resistant *Staphylococcus aureus*: mechanisms of resistance and implications for treatment. *Postgraduate Medicine*. 109, 43-50.
  150. Calfee, D.P., Salgado, C.D., Classen, D., Arias, K.M., Podgorny, K., Anderson, D.J., Burstin, H., Coffin, S.E., Dubberke, E.R., Fraser, V., 2008. Strategies to prevent transmission of methicillin-resistant *Staphylococcus aureus* in acute care hospitals. *Strategies*. 29, 62-80.
  151. Malhotra-Kumar, S., Haccuria, K., Michiels, M., Ieven, M., Poyart, C., Hryniewicz, W., Goossens, H., 2008. Current trends in rapid diagnostics for methicillin-resistant *Staphylococcus aureus* and glycopeptide-resistant enterococcus species. *Journal of Clinical Microbiology*. 46, 1577-1587.
  152. Clevn B.E., Palka-Santini, M., Gielen, J., Meembor, S., Krönke, M., Krut, O., 2006. Identification and characterization of bacterial pathogens causing bloodstream infections by DNA microarray. *Journal of Clinical Microbiology*. 44, 2389-2397.
  153. Towner, K., Talbot, D., Curran, R., Webster, C., Humphreys, H., 1998. Development and evaluation of a PCR-based immunoassay for the rapid detection of methicillin-resistant *Staphylococcus aureus*. *Journal of Medical Microbiology*. 47, 607-613.
  154. Watanabe, K., Kuwata, N., Sakamoto, H., Amano, Y., Satomura, T., Suye, S.-i., 2014. A smart DNA sensing system for detecting methicillin-resistant *Staphylococcus aureus* using modified nanoparticle probes, *Biosensors and Bioelectronics*. (In press).
  155. Wassenberg, M.W., Kluytmans, J.A., Box, A.T., Bosboom, R.W., Buiting, A.G., van-Elzakker, E.P., Melchers, W.J., van-Rijen, M.M., Thijsen, S.F., Troelstra, A., Vandenbroucke-Grauls, C.M., Visser, C.E., Voss, A., Wolffs, P.F., Wulf, M.W., van-Zwet, A.A., de-Wit, G.A., Bonten, M.J., 2010. Rapid screening of methicillin-resistant *Staphylococcus aureus* using PCR and chromogenic agar: a prospective study to evaluate costs and effects. *Clinical Microbiology and Infection*. 16, 1754-1761.
  156. Tatsumi, N., Kondou, K., Yamada, T., Sugiura, Y., Inuzuka, K., and Kaneko, T., 2011. Etiological bacterial level in enterohemorrhagic *Escherichia coli* infection feces and chromogenic culture medium CHROMagar STEC usefulness. *The Journal of the Japanese Association for Infectious Diseases*. 85, 664-669.
  157. Padhye, N., Doyle, M., 1991. Rapid procedure for detecting enterohemorrhagic *Escherichia coli* O157: H7 in food. *Applied and Environmental Microbiology*. 57, 2693-2698.

158. [www.abnova.com/](http://www.abnova.com/) November 10, 2014.
159. Call, D. R., Brockman, F. J., and Chandler, D. P., 2001. Detecting and genotyping *Escherichia coli* O157:H7 using multiplexed PCR and nucleic acid microarrays. *International Journal of Food Microbiology*. 67, 71-80.
160. Patrinos, G.P., Ansoorge, W.J., 2010. *Molecular diagnostics*. 2nd edition. Academic Press. London.
161. Allanach, K., Mengel, M., Einecke, G., Sis, B., Hidalgo, L., Mueller, T., Halloran, P., 2008. Comparing microarray versus rt-pcr assessment of renal allograft biopsies: similar performance despite different dynamic ranges. *American Journal of Transplantation*. 8, 1006-1015.
162. Fan, H., Wu, Q., Kou, X., 2008. Co-detection of five species of water-borne bacteria by multiplex PCR. *Life Science Journal*. 5, 47-54.
163. Settingington, E.B., Alcolija, E.C., 2012. Electrochemical biosensor for rapid and sensitive detection of magnetically extracted bacterial pathogens. *Biosensors*. 2, 15-31.
164. Xia, H., Wang, F., Huang, Q., Huang, J., Chen, M., Wang, J., Yao, C., Chen, Q., Cai, G., Fu, W., 2008. Detection of *Staphylococcus epidermidis* by a quartz crystal microbalance nucleic acid biosensor array using Au nanoparticle signal amplification. *Sensors*. 8, 6453-6470.
165. Chen, S-H., Wu, V.C., Chuang, Y-C., Lin, C-S., 2008. Using oligonucleotide-functionalized Au nanoparticles to rapidly detect foodborne pathogens on a piezoelectric biosensor. *Journal of Microbiological Methods*. 73, 7-17.
166. Taylor, A., Ladd, J., Homola, J., Jiang, S., 2008. Surface plasmon resonance (SPR) sensors for the detection of bacterial pathogens in: *Principles of bacterial detection: Biosensors, Recognition Receptors and Microsystems*. Springer, New York.
167. Li, D., Feng, Y., Zhou, L., Ye, Z., Wang, J., Ying, Y., Ruan, C., Wang, R., and Li, Y., 2011. Label-free capacitive immunosensor based on quartz crystal Au electrode for rapid and sensitive detection of *Escherichia coli* O157: H7, *Analytica Chimica Acta*. 687, 89-96.
168. D'Orazio, P., 2003. Biosensors in clinical chemistry. *Clinica Chimica Acta*. 334, 41-69.
169. Hardenbol, P., Banér, J., Jain, M., Nilsson, M., Namsaraev, E.A., Karlin-Neumann, G.A., Fakhrai-Rad, H., Ronaghi, M., Willis, T.D., Landegren, U., 2003. Multiplexed genotyping with sequence-tagged molecular inversion probes. *Nature Biotechnology*. 21, 673-678.
170. Raymond, F., Carbonneau, J., Boucher, N., Robitaille, L., Boisvert, S., Wu, W-K., De-Serres, G., Boivin, G., Corbeil, J., 2009. Comparison of automated microarray detection with real-time PCR assays for detection of respiratory viruses in specimens obtained from children. *Journal of Clinical Microbiology*. 47, 743-750.
171. Yang, J.R., Wu, F.T., Tsai, J.L., Mu, J.J., Lin, L.F., Chen, K.L., Kuo, S.H.S., Chiang, C.S., Wu, H.S., 2007. Comparison between O serotyping method and multiplex real-time PCR to identify diarrheagenic *Escherichia coli* in Taiwan, *Journal of Clinical Microbiology*. 45, 3620-3625.
172. <http://www.lifetechnologies.com/November12,2014>.
173. Oh, B.K., Lee, W., Lee, W.H., Choi, J.W., 2003b. Nano-scale probe fabrication using self-assembly technique and application to detection of *Escherichia coli* O157:H7. *Biotechnology and Bioprocess Engineering*, 8, 227-232.
174. Ertürk, G., Berillo, D., Hedström, M., Mattiasson, B., 2014. Microcontact-BSA imprinted capacitive biosensor for real-time, sensitive and selective detection of BSA. *Biotechnology Reports*. 3, 65-72.



# Paper I





## Use of a capacitive affinity biosensor for sensitive and selective detection and quantification of DNA—A model study



Ally Mahadhy, Eva Ståhl-Wernersson, Bo Mattiasson, Martin Hedström\*

Department of Biotechnology, Lund University, P.O. Box 124, SE-22100 Lund, Sweden

### ARTICLE INFO

#### Article history:

Received 8 April 2014

Received in revised form 2 June 2014

Accepted 2 June 2014

Available online 12 June 2014

#### Keywords:

Sandwich hybridization

DNA-sensor

Polytyramine

### ABSTRACT

A capacitive DNA-sensor model system was used to monitor the capture of complementary single-stranded DNAs. The sensor chip consisted of a gold electrode, which was carefully insulated with a polytyramine layer and covalently tagged with 25-mer oligo-C. As low as  $10^{-11}$  moles per liter of target oligo-G could be detected by injecting 250  $\mu$ L of sample. Elevated temperature was used to reduce non-specific hybridization. Less than 10% of non-target 25-mer oligo-T interacted nonspecifically with the oligo-C probes when hybridization process was performed at 50 °C. Studying the relationship of length of the analyte to the signal strength, the output from the capacitive DNA-sensor increased to almost the double; from 50 to 88-nF  $\text{cm}^{-2}$ , when a 25-mer oligo-G was used instead of a 15-mer. By sandwich hybridization at room temperature, it was possible to further increase the signal, from 78-nF  $\text{cm}^{-2}$  for the target 50-mer oligo-G alone, to 114-nF  $\text{cm}^{-2}$ .

© 2014 Published by Elsevier B.V. This is an open access article under the CC BY-NC-ND license (<http://creativecommons.org/licenses/by-nc-nd/3.0/>).

### 1. Introduction

The development of sensitive, selective and real-time sensors for monitoring DNA in biological samples is very important. Determination of specific DNA-sequences in clinical or food samples can result in the detection and identification of certain infectious organisms [1]. Various DNA-sensors with labeled probes have been reported; where the use of radioisotope-labeled ( $^{125}\text{I}$  or  $^{32}\text{P}$ ) DNA-probes have been reported frequently [2–4]. However, apart from high sensitivities, the use of isotope-labeled reagents is restricted because of the potential danger of radioactivity. Therefore, new strategies have been introduced for labeling of DNA such as use of avidin–biotin [5], ferrocenium [6], chemiluminescent agent [7,8], fluorescent dye [9], and various metal nanoparticles [10] such as gold-nanoparticles [11]. Assays based on labeled reagents are among the most sensitive reported, but in general they are costly, complex and time-consuming.

Alternatively, various DNA-sensors with label-free probes have been developed. Among these are piezoelectric [12], acoustic [13], optical [14] and electrochemical transduction [1]. In particular, electrochemical DNA sensors are robust, cheap and allow fast detection. They make use of single-stranded DNA probes that are attached to the surface of the sensing devices which have the potential to allow rapid and quantitative monitoring of label-free

hybridization. Electrochemical detection of DNA hybridization usually involves changes in electrochemical parameters such as; capacitance [15], impedance [16] and electrochemical quartz crystal microbalance measurements [17] at fixed potential or detecting complementary target, using both direct electrochemical oxidation of guanine and redox of the electroactive indicator methylene blue [17–19]. The above listed electrochemical DNA-sensors that use label-free probes are cost effective alternatives adopted for real-time monitoring, however with serious drawbacks; low selectivity and low sensitivity [15,17].

This paper describes the use of a capacitive DNA-sensor application, where a surface-bound label-free oligonucleotide probes captures a target complementary DNA-sequence and real time measurement is performed. Nevertheless, the application of elevated temperature to reduce non-specific hybridization (interaction of non-complementary oligos) in order to increase the selectivity, the influence of oligo length to the signal strength, and application of sandwich hybridization approach in order to amplify the signal strength of the long DNA molecules are reported.

### 2. Materials and methods

#### 2.1. Materials

All single stranded oligonucleotides were obtained from Eurofins MWG Operon (Ebersberg, Germany): 25-mer oligonucleotides-C (oligo-C); 15-, 25- and 50-mer oligonucleotides-G (oligo-G); and 25-mer oligonucleotides-T (oligo-T). Absolute

\* Corresponding author. Tel.: +46 46 222 75 78; fax: +46 46 222 47 13.  
E-mail address: [Martin.Hedstrom@biotek.lu.se](mailto:Martin.Hedstrom@biotek.lu.se) (M. Hedström).



ethanol and sodium hydroxide (NaOH) were obtained from VWR International (Leuven, Belgium). Tyramine, *N*-hydroxysuccinimide (NHS), *N*-(3-dimethylaminopropyl) *N*-ethylcarbodiimide hydrochloride (EDC), ethanesulfonic acid (MES), and 1-dodecane thiol were obtained from Sigma–Aldrich (Steinheim, Germany). All other chemicals used were of analytical grade. All buffers and regeneration solutions were prepared with double distilled water from a Milli-Q system (Millipore, Massachusetts, USA). All solutions were filtered through a membrane (pore size 0.22 μm) and degassed prior to use.

## 2.2. Methods

### 2.2.1. Electrode surface modification

A gold electrode (99.9% purity, custom-made,  $\phi = 3$  mm) with a surface area of 0.07 cm<sup>2</sup> was used as a working electrode. Prior to the modification with oligonucleotides, the gold electrode was polished with alumina slurry with a particle size of 0.1 μm (Struers, Ballerup, Denmark) and cleaned through sonication in distilled water and subsequently in absolute ethanol, for 15 min in each solvent. It was then washed with distilled water and dried with pure nitrogen gas [20], followed by plasma cleaning, PDC-3XG (Harrick, New York, USA) for 20 min, and after that coated by the electropolymerization of tyramine on the electrode surface [21]. The coated electrode was rinsed with distilled water to remove any loosely bound polymer and it was finally carefully dried with pure nitrogen gas prior to immobilization.

To immobilize nucleotide-probes on the modified electrode, 20 μL of a mixture that contained 20 μM 25-mer oligo-C, 9.9 μM NHS and 1.65 μM EDC in 40 mM MES buffer, pH 6.5 was added on the surface of the electrode. The reaction was left at room temperature for 30 min, while covered to prevent evaporation. The electrode was then transferred to 4 °C and kept there for 24 h. Prior to use, the sensor electrode was washed with 10 mM potassium phosphate buffer pH 7.2, and distilled water before being dried by pure nitrogen gas. The modified electrode was then immersed into 10 mM 1-dodecane thiol for 20 min in order to provide insulation and to block any pin holes. Cyclic voltammetry, CV/Auto-lab (Utrecht, Netherlands) was used to monitor the results of insulation and immobilization processes [21].

### 2.2.2. Experimental set up

All experiments were performed in a conventional four-electrode flow cell with a dead volume of 10 μL, using a data acquisition unit (Keithley Instruments, Cleveland, OH, USA) and a potentiostat interfaced with a personal computer (Fig. 1a). Details of the experimental set-up of the four-electrode flow cell injection capacitive sensor system were described previously [22]. A modified electrode, using 25-mer oligo-C probe immobilized on the surface, was placed into the flow cell and then equilibrated with running buffer (10 mM potassium phosphate buffer pH 7.2) at flow rate of 100 μL/min until a stable base line was obtained, followed by injecting 250 μL of a sample in the same buffer. NaOH (50 mM) was applied for intermediate regeneration after hybridization step [23] in order to break the binding between oligo-C probe and an analyte (oligo-G), and hence, to facilitate additional measurements. All the measurements made in this study were performed in triplicates, either at room temperature (23 °C, RT) or at elevated temperatures. For the studies that involve the use of elevated temperatures, a column-thermostat, Jetstream 2 (Vienna, Austria) was used.

In principle, when a bare electrode surface is subjected to the electrolyte solution, an electrical double layer which consists of adsorbed fixed layer (Stern layer) and a diffuse mobile layer (Gouy–Chapman diffuse layer) is formed at the electrode surface/electrolyte solution interface. The interface between electrode surface and the

electrolyte solution (the electric double layer) behaves like a capacitor; i.e., it is capable of storing electric charge [24]. The electrical double layer capacitance could be described by Eq. (1).

$$\frac{1}{C_{EDL}} = \frac{1}{C_{SL}} + \frac{1}{C_{CC}} \quad (1)$$

where,  $C_{EDL}$  is the capacitance of the electrical double layer,  $C_{SL}$  is the capacitance of Stern (adsorption layer) layer and  $C_{CC}$  is the capacitance of the Gouy–Chapman (diffuse mobile) layer.

However, in typical capacitive DNA-sensor, the capacitance at the electrode surface/electrolyte solution interface is built up of several capacitors in series [25]; (i) the capacitance of insulating layer (polytyramine layer),  $C_{ins}$  (ii) the capacitance of capture probe (immobilized DNA),  $C_{capt}$  and any contribution from adsorbed fixed layer (iii) and the capacitance of diffuse mobile layer,  $C_{dl}$  as depicted in Fig. 1b. Therefore total capacitance ( $C_{Tot}$ ) at electrode surface/electrolyte solution interface could be described by Eq. (2).

$$\frac{1}{C_{Tot}} = \frac{1}{C_{ins}} + \frac{1}{C_{capt}} + \frac{1}{C_{dl}} \quad (2)$$

When the analyte hybridizes on capture probe, consequently this increases the thickness and the length of the capture probe layer. The displacement of the diffuse mobile layer created during the potentiostatic pulse will cause a decrease in total capacitance, which is strictly proportional to the analyte concentration. The surface should be designed so that, the capacitance of the insulating layer,  $C_{ins}$  is high as possible that allows the capacitance from the binding of analyte to be detected. This change in capacitance due to binding of analyte was used for detection.

### 2.2.3. Capacitance measurement

A positive potential pulse of 50 mV was applied each sixty second at the modified electrode (working electrode), which gives a current response signal. The current was sampled and the total capacitance was obtained by taking the logarithm of Eq. (3)

$$i(t) = \frac{u}{R_s} \exp\left(-\frac{t}{R_s C_{Tot}}\right) \quad (3)$$

where,  $i(t)$  is the current in the open circuit (RC model) as a function of time,  $u$  is the applied pulse potential,  $R_s$  is the dynamic resistance of capture probe layer,  $C_{Tot}$  is the total capacitance measured between the gold electrode surface and the electrolyte solution interface, and  $t$  is the time elapsed after the potentiostatic step was applied. The technique is described in detail elsewhere [22].

Hybridization of single stranded DNA (ssDNA) on the capture probe caused  $C_{Tot}$  to decrease. Then, the capacitance change,  $\Delta C$ , could be determined as a difference between the two base lines, before and after injection of the sample. A baseline was considered stable when a standard deviation of an average of the last five measuring points of a registered total capacitance is <1 nF. The necessity to evaluate an average of five capacitance values was previously mathematically proved [26]. However, standard deviation of <1 nF was introduced based on previous observations (data not shown) that the signal for the lowest concentration ( $10^{-12}$  M) of the target analyte tested in this study, was clearly observed when the standard deviation of the 5 average points of the baseline before injection of the analyte was <1 nF.

### 2.2.4. DNA-hybridization on the electrode surface at different temperatures

Hybridization of target DNA was initially performed at RT. Oligo-G probes of different lengths (15-, 25- and 50-mer) were injected into the system at different concentrations, i.e.  $10^{-8}$ ,  $10^{-9}$ ,  $10^{-10}$  and  $10^{-11}$  M. The result in capacitance change of each oligo-probe length was registered and evaluated.

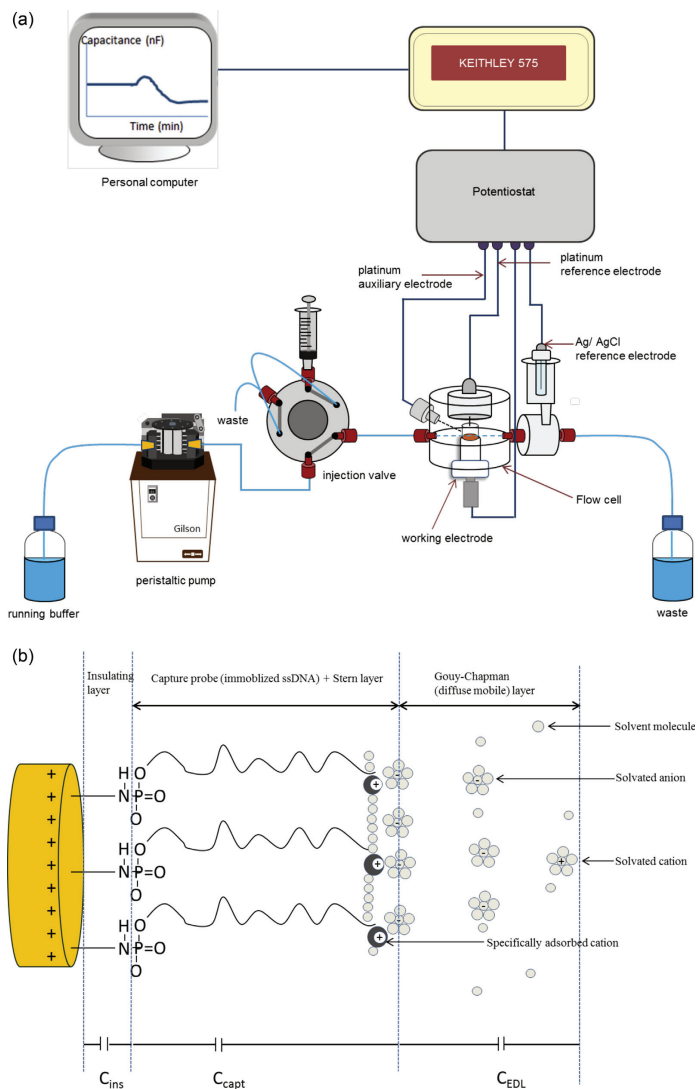


**Fig. 1.** (a) Experimental set up of the flow injection capacitive DNA-sensor system. (b) Schematic of the electrical double layer structure of a capacitive DNA-sensor electrode with the built-up of capacitors in series.

In the analytical step using DNA-sensors, higher temperatures are often needed in order to improve the selectivity of the sensor. However, it is necessary to know the influence of the temperature on the electrode modified surface in order to understand whether a measured capacitance is caused by changes to temperature or by any other event on the electrode surface. For this reason, the behavior of the modified electrode surface with respect to capacitance changes was initially studied at RT, 30, 40, 50, and 60 °C, and kept for 30 min at each temperature.

Specific and non-specific hybridizations at RT, 30, 40, 50, and 60 °C were also studied by applying target DNA,  $10^{-8}$  M of 25-mer oligo-G at the modified electrode surface. Later, the same concentration of non-specific DNA, 25-mer oligo-T was also applied under identical conditions and the results were compared to each other. This study offers a predictable optimum temperature that discriminates non-specific hybridization without significantly affecting the specific hybridization.

### 2.2.5. Sandwich hybridization

Sandwich hybridization was performed at RT by injecting 50-mer oligo-G at different concentrations ( $10^{-8}$ ,  $10^{-9}$ ,  $10^{-10}$  and  $10^{-11}$  M). Once a stable base line was observed, the same concentration of 25-mer oligo-C was injected. These results were compared with those obtained from injection of the 50-mer oligo-G, alone.

## 3. Results and discussion

### 3.1. Cyclic voltammetry

The electrochemical behavior of the electrode was studied after each modification step (Fig. 2) by oxidizing and reducing a redox couple on the bare gold electrode surface. After electropolymerization of tyramine on the electrode surface, the redox peak was decreased markedly. The deposited polytyramine, besides of providing free amino groups for covalent binding to the phosphate group of oligonucleotides by forming phosphoramidate bond [27], it also provides an insulating property on the electrode surface.

The oligo-C probe coupled to the polytyramine layer also contributed to the insulating behavior of the polytyramine layer. Therefore, a further decrease of redox peak was observed after subsequent immobilization of oligo-C. However, after treatment with 1-dodecanethiol the cyclic voltammograms showed complete blockage of redox reaction. The electrode surface was assumed to be

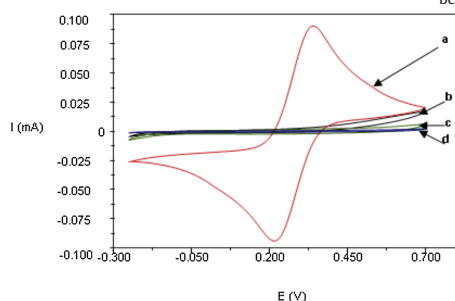


**Fig. 2.** Cyclic voltammograms recorded in 10 mM  $K_3[Fe(CN)_6]$  in 0.1 M KCl. The potential was swept in the range between  $-250$  and  $700$  mV (vs Ag/AgCl) with a sweep rate of  $100$  mV  $s^{-1}$ : (a) bare gold electrode (red); (b) gold electrode modified with polytyramine layer (black); (c) the same as (b) after immobilization of 25-mer oligo-C (green); (d) as in (c) after treatment with 1-dodecanethiol (blue). (For interpretation of the references to colour in this figure legend, the reader is referred to the web version of this article.)

completely covered so that the all influence from pin holes were considered negligible based on, that makes the electrode/solution interface to be described by resistor–capacitor in series (RC) model (Eq. (2)) above. Otherwise the capacitance would be in parallel with resistor (R/RC) model, resulting in a decrease in sensitivity due to leakage of current.

### 3.2. Analytical characterization

#### 3.2.1. Capacitance change due to hybridization of target DNA

The value of registered capacitance depends on the dielectric and insulating features at the working electrode and solution interface. Fig. 3 shows the basic features of the registered capacitance; before injection of analyte,  $C_{\text{beforeanalyte}}$ ; after injection of analyte,  $C_{\text{afteranalyte}}$ ; and after regeneration,  $C_{\text{afterregeneration}}$ .

Upon injection of oligo-G, the hybridization with immobilized oligo-C on the electrode surface took place that resulted into a decrease in capacitance. The observed little increase in capacitance immediately after injection of oligo-G might be due to an increase in negative charge density as the polyanion DNA-probes approach the electrode. A similar argument has been applied for 5'-end biotin modified oligo-C-avidin-polyaniline films system where a decrease in electron transfer resistance was observed during hybridization [16,18]. However, once the base-pairing between oligo-G and oligo-C took place, water and electrolyte ions (diffuse mobile layer) were displaced. The diffuse mobile layer contains high abundance of negatively charged ions that outweighed the polyanion on the DNA surface. The capacitance change was then dominated by the displacement of the diffuse mobile layer away from the electrode surface as a result of an increase in thickness and length of the capture probe layer; hence decrease in capacitance was registered [15]. Regeneration of the modified electrode surface by injecting 50 mM NaOH was used to disrupt the hydrogen bonds between the paired DNA strands (oligo-C and oligo-G) without damaging the oligo-C (capture probe). The capacitance was then returned to the original base line ready for additional measurements. Fig. 3 inset, shows how the capacitance change upon injection of analyte change was determined.

The capacitive change was proportional to the applied concentrations of the oligo-Gs, (15-, 25- and 50-mer) as depicted in Fig. 4. Applying higher number of oligo-G molecules, could lead to displacement of more number of electrolyte ions (the diffuse mobile layer) further away from the electrode surface, therefore a larger decrease in total capacitance was registered [28].

Nevertheless, the magnitude of registered capacitance change was also found to some extent to be dependent on the length of applied oligo-G. For instance, applying 25-mer oligo-G at electrode modified surface resulted in a capacitance shift which was approximately twice as high as that caused by a 15-mer oligo-G (Table 1). However, there was no significant difference for the capacitance change, when the same concentration of 25- and 50-mer oligo-Gs was applied on the surface. In theory, the effect of 50-mer oligo-G was expected to be twice of that 25-mer oligo-G and three times of that 15-mer oligo-G; this is because the longer DNA molecule hybridizes on the surface, the longer the capture probe layer it becomes, then the further distance the diffuse mobile layer is displaced, which would lead to larger decrease in total capacitance.

On the contrary, the bending behavior of the long molecules, like DNA, could be the explanation of the observed results for 50-mer oligo-G. The long DNA molecules exhibit intrinsic bending behavior due to various factors, such as van der Waals force and aromatic–aromatic ( $\pi$ – $\pi$ ) interaction between the bases of the same DNA molecule. Nonetheless, Kelly et al. (1998) reported that, when an electrode surface is positively charged (by applying a positive potential pulse), the intrinsic negatively charged DNA is pulled towards the electrode and hence adopts a tilted orientation

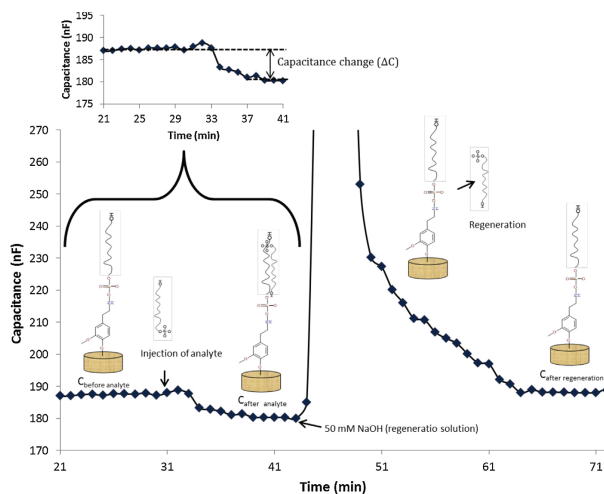


**Fig. 3.** Time course graph showing the capacitance: (i) before injection of analyte ( $C_{\text{before analyte}}$ ) (ii) after injection of analyte ( $C_{\text{after analyte}}$ ) and (iii) after regeneration ( $C_{\text{after regeneration}}$ ). Inset shows how to determine the capacitance change upon injection of analyte.

[29]. Since, the longer the DNA molecule the more negative charges it has, a 50-mer would be pulled towards the electrode surface even more (more tilted) than 25-mer oligo-G, resulted into less signal strength than expected. However, by introducing a sandwich hybridization approach, it was possible to increase the signal strength of the 50-mer oligo-G. The results of this approach are described in Section 3.2.3.

### 3.2.2. The effect of elevated temperature on hybridization of oligonucleotides on the sensor surface

Initially, the behavior of the modified electrode surface with reference to capacitance change at different temperatures was studied (Fig. 5a). It was observed that the capacitance increased with increasing temperature. It may be suggested that, with increasing temperature, the mobility of ions in the diffuse mobile layer increases too, resulting into an increase in electrical conductivity of the electrolyte. The latter leads to an increase in the dielectric “constant” of the medium [30], hence, resulted into an increase in registered capacitance. But also, the increase in temperature could lead to reorientation of the oligo-C (capture

probe) on the electrode surface from its initial tilted orientation [29], but also, became less dense which then allows the electrolyte ions to reach closer to the electrode surface and hence, a further increase in capacitance is observed.

The modified electrode surface seems to withstand temperatures up to 50 °C; however at 60 °C, the baseline became unstable. Observations indicated that the accumulation of released gas bubbles on the electrode surface was the probable cause of the baseline instability at higher temperatures. Therefore, it was concluded that, the maximum suitable temperature for the present experimental set-up was 50 °C. Since the hybridization of DNA is often carried out at even lower temperature, this temperature range is sufficient for most application of the DNA sensors.

The capacitance change,  $\Delta C$ , due to non-specific hybridization, 25-mer oligo-T was found to decrease drastically; from 48 to 3 nF cm<sup>-2</sup> as the temperature increased from RT to 50 °C, respectively (Fig. 5b). However, there was no significant decrease in target hybridization (25-mer oligo-G) capacitance change with respect to the increase in temperature. The capacitance changes at RT compared to 50 °C, were 84 and 77 nF cm<sup>-2</sup>, respectively.

The hybridization between the non-target (non-complementary) oligonucleotide with the capture probe could be explained by the different weak interactions such as aromatic–aromatic ( $\pi$ – $\pi$ ) interaction and van der Waals forces. The non-specific interaction could have been more efficiently reduced at 50 °C if small amounts

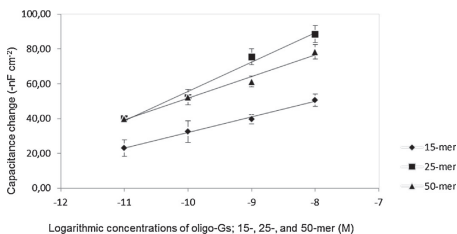


**Fig. 4.** Capacitance change with an increased concentration of 15-, 25- and 50-mer oligo-G.

**Table 1**  
Calculated capacitance change upon applying of oligo-G of different lengths on the electrode surface coupled with 25-mer oligo-C (capture probe).

Oligo-G length (-mer)	Capacitance change: average $\pm$ SD (nF cm <sup>-2</sup> )		
	at 10 <sup>-8</sup> M	at 10 <sup>-9</sup> M	at 10 <sup>-11</sup> M
15	51 $\pm$ 4	40 $\pm$ 3	23 $\pm$ 5
25	89 $\pm$ 5	76 $\pm$ 5	40 $\pm$ 2
50	78 $\pm$ 4	61 $\pm$ 3	40 $\pm$ 2

of formamide had been added in the running buffer, without affecting the target DNA. Formamide helps to reduce the thermal stability of double stranded nucleic acid [31,32]. However, our results suggest that, working at high temperature up to 50 °C, could efficiently reduce non-specific hybridization by more than 90% without significantly altering the specific interaction. Carrarra et al. [28] studied the efficiency of the hybridization reaction at elevated temperature (80 °C), and they found that 80% of the target DNA molecules reacted with probes forming double helix while less than 10% of the non-target DNA molecules reacted with probes forming double helix. As the temperature increases, the kinetic energy increases which causes increasing molecular motion and thereby breaking the weak interactions and hence, reducing non-specific DNA hybridization.

There must be a trade-off between raising the temperature to eliminate non-specific binding and the temperature effect on the specific binding. This is an aspect that needs to be kept under

control. However, it does not seem to be a problem at temperatures below 50 °C as were used in this study.

### 3.2.3. Sandwich hybridization

Hybridization of 50-mer oligo-G with immobilized 25-mer oligo-C on the electrode surface was initially performed. Subsequently, another 25-mer oligo-C was injected to the system at the same concentration as that of oligo-G. This resulted in a higher capacitive response as compared to response from hybridization of 50-mer oligo-G alone to the sensor surface (Fig. 6). In this study, the 50-mer oligo-G was expected to be long enough to give the intrinsic bending behavior, but also to experience higher attraction force towards the electrode surface than others (25- and 15-mer). For example, the signal from the 50-mer oligo-G at concentration of  $10^{-8}$  M was lower than expected,  $78\text{-nFcm}^{-2}$ , but after subsequent injection of the same concentration of the shorter 25-mer oligo-C, the hybridization of partial bent oligo-G with

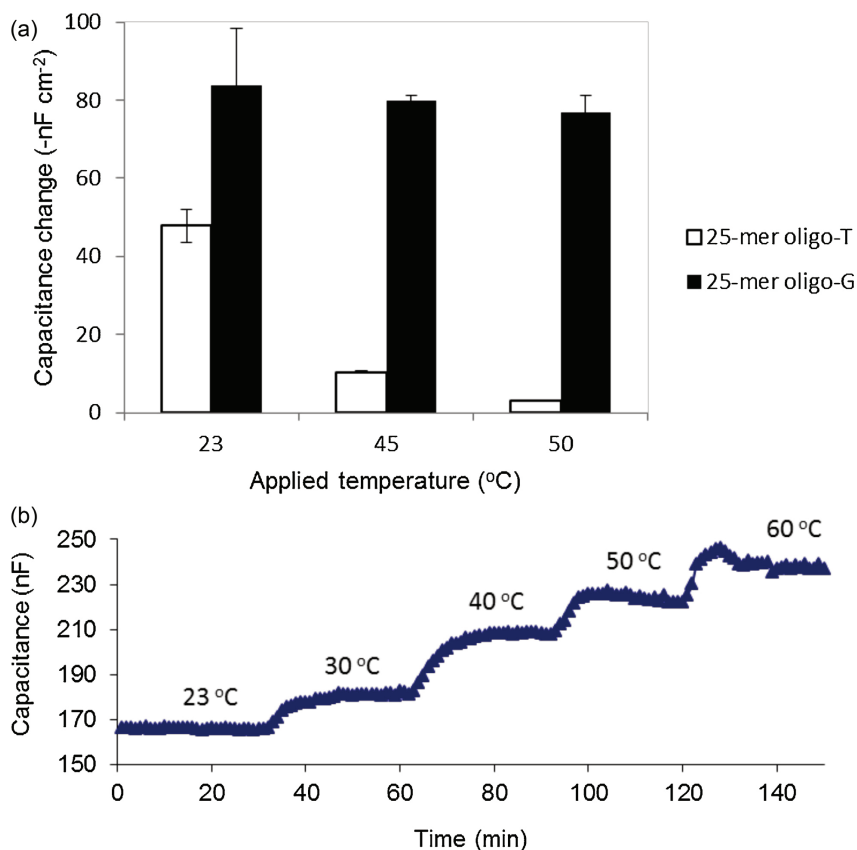
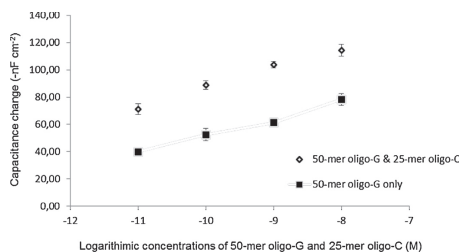


Fig. 5. (a) Capacitance change of modified electrode surface at different temperatures: 23, 30, 40, 50 and 60 °C. (b) Capacitance change from an electrode with immobilized 25-mer oligo-C, for injections of  $10^{-8}$  M complementary (oligo-G) and non-complementary (oligo-T), at different temperatures.



**Fig. 6.** Sandwich hybridization 50-mer oligo-G followed by 25-mer oligo-C (◆) compared with 50-mer oligo-G alone (■).

oligo-C occurs, resulting in further increase of capacitance change to  $114\text{-nF cm}^{-2}$ . The subsequent injected short complementary oligonucleotide hybridized with bases from a partially bent long oligonucleotide molecule, and resulted in an amplification of the signal, which has indicated that the diffuse mobile layer was even further displaced from the surface of the gold electrode due to hybridization of DNA molecules. Increasing in signal strength could lead to an increase in sensitivity of an analytical device too. However, in some cases, signal strength is somewhat not very important when improving sensitivity of an analytical device; because the signal can be very big but the detection limit cannot be very good due to poor signal to noise level.

#### 4. Conclusions

The application of polymer chemistry (polytyramine) for insulation of a gold electrode surface and immobilization of oligo-nucleotides to that surface is a simple and repeatable method for DNA based sensors. This work has demonstrated that the capacitance change,  $\Delta C$ , is proportional to the concentration of and the length of the hybridized oligo-G for the developed system. However, longer DNA molecules have to be treated differently. This was solved by using sandwich hybridization, which increased the amplitude of the signal. Non-specific hybridization was handled by elevating the temperature up to  $50^\circ\text{C}$ , resulting in a tenfold decrease of the signal compared to RT. In order to adopt the developed model system for diagnostic and research purposes, it is necessary to use real bacteria/virus DNA samples. This will be the future work, to further optimize selectivity and sensitivity for the developed model system.

#### Acknowledgements

This work was funded by World Bank supported project titled "Capacity Building in Science, Technology and Higher education" (STHEP) which is being implemented at University of Dar es salaam, Tanzania. The support from the Swedish Research Council is gratefully acknowledged.

#### References

- [1] P. Basselet, G. Wegrzyn, S.O. Enfors, M. Gabig-Ciminska, Sample processing for DNA chip array-based analysis of enterohemorrhagic *Escherichia coli* (EHEC), *Microb. Cell Fact.* 7 (2008) 29, doi:10.1186/1475-2859-7-29.
- [2] T.A. Drake, J.A. Hindler, O.G.W. Berlin, D.A. Bruckner, Rapid identification of mycobacterium-avium complex in culture using DNA probes, *J. Clin. Microbiol.* 25 (1987) 1442–1445.
- [3] H. Sakamoto, O. Lemaire, D. Merdinoglu, J.L. Guesdon, Comparison of enzyme-linked immunosorbent-assay (ELISA) with dot hybridization using P-32 acetylaminofluorene or 2-acetylaminofluorene (AFF)-labeled cDNA probes for

the detection and characterization of beet necrotic yellow vein virus, *Mol. Cell. Probe* 3 (1989) 159–166, doi:10.1016/0890-8508(89)90026-1.

- [4] B.L. Wetherall, P.J. McDonald, A.M. Johnson, Detection of campylobacter-pylori DNA by hybridization with non-radioactive probes in comparison with a P-32-labeled probe, *J. Med. Microbiol.* 26 (1988) 257–263.
- [5] Y. Liu, B. Elsholz, S.O. Enfors, M. Gabig-Ciminska, Confirmative electric DNA array-based test for food poisoning *Bacillus cereus*, *J. Microbiol. Method* 70 (2007) 55–64, doi:10.1016/j.mimet.2007.03.011.
- [6] R. Teles, F. Rodrigues, F. Prazeres, D.M. Lima-Filho, J. Luiz, Electrochemical detection of a dengue-related oligonucleotide sequence using ferrocenium as a hybridization indicator, *Sensors* 7 (2007) 2510–2518.
- [7] X. Chen, X.-E. Zhang, Y.Q. Chai, W.-P. Hu, Z.-P. Zhang, X.-M. Zhang, E.A.G. Cass, DNA optical sensor: a rapid method for the detection of DNA hybridization, *Biosens. Bioelectron.* 13 (1998) 451–458.
- [8] D.-K. Xu, L.-R. Ma, Y.-Q. Liu, Z.-H. Jiang, Z.-H. Liu, Development of chemiluminescent biosensing of nucleic acids based on oligonucleotide-immobilized gold surfaces, *Analyst* 124 (1999) 533–536, doi:10.1039/a809057b.
- [9] T. Livache, B. Fouque, A. Roget, J. Marchand, G. Bidan, R. Téoule, G. Mathis, Polypyrrole DNA chip on a silicon device: example of hepatitis C virus genotyping, *Anal. Biochem.* 255 (1998) 188–194.
- [10] W. Fritzsche, T.A. Taton, Metal nanoparticles as labels for heterogeneous, chip-based DNA detection, *Nanotechnology* 14 (2003) 63–73.
- [11] M.L. Sauthier, R.L. Carroll, C.B. Gorman, S. Franzen, Nanoparticle layers assembled through DNA hybridization: characterization and optimization, *Langmuir* 18 (2002) 1825–1830.
- [12] S. Tombelli, M. Minunni, M. Mascini, Piezoelectric biosensors: strategies for coupling nucleic acids to piezoelectric devices, *Methods* 37 (2005) 48–56, doi:10.1016/j.jymeth.2005.05.005.
- [13] H. Zhang, H. Tan, R. Wang, W. Wei, S. Yao, Immobilization of DNA on silver surface of bulk acoustic wave sensor and its application to the study of UV-C damage, *Anal. Chim. Acta* 374 (1998) 31–38.
- [14] G.D. Francia, V.L. Ferrara, S. Manzo, S. Chiavarini, Towards a label-free optical porous silicon DNA sensor, *Biosens. Bioelectron.* 21 (2005) 661–665, doi:10.1016/j.bios.2004.12.008.
- [15] C. Berggren, P. Saelhandske, J. Brundell, G. Johansson, A feasibility study of a capacitive biosensor for direct detection of DNA hybridization, *Electroanalysis* 11 (1999) 156–160.
- [16] V. Dharuman, T. Grunwald, E. Nebling, J. Albers, L. Blohm, R. Hintsche, Label-free impedance detection of oligonucleotide hybridisation on interdigitated ultramicroelectrodes using electrochemical redox probes, *Biosens. Bioelectron.* 21 (2005) 645–654, doi:10.1016/j.bios.2004.12.020.
- [17] A. Tenreiro, C.M. Cordas, L.M. Abrantes, Oligonucleotide immobilisation on polytyramine-modified electrodes suitable for electrochemical DNA biosensors, *Portugaliae Electrochim. Acta* 21 (2003) 361–370.
- [18] K. Arora, N. Prabhakar, S. Chand, B.D. Malhotra, Ultrasensitive DNA hybridization biosensor based on polyaniline, *Biosens. Bioelectron.* 23 (2007) 613–662, doi:10.1016/j.bios.2007.07.010.
- [19] M. Mascini, Affinity electrochemical biosensors for pollution control, *Pure Appl. Chem.* 73 (2001) 23–30.
- [20] W. Limbut, P. Kanatharana, B. Mattiasson, P. Asawatreratanakul, P. Thavarungkul, A comparative study of capacitive immunosensors based on self-assembled monolayers formed from thiourea, thioctic acid, and 3-mercaptopropionic acid, *Biosens. Bioelectron.* 22 (2006) 233–240, doi:10.1016/j.bios.2005.12.025.
- [21] K. Teeparuksapin, M. Hedström, E.Y. Wong, S. Tang, I.K. Hewlett, B. Mattiasson, Ultrasensitive detection of HIV-1 p24 antigen using nanofunctionalized surfaces in a capacitive immunosensor, *Anal. Chem.* 82 (2010) 8406–8411.
- [22] W. Limbut, M. Hedström, P. Thavarungkul, P. Kanatharana, B. Mattiasson, Capacitive biosensor for detection of endotoxin, *Anal. Bioanal. Chem.* 389 (2007) 517–525, doi:10.1007/s00216-007-1443-4.
- [23] C. Ananthanawat, T. Vilaivan, W. Mekboonsonglar, V.P. Hoven, Thiolated pyrroldinyl peptide nucleic acids for the detection of DNA hybridization using surface plasmon resonance, *Biosens. Bioelectron.* 24 (2009) 3544–3549.
- [24] A.J. Bard, L.R. Faulkner, *Electrochemical Methods: Fundamentals Applications*, second ed., John Wiley & Sons, New York, 2001.
- [25] C. Berggren, B. Bjarnason, G. Johansson, Capacitive biosensors, *Electroanalysis* 13 (2001) 3.
- [26] A. Ramanaviciene, A. Ramanavicius, Pulsed amperometric detection of DNA with an ssDNA/polypyrrole-modified electrode, *Anal. Bioanal. Chem.* 379 (2004) 287–293.
- [27] Y.-D. Zhao, D.-W. Pang, S. Hu, Z.-L. Wang, J.-K. Cheng, H.-P. Dai, DNA-modified electrodes: part 4: optimization of covalent immobilization of DNA on self-assembled monolayers, *Talanta* 49 (1999) 751–756.
- [28] S. Carrara, F.K. Gürkaynak, C. Guiducci, C. Stagnic, L. Beninic, Y. Leblebici, S. Bruno, G. Michelib, Interface layering phenomena in capacitance detection of DNA with biochips, *Sens. Transducers* 76 (2007) 969–977.
- [29] S.O. Kelly, J.K. Barton, N.M. Jackson, L.D. McPherson, A.B. Potter, E.M. Spain, M.J. Allen, M.G. Hill, Orienting DNA helices on gold using applied electric fields, *Langmuir* 14 (1998) 6781–6784.
- [30] J. Hong, D.S. Yoon, M. Park, J. Choi, T.S. Kim, G. Im, S. Kim, Y.E. Pak, K. No, A dielectric biosensor using the capacitance change with ac frequency integrated on glass substrates, *Jpn. J. Appl. Phys.* 43 (2004) 5639–5645.
- [31] B.L. McConaughy, C.D. Laird, B.J. McCarthy, Nucleic acid reassociation in formamide, *Biochemistry* 8 (1969) 3289–3295.
- [32] R.D. Blake, S.G. Delcourt, Thermodynamic effects of formamide on DNA stability, *Nucleic Acid Res.* 24 (1996) 2095–2103.



## Paper II







## PCR-Free Ultrasensitive Capacitive Biosensor for Selective Detection and Quantification of Enterobacteriaceae DNA

Ally Mahadhy<sup>1</sup>, Gashaw Mamo<sup>1</sup>, Eva Ståhl-Wernersson<sup>1</sup>, Bo Mattiasson<sup>1,2</sup> and Martin Hedström<sup>1,2\*</sup>

<sup>1</sup>Department of Biotechnology, Lund University, P.O. Box 124, SE-22100 Lund, Sweden

<sup>2</sup>CapSenze HB, Medicion Village, SE-22838 Lund, Sweden

### Abstract

This paper presents a flow-based ultrasensitive capacitive biosensor for the detection of bacterial DNA. The used sensor chip consists of a gold electrode, insulated with a polytyramine layer and covalently tagged with a DNA capture probe. The hybridization of target DNA to the capture probe resulted in sensor response. The sensor response was linear vs. log concentration in the range  $1.0 \times 10^{12}$  to  $1.0 \times 10^7$  moles per litre with a detection limit of  $6.5 \times 10^{-13}$  M. An alternative approach to bacterial DNA sample preparation for a flow-based analysis is also reported. The approach involved application of a thermostable ssDNA binding protein to prevent re-annealing of a heat-denatured target DNA prior to analysis. During analysis, formamide was integrated in the running buffer to denature ET SSB. *E. coli* DNA corresponding to 10 cells per millilitre of sample was detected in 15 min by this DNA-sensor. The sensor chip could be re-used up to 20 times with RSD of < 6%. The DNA-sensor chip was able to discriminate between Enterobacteriaceae (*E. coli*) and Lactobacillaceae (*L. reuteri*) DNAs. The reported DNA-sensor lays the groundwork for incorporating the method into an integrated system for in-field bacteria detection.

**Keywords:** DNA-sensor; Capacitance; Formamide; Enterobacteriaceae; ssDNA-binding-protein

### Introduction

There is a need for rapid and field-adopted assays for detection of pathogenic microorganisms. This need is reflected in most diagnostic assays of pathogenic organisms that are still made in clinical laboratories. For instance, the source of food-borne illness is determined in less than 50% of the cases, usually because of limited diagnostic capabilities [1,2]. Most of the hospital, clinical and quality control laboratories use a traditional method, plate counting, as a primary method for detection and quantification of infectious pathogens. The method is laborious and time consuming; it takes 24 to 48 hr to obtain initial results [3,4].

The limitations of diagnostic capabilities have greatly increased the demand for developing a fast, selective and sensitive bioanalytical technique for the detection and quantification of infectious pathogens in the samples. Various DNA-based sensor models have been reported for detection of different pathogenic organisms; *E. coli* [5-7]; *Neisseria meningitidis* [8]; *Staphylococcus aureus* [9]; and *Mycobacterium tuberculosis* [10]. The DNA-sensors make use of genetic markers of microorganisms for their identification and quantification. A genetic marker could be a DNA sequence that is responsible for pathogenicity or a unique DNA sequence for a particular microorganism [11]. However, a main problem in detection of DNA at physiological levels is that the target DNA is in a very low concentration, usually lower than the detection limits of many reported analytical techniques. Thus, amplification of the sample by polymerase chain reaction (PCR) has been the best choice [12]. On the other hand, the use of PCR is not only expensive but it is also limited in part by presence of inhibitory substances in complex biological samples, which reduce or even block the amplification capacity of PCR. For example, PCR mixture containing widely used *Taq* polymerase is totally inhibited by the presence of 0.004% (v/v) red blood cells [13].

This paper presents a real-time, PCR-free, selective and sensitive capacitive DNA-sensor, for the identification and quantification of

Enterobacteriaceae DNA. Rod-shaped bacteria of the Enterobacteriaceae family are one of the major worldwide health hazards and particularly in developing countries where sanitation standards are low. Strains of *Escherichia coli*, *Shigella*, *Salmonella* and *Yersinia pestis* are responsible for diarrhea, severe bacillary dysentery, typhoid and other intestinal diseases, as well as genitourinary tract and blood infections. According to the World Health Organization report, there are 4.5 billion cases every year, out of which approximately 1.9 million have a lethal outcome. This makes intestinal infections the third most mortal group of human diseases [14].

We have developed a DNA based sensor, as DNA probes are more cheaper and reliable than protein probes. As such, antibodies are very expensive and the proteins that they target can be degraded during sample preparation, where as targeted ssDNAs by ssDNA probes are much more stable.

The hybridization between the capture DNA probes and targeted DNAs was monitored by capacitance measurements [15]. *E. coli* BL21 (DE3), family Enterobacteriaceae was selected as a candidate and model for this study. However, the capacitive DNA-sensor can be used to target a broader range of bacteria that share a certain gene. Time consumption and sensitivity of the capacitive DNA-sensor and the total plate counting technique were compared as well.

\*Corresponding author: Martin Hedström, Department of Biotechnology, Lund University, P.O. Box 124, SE-22100 Lund, Sweden, Tel: +46 46-222 75 78; Fax: +46 46-222 47 13; E-mail: Martin.Hedstrom@biotek.lu.se

Received September 12, 2014; Accepted October 07 2014; Published October 10, 2014

Citation: Mahadhy A, Mamo G, Ståhl-Wernersson E, Mattiasson B, Hedström M (2014) PCR-Free Ultrasensitive Capacitive Biosensor for Selective Detection and Quantification of Enterobacteriaceae DNA. J Anal Bioanal Tech 5: 210 doi:10.4172/2155-9872.1000210

Copyright: © 2014 Mahadhy A, et al. This is an open-access article distributed under the terms of the Creative Commons Attribution License, which permits unrestricted use, distribution, and reproduction in any medium, provided the original author and source are credited.

## Experimental section

### Reagents

Single stranded 30-mer oligonucleotides; capture probe and target (complementary) probe designed from *E. coli* BL21(DE3) 16S rDNA were custom-made by Integrated DNA Technologies, Inc. (Leuven, Belgium), while 16S rDNA universal primers: forward (63F) and reverse (1389R) were available in our lab. The sequences of all oligonucleotides are listed in Table 1. Extremely thermostable single-stranded DNA binding protein (ET SSB) was purchased from New England Biolabs (Ipswich, MA, USA). Restriction enzyme, FastDigest *AclI* (SsiI) from Fermentas (Glen Burnie, MD, USA). Dream Taq PCR master mix (2X); GeneRuler Ultra low range DNA ladder and GeneRuler (1 kb) were all purchased from Thermo Fisher Scientific, Inc. (Göteborg, Sweden). DNA extraction/purification kit (ZR Fungal/Bacterial DNA MiniPrep™) was purchased from Zymo research corporation (Irvine, CA, USA), and 5X Phusion buffer from Finnzymes (Espoo, Finland). Ethanol, sodium hydroxide and Omega Bio-tek's gel extraction kit were obtained from VWR International (Leuven, Belgium). Tyramine, N-hydroxysuccinimide (NHS), N-(3-dimethylaminopropyl) N-ethylcarbodiimide hydrochloride (EDC), agarose type I, Luria-Bertani (LB) agar, formamide and 1-dodecane thiol were obtained from Sigma-Aldrich (Steinheim, Germany). *E. coli* BL21 (DE3) strain; *L. reuteri* DSM 20016; were available in our Department. All other chemicals used were of analytical grade. Buffers and solutions were prepared with double distilled water from a Milli-Q system by Millipore (Massachusetts, USA). Water were filtered through nitrocellulose membrane of a pore size 0.22 µm, from Sigma-Aldrich (Steinheim, Germany), and degassed prior to use.

### Instruments

NanoDrop ND 1000 UV-Vis spectrophotometer, from NanoDrop Technologies (San Jose, CA, USA), an ultrasonicator, Hielscher UP 400S (Teltow, Germany), a water bath from Haake TP 42 (Karlsruhe, Germany), a cryostat, Neslab RTE-200 (Portsmouth, NH, USA), a PCR machine, Thermocycler Biometra RS 232 (Göttingen, Germany). Light-inverted microscope from Nikon. (Japan). Gel electrophoresis equipment; Electrophoresis Power Supply/ EPS 500/400 was from Pharmacia Fine Chemicals, Inc. (New Jersey, USA), while a gel visualizing equipment, MiniBis Pro 16 mm was from DNR Bio-Imaging system Ltd (Jerusalem, Israel). Plasma cleaning system from Harrick (New York, USA), a column thermostat (oven), Jetstream 2 from LabVision (Vienna, Austria) and Fast data acquisition unit from Keithley Instruments (Cleveland, OH, USA).

### Procedures

**Preparation of working electrode:** The study used a custom-made 3 mm diameter disposable gold working electrode (Academic workshop, Linköping University, Sweden). The electrode was initially cleaned in acetone, then followed by ethanol and finally piranha

solution (3:1) concentrated sulfuric acid: 30% hydrogen peroxide) for 5 min in each solution, while sequentially rinsed with distilled water before being placed in the plasma cleaning for 20 min. The cleaned working electrode was coated by electropolymerization of tyramine on the electrode surface [16]. The coated electrode was then rinsed with distilled water to remove any loosely bound polymer. The electrode was carefully dried with a stream of nitrogen gas after each step.

The immobilization of the capture probe on the surface of polytyramine coated electrode was carried out under optimized conditions [17], by applying 20 µL of 10 µM capture probe (DNA) in 10 mM potassium phosphate buffer (PB) solution, pH 7.2, containing 5 mM EDC, 8 mM NHS. The electrode was incubated during two hours at room temperature. After immobilization, DNA modified electrode was rinsed with double distilled water and 10 mM PB, pH 7.2, with 30% formamide. Finally, the electrode was immersed in 1-dodecanethiol (10 mM in ethanol) in order to block pinholes in the affinity surface [15], and was then stored at 4°C until use.

**Capacitance measurements:** The prepared working electrode was mounted in a four-electrode flow-injection cell with a dead volume of 10 µL and connected to a potentiostat, two platinum wires; one was used as the auxiliary and the other as the reference electrode. An external reference (Ag/AgCl) was placed in the outlet stream. A fast data acquisition unit was connected between a personal computer and the potentiostat. To reduce the noise in the system, the potentiostat is powered from data acquisition unit, which in turn was powered by the computer through a galvanometrically insulated power supply. A schematic drawing of the system set up is provided elsewhere [15], the four-electrode flow-injection cell with the mounted electrodes was kept in the column thermostat; the working (hybridization) temperature was kept at 30°C, unless stated otherwise. The mobile phase (10 mM PB, pH 7.2, with 30% formamide) was infused using a peristaltic pump at a flow rate of 100 µL min<sup>-1</sup>. Samples were injected into the flow via a 250 µL loop. The DNA-sensor was regenerated with 0.5 M NaOH after each sample injection. The total capacitances and capacitance change (ΔC) were calculated from the current response as previously described in details [15]. All experiments were performed in triplicates.

**Preparation of calibration curve:** A standard stock solution of 1.0 × 10<sup>6</sup> M synthesised 30-mer ss16S rDNA, which is complementary to the capture probe, was prepared and serially diluted by a factor of 10, to make 9 solutions of concentrations from 1.0 × 10<sup>6</sup> to 1.0 × 10<sup>-14</sup> M. Aliquots of each concentration and a blank (mobile phase) were injected in triplicate and capacitance change (ΔC) for each sample was calculated. A calibration curve of a logarithmic concentration of injected DNA sample *versus* registered signal was plotted. From the calibration curve, a linear range and the limit of detection (LOD) was determined. Using the same plotted curve as a reference, DNA samples from bacteria were analysed.

**Re-usability:** The re-usability of 30-mer 16S rDNA-sensor chip was investigated by monitoring the ΔC when repeatedly injecting the

Oligonucleotide	Sequence (5' → 3')	Size
Capture probe	GAGTAAAGTTAATACCTTTGCTCATTGACG	30-mer
Target Probe	CGTCAATGAGCAAAGGTATTAACCTTTACTC	30-mer
Forward primer (63F)	CAGGCCTAACACATGCAAGTC	21-mer
Reverse primer (1389R)	ACGGGCGGTGTGTACAAG	18-mer
<i>E. coli</i> 16S r-DNA (amplified sequence)	-	1447 bp
Target fragment of <i>E. coli</i> 16S rDNA (restriction enzyme product)	GGTAAACGTC AATGAGCAAAGGTA TTAACCTTTA CTCCCTCCTCC	44-bp

Table 1: Different oligonucleotide sequences and their sizes used in this study.

same concentration of the standard complementary 30-mer ss16S rDNA ( $10^{11}$  M) up to 23 times in 2 days, with regeneration after each assay. The residual capacity was calculated (Eq. 1 below) and the values of the percentage residual capacity of the 30-mer 16S rDNA-sensor chip versus the number of injections.

$$\text{Residual capacity (\%)} = 100 - ((\Delta C_i - \Delta C_f) / \Delta C_i) \times 100 \quad (1)$$

where,  $\Delta C_i$  is the initial capacitance change and  $\Delta C_f$  is the final capacitance change.

**Stock solution of bacterial cells:** *E. coli* was cultivated on LB- agar plates at 37°C for 24 hr., while *L. reuteri* cell mass was provided by Dr. Tarek Dishisha (Department of Biotechnology Lund, University). The cells of *E. coli* and *L. reuteri* were harvested by spinning down the cells at 3000 × g for 5 min. The cells were thereafter re-suspended in a saline solution (0.9% (w/v) NaCl) and kept at 4°C until further use. The number of cells per ml of each culture was determined microscopically using a hemocytometer [18] just before use.

**DNA sample preparation from bacterial cells:** It should be noted that, both *E. coli* and *L. reuteri* samples were treated in a similar manner throughout the study.

The whole sample preparation took less than 90 min and the hybridization time was 15 min. The preparation started by (1) Whole genomic DNA extraction (2) DNA fragmentation by restriction enzyme (3) DNA heat denaturation (4) Preventing re-annealing of single stranded DNA by adding ET SSB and (5) Injecting DNA sample into the capacitive DNA-sensor for analysis, immediately after adding formamide to 30% (v/v), as shown in Figure 1.

**DNA extraction:** Genomic DNA were extracted from *E. coli* and *L. reuteri* cultures (about  $10^8$  cells ml<sup>-1</sup>) using ZR Fungal/Bacterial DNA MiniPrep™. The concentration of the extracted genomic DNAs was

estimated using a NanoDrop spectrophotometer.

**DNA fragmentation:** *Acil* (*Ssi*I) restriction enzyme was used as described in the protocol (Fermentas) for digestion of genomic DNA. In order to produce suitable and consistent targeted fragments, the digestive efficiency of *Acil* restriction enzyme was previously studied. Whereas the 16S rDNA was initially amplified from 2 μL *E. coli* DNA extract with 10 μL *Dream Taq* polymerase (dNTPs and polymerase), the set of primers, 1 μL 63F and 1 μL 1386R, and 6 μL water; to make a PCR reaction mixture of 20 μL. PCR was performed for 30 cycles, starting at initial denaturation temperature, 95°C for 3 min, at the first cycle, for the consecutive 29 cycles the same denaturation temperature was kept for 30 s. The annealing and extension temperatures were 50°C for 30 s and 72°C for 2.5 min throughout the PCR run, respectively. However, for the final step, the extension temperature was kept for 7.5 min. Then, the PCR product was digested using *Acil* (*Ssi*I) enzyme.

Both, whole PCR product and fragments were analysed by electrophoresis on 3% agarose gel, run at 80 V for 2 hr. The gel was stained in GelRed™ 3X staining solution and then visualized and photographed with MiniBis Pro 16 mm from DNR Bio-Imaging system.

**Heat denaturation of DNA:** In order to produce single stranded DNA for DNA-sensor analysis, a mixture which contained: 50 μL of 14 ng μL<sup>-1</sup> fragmented DNA sample, 29 μL nuclease free water, and 20 μL 5X Phusion buffer was heated at 95°C for 5 min. Then, 1 μL (0.5 μg) of ET SSB was added to the mixture while heated in order to prevent re-annealing of denatured DNA. Finally, the sample was ready for analysis.

The effect of addition of *ET SSB* was previously compared with a rapid-cooling approach for preventing re-annealing of denatured DNA, whereas three different cooling media were studied (Figure 2).

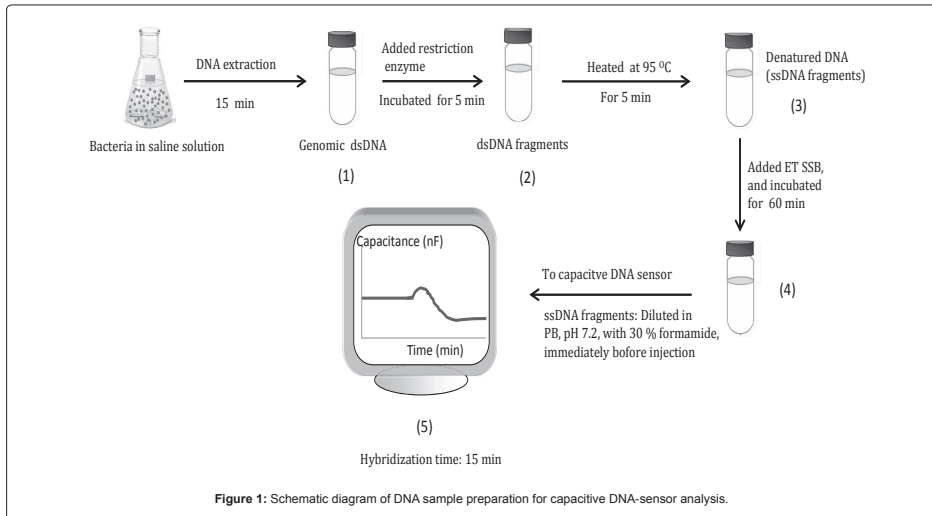
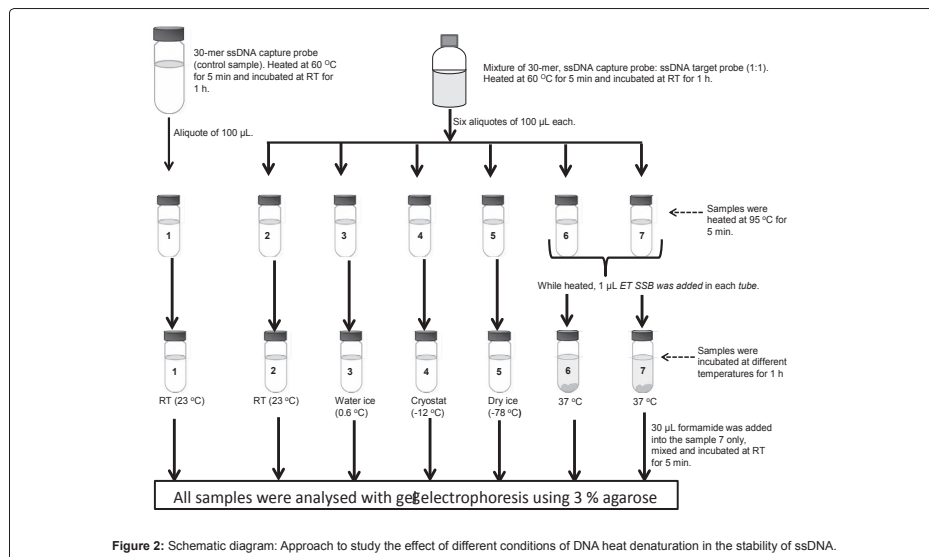


Figure 1: Schematic diagram of DNA sample preparation for capacitive DNA-sensor analysis.



Two complementary single stranded 30-mer 16S rDNAs were mixed at 1:1 ratio and heated on a water bath, 60°C for 5 min and left to hybridize at room temperature for 1 h. Six aliquotes of 100 µL each; named 2, 3, 4, 5, 6 and 7 were taken from the reaction mixture. The aliquotes and a 100 µL single stranded 30-mer 16S rDNA control sample solution (named 1), were then heated in the water bath at 95°C for 5 min; while heated, total volume of two microliter *ET SSB* solution was added in to samples 6 and 7, one microliter each. After the heating, samples 1 and 2 were left at room temperature (23°C), samples 6 and 7 were incubated at 37°C; samples 3, 4, and 5 were immediately transferred to ice water (0.6°C), a cryostat (-12°C, ethanol as cryo-solvent), and dry ice (-78°C), respectively. All samples were left at their respectively temperatures for 1 h. After that, in sample 7 about 30 µL of formamide was added, mixed and the mixture incubated at room temperature for 5 min. All samples were then analysed with gel electrophoresis using 3% agarose gel, 80 V for 2 h 45 min.

#### *E. coli* sample analysis

**Capacitive DNA-sensor:** Since the initial concentration used for extraction of genomic DNA was  $10^8$  cells  $ml^{-1}$ , it was considered that the extract contained a concentration of genomic DNA corresponding to the concentration of the starting amount the cells ( $10^8$  cells  $ml^{-1}$ ). It was considered that 100% recovery of genomic DNA was achieved using ZR Fungal/Bacterial DNA MiniPrep™ extraction kit under optimum conditions. Moreover, following dilutions during the DNA fragmentation and denaturation steps, the genomic DNA ended up being 10 times diluted. Prior to DNA-sensor analysis, the pre-treated genomic DNA was even further serially diluted to  $1/10^1$ ,  $1/10^2$ ,  $1/10^3$ ,  $1/10^4$ ,  $1/10^5$  and  $1/10^6$ . Based on the assumption above, these dilutions were assumed to correspond to concentrations of  $10^5$ ,  $10^4$ ,  $10^3$ ,  $10^2$ ,  $10^1$  and 1 *E. coli* cell(s)  $ml^{-1}$ , respectively. The assumption above was

made for the sake of comparison between capacitive DNA-sensor and the plate counting techniques. Finally, an aliquot of each dilution was injected into the capacitive DNA-sensor in triplicate, and  $\Delta C$  for each dilution was determined. Sensitivity of the sensor was then compared with the plate counting technique.

**Plate counting:** Five different concentrations of *E. coli* cells:  $10^1$ ,  $10^2$ ,  $10^3$ ,  $10^4$  and  $10^5$  cells  $ml^{-1}$  were prepared by serially diluting a  $10^8$  cells  $ml^{-1}$  stock suspension by a factor of 10. Each concentration above was treated as an individual sample. The LB agar plates in triplicates were then streaked with 10 µl of each sample and incubated at 37°C for 24 h. Samples with  $10^3$  to  $10^5$  cells  $ml^{-1}$  were initially diluted to obtain an acceptable range of colony forming unit per plate (CFU/plate). Finally, the CFU  $ml^{-1}$  of each sample was determined [19].

#### Selectivity of the DNA-sensor chip

**Whole genomic DNA:** An aliquot of each dilution of *L. reuteri* (family Lactobacillaceae) genomic DNA were analysed by the capacitive DNA-sensor. The analyses were done in triplicate, and  $\Delta C$  for each dilution was determined and compared with that of the *E. coli* (family Enterobacteriaceae) genomic DNA. The experiment was repeated by injecting samples of *E. coli* and *L. reuteri* at a dilution corresponding to  $10^5$  cells  $ml^{-1}$ , while changing the working temperature from initially 30 to 40°C, but keeping the same concentration of formamide in the mobile phase.

**Amplified 16S rDNA:** Genomic DNAs of *E. coli* and *L. reuteri* samples were initially extracted as explained in DNA extraction section, and then 16S rDNA from diluted DNA extract (1:10) of each sample was amplified with *Dream Taq PCR master mix* and the set of primers 63F and 1386R. PCR was performed for 30 cycles (in the same way as in DNA fragmentation section). PCR products of each sample

were analysed on 1% agarose gel, run at 120 V for 55 min. A band for 16S rDNA from each sample was carefully excised, and then 16S rDNA was extracted from the gel using Omega Bio-tek's gel extraction kit. Equal volume of  $10^{10}$  M 16S rDNA samples from *L. reuteri* and *E. coli* separately, were enzymatically fragmented and heat-denatured as described in DNA fragmentation section and Heat denaturation of DNA section, respectively. Thereafter, each sample was injected into the capacitive DNA-sensor system, which was previously modified by immobilizing a synthesized 30-mer *E. coli* 16S rDNA. The  $\Delta C$  for each sample was determined and compared to each other.

## Results and discussion

### Modification of sensor electrode surface

Cyclic voltammogram of each electrode surface modification was recorded as shown in Figure 3 and compared with a cyclic voltammogram of a bare electrode surface (insert, a).

The electrode surface was initially functionalized with amine groups via the polytyramine layer that was electro-deposited onto the electrode surface. The dramatic decrease in redox peak currents after deposition of polytyramine layer (**b, red**) reflects the passivation of the electrode surface, because the formed non-conducting layer hampers the electron transfer between electrode surface and redox species. Following immobilization of the capture probe onto the surface, the redox peak currents were further decreased (**c, black**). Finally, a pinhole-free surface was formed by depositing 10 mM 1-dodecanethiol (in ethanol) on the surface, which resulted in an even further decrease in redox peak currents (**d, green**).

### Capacitive DNA-sensor for assay of hybridization of complementary probes

**Linear dynamic range and detection limit:** The fundamental principle of the capacitive transducer is based on the theory of double layer (DL) which was well described previously by Berggren et al. [20]. During the capacitance measurement, charge transfer is taking place at the DL [15]. The modified gold electrode when placed in an electrolyte solution (PB), behaves like several capacitors arranged in series (Figure 4) with;  $C_{ins}$  capacitance of the insulating layer on the surface;  $C_{cp}$  capacitance of immobilized capture probe; and  $C_{dl}$  capacitance of the double layer.

Therefore, the total capacitance ( $C_{tot}$ ) of the modified electrode is defined by Eq. (2):

$$\frac{1}{C_{tot}} = \frac{1}{C_{ins}} + \frac{1}{C_{cp}} + \frac{1}{C_{dl}} \quad (2)$$

When target ssDNA hybridizes to the capture probe, the dielectric constant of the electrode surface layer will decrease [21], and the double layer will be pushed away from the electrode surface [20]. The decrease in the dielectric constant and the displacement of the double layer will result in the decrease of relative permittivity of the electrode/solution interface, and in an increase of the distance between ions and the electrode surface layer, respectively. The former will result in the decrease of  $C_{cp}$ , whereas, the latter will cause the decrease of  $C_{dl}$ ; and therefore, both will result in the decrease of the  $C_{tot}$  registered.

Here, the change in capacitance i.e., the difference of the  $C_{tot}$  before and after sample injection ( $\Delta C$ ) was found to be proportionally related

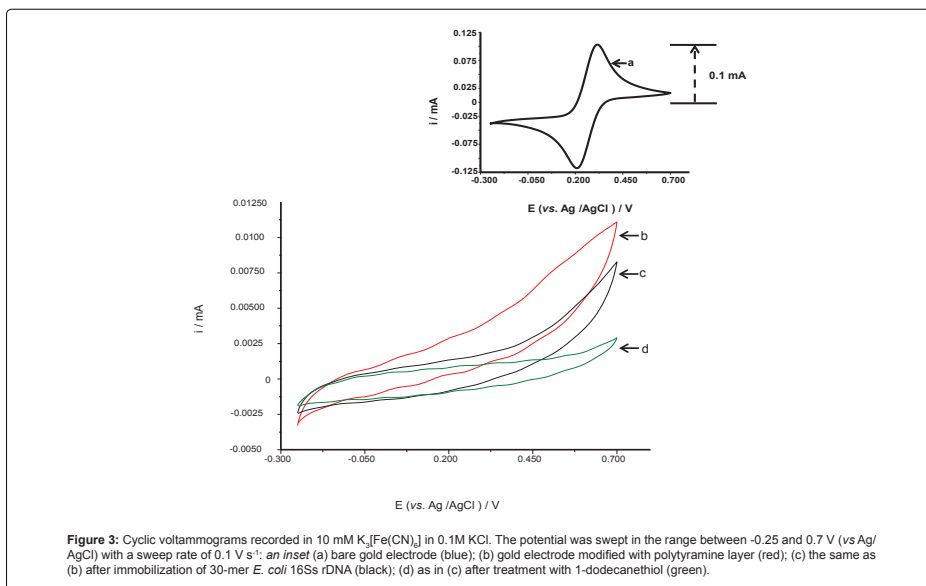
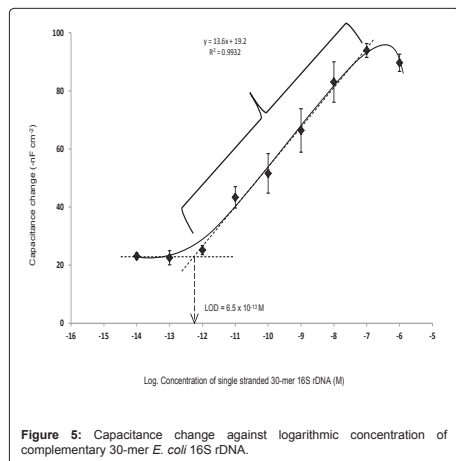
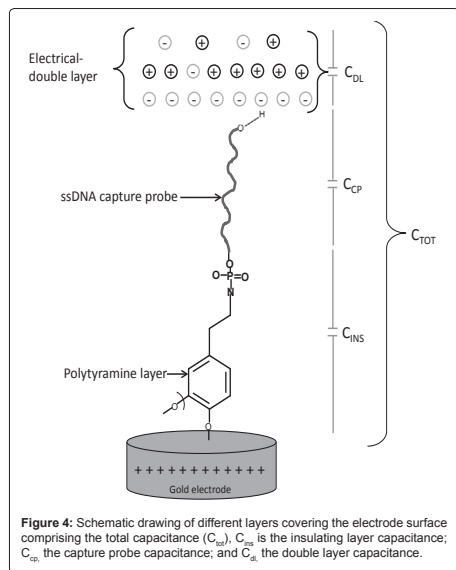


**Figure 3:** Cyclic voltammograms recorded in 10 mM  $K_3[Fe(CN)_6]$  in 0.1M KCl. The potential was swept in the range between -0.25 and 0.7 V (vs Ag/AgCl) with a sweep rate of 0.1 V  $s^{-1}$ : *an inset* (a) bare gold electrode (blue); (b) gold electrode modified with polytyramine layer (red); (c) the same as (b) after immobilization of 30-mer *E. coli* 16Ss rDNA (black); (d) as in (c) after treatment with 1-dodecanethiol (green).



to the logarithmic concentrations of the target ssDNA sample. The linear dynamic range and LOD of the capacitive DNA-sensor is shown in Figure 5.

The linear range vs. logarithmic concentration of capacitive DNA-sensor was between  $1.0 \times 10^{-12}$  to  $1.0 \times 10^{-7}$  M, with the sensitivity of

$13.6 \text{ nF cm}^{-2} \text{ M}^{-1}$  and LOD of  $6.5 \times 10^{-13}$  M, determined according to IUPAC recommendation [22]. The detection limit of the capacitive DNA-sensor reported here is in agreement with Sankoh et al. [23] who reported the limit of detection of  $2.0 \times 10^{13}$  M and linear range of  $1.0 \times 10^{-12}$  to  $1.0 \times 10^{-8}$  M. The obtained linear range from Figure 5 above, represents a slightly wider range than what is reported previously [23].

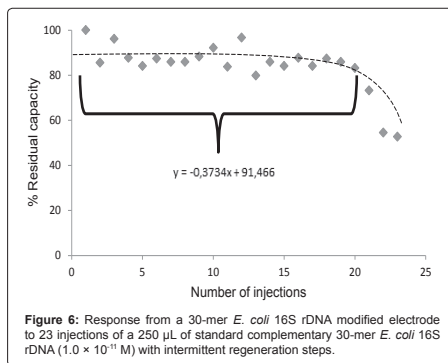
**Reproducibility:** The reproducibility of the analysis involving the 30-mer 16S rDNA-sensor chip was investigated. The residual capacity of the 30-mer 16S rDNA-sensor chip versus the number of injections is depicted in Figure 6. After the first 20 injections, the hybridization capacity of the 30-mer 16S rDNA-sensor chip retained about  $88 \pm 5\%$  of the original capacity.

Thus, the 30-mer 16S rDNA-sensor chip could be re-used with good reproducibility up to 20 times (relative standard deviation (RSD) of 5.8%). After 20 times of hybridization and regeneration (0.5 M NaOH), the sensor chip hybridization capacity dramatically decreased to ca 50%. The reduction of capacity may be caused by the loss of ssDNA capture probe on the sensor chip after repeated hybridization and regeneration cycles. Another explanation for the decrease of the DNA-sensor capacity could be microbial and nuclease contamination because the assay procedure was conducted under non-sterile condition.

#### Assay for real bacterial DNA sample

**Pre-capacitive DNA-sensor processing:** A diagnostic label-free capacitive DNA-sensor could be an extremely powerful and rapid tool for clinical diagnosis of microbial infections and genetic diseases, as well as for detecting microorganisms in environmental and food samples. The usefulness of the capacitive DNA-sensor technique is limited by the ability of the single-stranded DNA to rebind after dissociation which can lead to the false-negative results even if the DNA fragment of the targeted gene is abundantly present in the sample. Therefore, DNA sample processing prior to the assay is required. In this work, a commercial kit was used to extract genomic DNA samples from *E. coli* and *L. reuteri* cultures containing  $10^8$  cells  $\text{ml}^{-1}$  each.

The method is based on the selective adsorption of nucleic acids to a silica-gel membrane in the presence of high concentrations of chaotropic salts as it was described elsewhere [24]. The genomic DNA



was extracted in order to reduce background noise due to matrix effects of the sample by excluding other cellular components such as proteins, but also to get rid of RNA. Infact, the presence of RNA similar to the complementary targeted ssDNA probes could lead to the false-positive results. The DNA extraction step yielded genomic DNA with total concentrations of about 70 ng/ $\mu$ l.

The genomic DNA was fragmented to produce a suitable size of targeted complementary sequence (30-mer) with respect to the capture probe on the DNA-sensor chip. DNA fragments were produced using *Acil* restriction enzyme, of which according to Webcutter software *Acil* enzyme recognizes CCGC (-3/-1)<sup>^</sup> sites and cuts *E. coli* 16S rDNA at 17 different positions, including sites 374 and 421, between which the targeted complementary sequence is found. To demonstrate this concept, the PCR product of 16S rDNA was digested with *Acil* restriction enzyme and the fragments were run in gel electrophoresis. The results are shown in Figure 7; the product includes the targeted complementary fragment on *lane D* of about 44 bp in size.

When a double-stranded DNA is heated close to the boiling point of water, the hydrogen bonds that bind the two strands together in a double helix structure break and the DNA is separated into two complementary strands. However, if the denatured DNA sample is allowed to cool to between 50 and 60°C, the single strands will re-associate with their complementary partners and reform a double helix. Therefore, one of the challenges in preparation for DNA-sensor analysis is to prevent the separated single stranded DNA from re-annealing prior to analysis. Figure 8 represents a photograph of the electrophoretic gel, showing the results of two approaches investigated in this study by using the standard solutions of two complementary 30-mer 16S rDNAs: cooling approach; ice water (0.6°C) (lane #3), ethanol in cryostat (-12°C) (lane #4) and dry ice (-78°C) (lane #5); addition of ET SSB; (lane #6). Lane #7 is the same as lane #6 but followed by addition of formamide. All samples on the gel were run against single

stranded DNA (lane #1) and double stranded DNA (lane #2) as a positive and negative control, respectively, as well as DNA ladder (lane L).

The principle for immediate rapid cooling of denatured DNA is to cause a rapid aggregation to the individual generated single stranded DNAs and hence, preventing them from re-annealing. The application of rapid cooling on ice water to prevent re-annealing of single stranded DNA sample was previously reported [5]. In contrast, in the present study heat denaturation (95°C, for 5 min) followed by rapid cooling did not result in detectable ssDNA on the 3% agarose gel; as depicted in Figure 8, all the bands obtained from the rapid cooling approach; water ice (lane #3), cryostat (lane #4), and dry ice 5 (lane #5), migrated to the same position as that for double stranded DNA sample (lane #2), and it is found between 25 and 35 bp bands on the DNA ladder (L), which is equivalent to 30 bp. Hence, the rapid cooling approach could not produce a meaningful amount of ssDNA for analysis. Also, Thompson has previously reported that, chilling solution of denatured DNA at usual concentrations of 8 - 12 mg/ml did not result in aggregate formation [25]. He further demonstrated that, DNA aggregation positively is favoured by a high concentration and substantial length of a DNA. Therefore, a possible explanation for the obtained result could be the low concentration (14 ng  $\mu$ l<sup>-1</sup>) and short DNA sequence (30-mer) used in this study.

The band for heat-denatured DNA sample treated with ET SSB (lane #6) has migrated to the position of the 30-mer single stranded DNA (lane #1), which is equivalent to the band of about 25 bp on the DNA ladder (L). This study has verified that the heat-denatured DNA sample can be prevented from re-annealing by the addition of ET SSB. The interactions between single stranded DNA and the binding proteins (SSBs)-DNA was previously studied using surface plasmon resonance imaging [26], whilst the mechanisms of SSBs-DNA interaction was described well by Kunzelmann et al. [27]. The SSB prevents complementary ssDNA from re-annealing by binding specifically with high affinity to single-stranded DNAs [28]. The combination of electrostatic, hydrogen-bonding and stacking interactions from SSB to ssDNA forms the basis for ssDNA binding and specificity. However, the hydrophobic nature of stacking interactions provides the SSB with an additional strategy for ssDNA binding that does not require specialization of the nucleic acid-binding surface into specific DNA binding pockets or hydrogen-bonding patterns that would favour one sequence over another [29].

Then, one needs to remove ET SSB from ssDNA sample prior to injection into the DNA-sensor to allow the hybridization with the ssDNA-capture-probe on the sensor-chip. Therefore, the sample was mixed with formamide prior to injection such that the mobile phase contained a final concentration of 30% formamide. In the same figure (Figure 8), lane 7 shows that, the band for the denatured DNA sample that was treated with ET SSB to prevent re-annealing, but later on mixed with formamide to final concentration of 30% and left to re-associate, has migrated to the same position of that for 30-mer double stranded DNA (lane #2), suggesting that addition of formamide to final concentration of 30% was enough to denature and remove ET SSB from the ssDNAs without affecting a hybridization with the complementary probe.

Sadhu and Dutta [30] have demonstrated that, the addition of formamide to a mixture of complementary ssDNA solution to final concentration of 30%, did not affect the rate of hybridization [30]. Also, Knubovets et al. [31] have studied the behaviour of a protein in organic solvents and reported that, the protein (e.g. ET SSB) unfolds

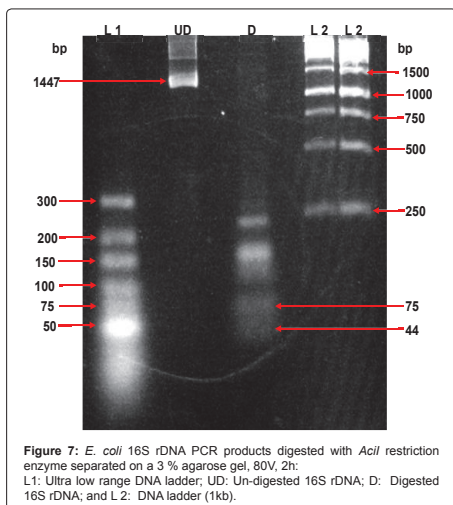
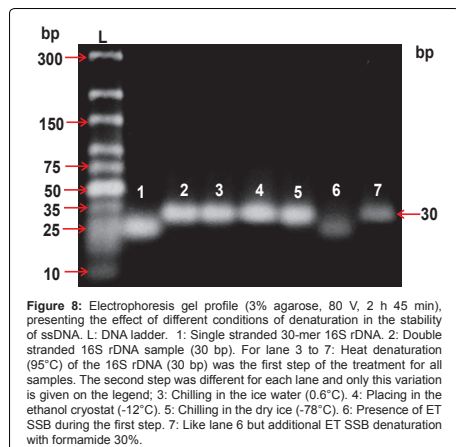


Figure 7: *E. coli* 16S rDNA PCR products digested with *Acil* restriction enzyme separated on a 3% agarose gel, 80V, 2h: L1: Ultra low range DNA ladder; UD: Un-digested 16S rDNA; D: Digested 16S rDNA; and L2: DNA ladder (1kb).





Applied no. of cells (mL <sup>-1</sup> )	Plate counting (CFU mL <sup>-1</sup> )	DNA sensor (-nF cm <sup>2</sup> )
10 <sup>5</sup>	(9.5 ± 0.5) × 10 <sup>4</sup>	84 ± 9
10 <sup>4</sup>	(7.8 ± 0.3) × 10 <sup>3</sup>	57 ± 5
10 <sup>3</sup>	(8.8 ± 0.2) × 10 <sup>2</sup>	40 ± 4
10 <sup>2</sup>	(9.2 ± 0.2) × 10 <sup>1</sup>	27 ± 4
10 <sup>1</sup>	ND	21 ± 3
10 <sup>0</sup>	ND	10 ± 1*

\*Below Limit of Detection. ND = Not Detected

**Table 2:** Comparison: Detection of *E. coli* cells at concentration range 1 to 10<sup>5</sup> cells ml<sup>-1</sup> using plate counting method and DNA based technique, capacitive DNA-sensor.

in solvents like formamide which competes for backbone hydrogen bonds. However, the addition of formamide in the sample should be done immediately before applying the sample on the DNA-sensor chip, the addition of formamide will cause the re-annealing if the sample is left for long time before applying on the DNA-sensor chip such that one loses ability to see the binding to the probe on the sensor surface.

**Analysis of *E. coli* using capacitive DNA-sensor versus plate counting:** Table 2 shows the results obtained by the capacitive DNA-sensor and plate counting techniques.

The capacitive DNA-sensor proved more sensitive than plate counting, with a detection limit of 10 *E. coli* cells ml<sup>-1</sup>. This is a value ten times lower than that detected by the plate counting technique (100 cells ml<sup>-1</sup>). In addition, the capacitive DNA-sensor can detect both viable and dead cells from the sample; which in many aspects could be regarded as advantageous. In fact, as other pathogens such as *Staphylococcus aureus*, *Bacillus cereus* and *Clostridium botulinum* are capable of producing toxins in the food sample [32] and thus, actively living bacterial cells do not need to be present for food illness to develop. However, even if the bacterial cell walls already have been destructed and the cells are dead, the DNA is stable and available in the sample. Hence, pathogens will be positively detected. In addition to that, capacitive DNA-sensor provides a detection solution for the problem of the bacteria in a viable but non-culturable (VBNC) state;

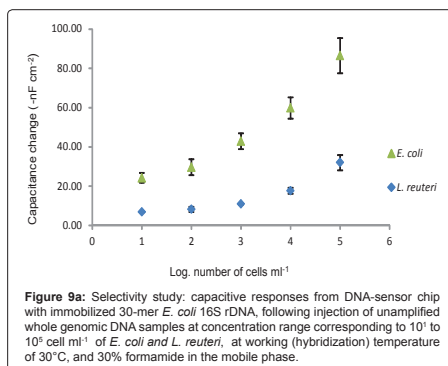
unlike for the plate counting method, which would only propagate viable and cultivable cells.

This capacitive DNA-sensor is even more sensitive than other biosensors reported in the literatures; Lijiang et al. [33] and Luo et al. [34], reported detection of approximately 2000 Cfu ml<sup>-1</sup> of *E. coli* O157:H7 and 40 Cfu ml<sup>-1</sup> of Enterobacteriaceae bacteria using a gold nanoparticle-enhanced piezoelectric biosensor and exonuclease III-enhanced-electrochemical DNA biosensor, respectively. Muhammad-Tahir and Alolcija (2003) [35] reported on an electrochemical sandwich immunoassay that could detect about 78 Cfu ml<sup>-1</sup> of *E. coli* O157:H7.

**Selectivity:** To investigate a cross reactivity of DNA-sensor chip at a family level; *L. reuteri* DSM 20016 (*Lactobacillaceae*) was used as a candidate, and both un-amplified genomic DNA and amplified 16S rDNA were tested. According to Blast analysis on NCBI (<http://blast.ncbi.nlm.nih.gov/Blast.cgi>) [36], *L. reuteri* DSM 20016 has 45 sites on its genomic DNA that match with the capture probe. Five of these matching sites were found to have thirteen matching bases with the capture probe, that make upto 43% of the total number of bases on the capture probes. Nevertheless, among the 45 matching sites, three are from its 16S rDNA sequence and were found to have only 7 matching bases with the capture probe, about 23% of the total bases on the capture probe.

Figure 9a presents the results of the capacitance change from the hybridization of equal concentration range of un-amplified single stranded genomic DNAs of *E. coli* and *L. reuteri*. The maximum capacitance change obtained from the injection of whole genomic DNA of *L. reuteri* corresponded to 10<sup>3</sup> cells ml<sup>-1</sup> is 32 ± 4 -nF cm<sup>2</sup>, which is almost three times lower than the response obtained from the injection of non-amplified whole genomic DNA of *E. coli* at equal concentration (84 ± 9 -nFcm<sup>2</sup>).

The response of *L. reuteri* (7-nF cm<sup>2</sup>) was 3 times lower than the response of *E. coli* genomic DNA (21 ± 3 -nF cm<sup>2</sup>) corresponding to concentration of 10<sup>1</sup> cells ml<sup>-1</sup>, which approaches the detection limit of the technique, indicating that the developed DNA chip has high selectivity to the *E. coli* DNA at the given working conditions: 30°C working temperature and 30% formamide added in the mobile phase. Several authors have reported the non-specific hybridization between capture probe and non-perfectly matched DNA probe [20,23,37-39].

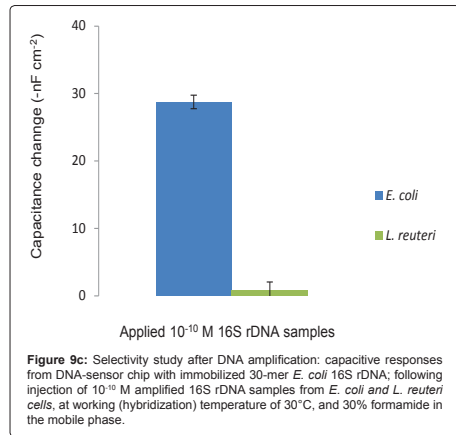
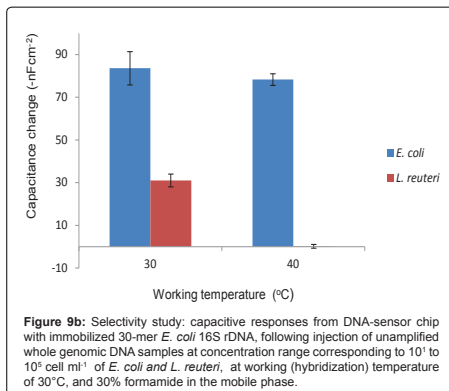


However, the selectivity of the DNA-sensor chip was further studied at elevated working temperature of 40°C, while keeping the same formamide concentration (30%) in the mobile phase, by injecting the un-amplified genomic DNA of *L. reuteri* and *E. coli* at a DNA concentration that is corresponding to  $10^5$  cell  $\text{ml}^{-1}$ . Similarly, the experiment was repeated at 30°C, while keeping other conditions the same. The results obtained from both working temperatures are compared as shown in Figure 9b.

The capacitance change obtained from injecting *L. reuteri* was efficiently reduced from,  $32\text{-nF cm}^{-2}$  (at 30°C), to  $0.14\text{-nF cm}^{-2}$  at the elevated working temperature of 40°C, without significantly altering the specific interaction of the applied *E. coli* BL21(DE3) genomic DNA. The responses due to specific hybridizations are 84 and  $78\text{-nF cm}^{-2}$  for working temperatures of 30 and 40°C, respectively. Besides, the observed non-specific signal ( $0.14\text{-nF cm}^{-2}$ ) at working temperature of 40°C, was below the lowest detection limit of the system. In particular, the hybridization was performed at very high stringency conditions; in other words, the presence of 30% formamide in the mobile phase, lowers the melting temperature of the complementary probes from  $57.5^\circ\text{C}$  to  $35.9^\circ\text{C}$ ; since for every 1% of formamide reduces the melting temperature by  $0.72^\circ\text{C}$  [30,40,41], consequently, raising the working temperature to 40°C, makes the hybridization temperature to be slightly higher than the melting temperature. These results suggest that one could discriminately detect *E. coli* by injecting its whole genomic DNA in the presence of whole genomic DNA of *L. reuteri* at 40°C hybridization temperature, and 30% formamide in the mobile phase, without involving any DNA amplification step.

To demonstrate that the non-selectivity observed at 30°C and 30% formamide was due to other genes on the whole *L. reuteri* DSM 20016 genomic DNA (with matching bases are more than 7), rather than its 16S rDNA sequence, the 16S rDNAs of *E. coli* and *L. reuteri* were each amplified and purified. Thereafter, the DNA material was injected in the capacitive DNA-sensor, at working temperature 30°C containing 30% formamide in the mobile phase. The results are shown in Figure 9c.

The capacitive DNA-sensor showed no significant responses towards *L. reuteri* 16S rDNA samples; on the other hand for *E. coli* 16S rDNA sample, a clear and significant signal was observed.



These results indicate that, the non-specific signals that were observed when the whole genomic DNA of *L. reuteri* was applied, were due to hybridization of the capture probe with other genes on the *L. reuteri* genomic DNA, probably those five genes with 13 matching bases to capture probes.

When whole genomic DNA is used for selective identification of a target bacteria based on its 16S rDNA (for example the hyper variable region), a capture probe should be design in such that, it does not match with 16S rDNA or any part of the genomic DNA of other bacteria. This may be a complex task, especially when a designed capture probe is as short as 15-30 mer. Particularly, since the shorter the sequence of the capture probe the higher probability of non-selectivity can be expected [20]. Otherwise, working close to the melting temperature of the capture probe could be the best alternative approach. Most of the sensor flow cell materials however do not withstand the temperature above  $45^\circ\text{C}$  [20]. Hence, the addition of formamide in the mobile phase has been demonstrated in this study, eliminating the need of equipment that tolerates higher temperature. Formamide reduces the thermal stability of DNA probes and hence, allows operation at suitable temperature for the sensor set ups with higher selectivity.

## Conclusion

We have reported a flow-based ultrasensitive PCR-free capacitive DNA-sensor for detecting the complementary sequence from unamplified Enterobacteriaceae genomic DNA. The reported sensor was relatively fast, 15 min hybridization time; and tenfold more sensitive than plate counting, and even more sensitive than other biosensors reported in the literatures; [33-35]. Also, for the first time we have demonstrated the alternative approach to bacterial DNA sample preparation for flow-based DNA analysis. The approach involved using an extreme thermostable ssDNA binding protein (ET SSB), to prevent re-annealing of a heat-denatured target ssDNA prior to analysis; and during analysis formamide integrated in the running buffer to denature ET SSB. In addition, the DNA-sensor chip could be reused with reproducibility up to 20 times with a RSD of <6%. The DNA-sensor chip has shown selectivity for Enterobacteriaceae DNA over

Lactobacillaceae DNA at elevated working temperature and presence of upto 30% formamide in the running buffer. Thus, it is practical to develop a PCR-free, sensitive and selective flow-based capacitive DNA-sensor for bacteria detection via specific DNA analysis.

The reported capacitive DNA-sensor has potential for several applications in the health care sector, in food/water quality control and in research institute laboratories. In addition, the reported DNA-sensor lays the groundwork for incorporating the method into an integrated system for in-field bacteria detection. However, in order to be able to use the DNA-sensor at physiological level, one needs to have a full understanding of the electrochemical and topographical properties of the surface of the DNA-sensor chip. Therefore, future work will be needed to give the necessary insight of electrode surface roughness properties, and packing arrangement of the insulating matrices and capture probes.

#### Acknowledgements

Financial support from World Bank supported project titled "Capacity Building in Science, Technology and Higher education" at University of Dar es Salaam, Tanzania, is gratefully acknowledged. Also, technical and logistical support from Higher education and Swedish Research Council is highly appreciated.

#### References

- Janda JM, Abbott SL (2002) Bacterial identification for publication: when is enough enough? *J Clin Microbiol* 40: 1887-1891.
- Taege AJ (2002) The new American diet and the changing face of foodborne illness. *Cleve Clin J Med* 69: 419-424.
- Madigan MT, Martinko JM, Stahl DA, Clark DP (2012) *Brock Biology of Microorganisms*. 13<sup>th</sup> edition, Pearson, San Francisco.
- Weenk GH (1992) Microbiological assessment of culture media: comparison and statistical evaluation of methods. *Int J Food Microbiol* 17: 159-181.
- Arora K, Prabhakar N, Chand S, Malhotra BD (2007) *Escherichia coli* genosensor based on polyaniline. *Anal Chem* 79: 6152-6158.
- Jiang D, Liu F, Liu C, Liu L, Pu X (2013) An Electrochemical Sensor Based on Allosteric Molecular Beacons for DNA Detection of *Escherichia coli*. *O157:H7*. *Int J Electrochem Sci* 8: 9390-9398.
- Rijal K, Mutharasan R (2013) A method for DNA-based detection of *E. coli* O157:H7 in a proteinous background using piezoelectric-excited cantilever sensors. *Analyst* 138: 2943-2950.
- Patel MK, Solanki PR, Kumar A, Khare S, Gupta S, et al. (2010) Electrochemical DNA sensor for *Neisseria meningitidis* detection. *Biosens Bioelectron* 25: 2586-2591.
- Pang S, Gao Y, Li Y, Liu S, Su X (2013) A novel sensing strategy for the detection of *Staphylococcus aureus* DNA by using a graphene oxide-based fluorescent probe. *Analyst* 138: 2749-2754.
- Hsu SH, Lin YY, Lu SH, Tsai IF, Lu YT, et al. (2013) Mycobacterium tuberculosis DNA detection using surface plasmon resonance modulated by telecommunication wavelength. *Sensors (Basel)* 14: 458-467.
- Naravani R, Jamil K (2005) Rapid detection of food-borne pathogens by using molecular techniques. *J Med Microbiol* 54: 51-54.
- Ye Y, Ju H (2003) DNA Electrochemical behaviours, Recognition and Sensing by Combining with PCR Technique. *Sens* 3: 128-145.
- Rådström P, Knutsson R, Wolffs P, Lövenklev M, Löfström C (2004) Pre-PCR processing: strategies to generate PCR-compatible samples. *Mol Biotechnol* 26: 133-146.
- Jarżab A, Gorska-Fraczek S, Rybka J, Witkowska D (2011) Enterobacteriaceae infection - diagnosis, antibiotic resistance and prevention. *Postepy Hig Med Dosw* 65: 55-72.
- Mahadhy A, Ståhl-Wernersson E, Mattiasson B, Hedström M (2014) Use of capacitive affinity biosensor for sensitive and selective detection and quantification of DNA- A model study. *Biotechnol Rep* 3: 42-48.
- Teeparuksapun K, Hedström M, Wong EY, Tang S, Hewlett IK, et al. (2010) Ultrasensitive detection of HIV-1 p24 antigen using nanofunctionalized surfaces in a capacitive immunosensor. *Anal Chem* 82: 8406-8411.
- Tichoniuk M, Ligaj M, Filipiak M (2008) Application of DNA Hybridization Biosensor as a Screening Method for the Detection of Genetically Modified Food Components. *Sens* 8: 2118-2135.
- Strober W (2001) Monitoring cell growth. *Curr Protoc Immunol*.
- Sutton S (2011) Accuracy of Plate Counts. *J Valid Technol* 17: 42-46.
- Berggren C, Bjarnason B, Johansson G (2001) Review: Capacitive Biosensors. *Electroanal* 13: 173-180.
- Rivera-García J, Cabrera CR (2007) Self-assembled monolayers of 6-mercapto-1-hexanol and mercapto-n-hexyl-poly(OT)18-fluorescein on polycrystalline gold surfaces: An electrochemical impedance spectroscopy study. *Electroanal Chem* 605: 145-150.
- Buck RP, Lindner E (1994) Recommendations for Nomenclature of Ion-selective Electrodes. *Pure Appl Chem* 66: 2527-2536.
- Sankoh S, Samanman S, Thipmanee O, Numnuam A, Limbut W, et al. (2013) A comparative study of a label-free DNA capacitive sensor using a pyrrolidiny peptide nucleic acid probe immobilized through polyphenylene diamine and polytyramine non-conducting polymers. *Sens Actuators B* 177: 543-554.
- Melzak KA, Sherwood CS, Turner RFB, Haynes CA (1996) Driving Forces for DNA Adsorption to Silica in Perchlorate Solutions. *J Colloid Interface Sci* 181: 635-644.
- Thompson WF (1976) Aggregate formation from short fragments of plant DNA. *Plant Physiol* 57: 617-622.
- Brockman JM, Frutos AG, Corn RM (1999) A Multistep Chemical Modification Procedure to Create DNA Arrays on Gold Surfaces for the Study of Protein-DNA Interactions with Surface Plasmon Resonance Imaging. *J Am Chem Soc* 121: 8044-8051.
- Kunzelmann S, Morris C, Chavda AP, Eccleston JF, Webb MR (2010) Mechanism of interaction between single-stranded DNA binding protein and DNA. *Biochemistry* 49: 843-852.
- Jain S, Zweig M, Peeters E, Siewering K, Hackett KT, et al. (2012) Characterization of the single stranded DNA binding protein SsbB encoded in the *Gonococcal Genetic Island*. *PLoS One* 7: e35285.
- Shamoo Y (2001) Single-stranded DNA-binding Proteins. eLS.
- Sadhu C, Dutta S, Gopinathan K (1984) Influence of formamide on the thermal stability of DNA. *J Biosci* 6: 817-821.
- Knubovets T, Osterhout JJ, Kilbanov AM (1999) Structure of lysozyme dissolved in neat organic solvents as assessed by NMR and CD spectroscopies. *Biotechnol Bioeng* 63: 242-248.
- Adams MR, Moss MO (2008) *Food Microbiology*, 3<sup>rd</sup> Edition, Royal Society of Chemistry, Cambridge.
- Lijiang W, QingShan W, ChunSheng W, Zhao-Ying H, Jian J, et al. (2008) The *Escherichia coli* O157:H7 DNA detection on a gold nanoparticle-enhanced piezoelectric biosensor. *Chin Sci Bull* 53: 1175-1184.
- Luo C, Tang H, Cheng W, Yan L, Zhang D, et al. (2013) A sensitive electrochemical DNA biosensor for specific detection of Enterobacteriaceae bacteria by Exonuclease III-assisted signal amplification. *Biosens Bioelectron* 48: 132-137.
- Muhammad-Tahir Z, Alolici EC (2003) Fabrication of a Disposable Biosensor for *Escherichia coli* O157:H7 Detection. *Sens J IEEE* 3: 345-351.
- NCBI (2013) Basic Local Alignment Search Tool.
- Carrara S, Gürkaynak FK, Guiducci C, Stagni C, Benini L, et al. (2007) Interface Layering Phenomena in Capacitance Detection of DNA with Biochips. *Sens Transducers J* 76: 969-977.
- Tombelli S, Minunni M, Mascini M (2005) Piezoelectric biosensors: Strategies for coupling nucleic acids to piezoelectric devices. *Methods* 37: 48-56.
- Yu CJ, Wan Y, Yowanto H, Li J, Tao C, et al. (2001) Electronic detection of single-base mismatches in DNA with ferrocene-modified probes. *J Am Chem Soc* 123: 11155-11161.
- Yilmaz LS, Loy A, Wright ES, Wagner M, Noguera DR (2012) Modeling formamide denaturation of probe-target hybrids for improved microarray probe design in microbial diagnostics. *PLoS One* 7: e43862.
- McConaughy BL, Laird CD, McCarthy BJ (1969) Nucleic acid reassociation in formamide. *Biochemistry* 8: 3289-3295.

## Paper III



# Comparison: Polytyramine-Film and 6-Mercaptohexanol-Self-Assembled Monolayers as the Immobilization Layers for a Capacitive DNA-Sensor-chip

Ally Mahadhy<sup>1</sup>, Bo Mattiasson<sup>1,2</sup>, Eva StåhlWernersson<sup>1</sup>, Martin Hedström<sup>1, 2\*</sup>

<sup>1</sup>Department of Biotechnology, Lund University, P.O. Box 124, SE-22100 Lund, Sweden.

<sup>2</sup>CapSenze HB, Medicon Village, SE-22838 Lund, Sweden.

\*Corresponding author. Tel.: +46 46-222 75 78; fax: +46 46-222 47 13. E-mail address: *Martin.Hedstrom@biotek.lu.se*

## Abstract

Performance of a biosensor is in part associated with the properties of immobilization layer on the sensor-chip. In this study sensor-chips were modified with two different immobilization layers, polytyramine (Pty)-film and 6-mercaptohexanol (MCH)-self-assembled monolayer (SAM). The physical, electrochemical and analytical properties of Pty-film and MCH-SAM modified sensor-chips were studied and compared. The study was conducted using atomic force microscope, cyclic voltammetry and capacitive DNA-sensor system (CapSenze™ Biosystem).

Results obtained by AFM and CV indicated that, Pty-film on the sensor-chip possesses better insulating properties and provides more spaces for immobilization of capture probe (ssDNA) than MCH-SAM on the sensor-chip. A Capacitive DNA-sensor hosting Pty-ssDNA modified sensor-chip displayed higher sensitivity and larger signal amplitude than that of the MCH-ssDNA modified sensor-chip. The linearity responses for Pty-ssDNA and MCH-ssDNA modified sensor-chips were obtained at log concentration ranges, equivalent to  $10^{-12}$  to  $10^{-8}$  M and  $10^{-10}$  to  $10^{-8}$  M, with detection limits (LODs) of  $4.0 \times 10^{-13}$  M and  $7.0 \times 10^{-11}$  M of target ssDNA, respectively. Pty-ssDNA and MCH-ssDNA sensor-chips exhibited notable selectivity at hybridization temperature of 50 °C. However, in MCH-ssDNA modified sensor-chip, the signal amplitude for the target DNA was reduced by almost 20 %. In contrast, Pty-ssDNA modified sensor-chip, the signal amplitude for target DNA was slightly affected (less than 5 %).

**Key words:** Polytyramine; 6-mercaptohexanol; Sensor-chip; Immobilization; Atomic Force Microscopy; Self-assembled monolayer; Electropolymerization.

## 1. Introduction

The physical and chemical properties of a sensor-chip surface determine the selectivity, sensitivity and stability of an electrochemical biosensor. Consequently, different immobilization layers have been used for fabrication of biosensor gold-sensor-chip surfaces. The most reported immobilization layers for fabrication of biosensor gold-sensor-chip surfaces are polymers of both, conducting polymer for example, polypyrrole (Ates, 2013; Malhotra et al., 2006; Kros et al., 2005; Peng et al., 2004) and non-conducting polymer, for example polytyramine (Pty) (Mahadhy et al., 2014a; Mahadhy et al., 2014b; Lebogang et al., 2014, Sankoh et al., 2013; Labib et al., 2010; and Teeparuksapun et al., 2010); as well as self-assembled monolayers (SAMs) of mercapto-containing organosilanes (Campuzano et al., 2006; Fu et al., 2005; Piwonski et al., 2005; Choi et al., 2004; Blasini et al., 2003; and Park and Weaver, 2002) and organosulfur compounds (Teeparuksapun et al., 2012; Labib et al., 2009; Zhao et al., 1999; and Limbut et al., 2006). A major area of concern is modification of the sensor-chip with a layer that provides active groups for immobilization of biomolecules in a defined manner, such that steric hindrance between molecules and their binding counterparts can be avoided. In capacitive biosensor measurements, insulating property of the immobilization layer is also an important factor. The surface of sensor-chip is designed to be highly insulated in a way that the capacitive biosensor system can be described as simple model circuit, RC-circuit (Erlandsson et al., 2014). The RC model fits well with capacitive measurements using an exponential decay current-curve (Berggren et al., 1999). Moreover, if the sensor-chip is not sufficiently insulated, ions can move through the layer and causing a short circuit in the system, which leads to a deformed or omitted signal (Erlandsson et al., 2014).

Here we report results from a study where two different chemistries, electropolymerization of Pty-film and adsorption of 6-mercaptohexanol (MCH)-SAM were used for modification of gold-sensor-chip surfaces for capacitive DNA-sensor analysis. Properties of the modified gold sensor-chip surfaces were characterised by three different approaches: i) electrochemical characterisations, using cyclic voltammetry, CV (AUTOLAB, Utrecht, Netherlands) and CapSense™ Biosystem (CapSense HB, Lund, Sweden) measurements for determining insulating and hydrophobicity properties; ii) topographical characterisations using atomic force microscopy, AFM, (XE-100 Park system, Suwon, Korea) for the quality and uniformity of the sensor surface layer directly by imaging the surface, and iii) analytical characterisations using CapSense™ Biosystem when selectivity, sensitivity and re-usability were also determined and compared. The aim was to determine the immobilization layer that offers the best insulating properties and enough active sites for immobilization of capture probe as well as excellent analytical characteristics.

## 2. Materials and methods

### 2.1 Materials

Two complementary single-stranded 30-mer oligonucleotides: capture probe, 5'-GAGTAAAGTTAATACCTTTGCTCATTGACG-3'; and target probe, 3'-CTCATTTC AATTATGGAAACGAGTAACTGC-5' were obtained from Intergrated DNA Technologies, Inc. (Leuven, Belgium). Tyramine, *N*-hydroxysuccinimide (NHS), *N*-(3-dimethylaminopropyl) *N*-ethylcarbodiimide hydrochloride (EDC), 6-mercaptohexanol (MCH) and 1-dodecane thiol were obtained from Sigma-Aldrich (Steinheim, Germany), while sodium hydroxide and absolute ethanol were obtained from VWR international (Leuven, Belgium). Regeneration solution and buffers and were prepared in ultrapure water (Millipore purification system, Massachusetts, USA), filtered through a 0.22  $\mu\text{m}$  membrane and degassed prior to use.

### 2.2 Methods

#### 2.2.1 *Cleaning and modification of sensor-chips*

In this study the custom-made 3 mm diameter disposable gold electrodes from Academic workshop (Linköping University, Sweden) were used as sensor-chips. The sensor-chips were cleaned in acetone, ethanol and finally in piranha solution as described elsewhere (Mahadhy et al., 2014b),

The modification with Pty-film was made by coating the cleaned sensor-chip with Pty-film. The coating of the sensor-chip was done by electropolymerization of tyramine on the sensor-chip surface using CV (Teeparuksapun et al., 2010). The coated sensor-chip was then rinsed with ultrapure water to remove any loosely bound polymer.

The modification with MCH was made by adsorption of SAMs of MCH on the cleaned sensor-chip. The sensor-chip was dipped in 3.7 mM MCH solution (in ethanol) for 1 h, followed by rinsing with ultrapure water to remove any loosely bound MCH (Zhao et al., 1999).

#### 2.2.2 *Immobilization of capture probe on the modified sensor-chips*

Each one, Pty and MCH modified sensor-chips were placed on the petri dish. Then, a 10  $\mu\text{L}$  of 10  $\mu\text{M}$  capture probe in 10 mM potassium phosphate buffer (PB) solution, pH 7.2, containing 5 mM EDC and 8 mM NHS was dropped on each sensor-chip surface (Tichoniuk et al., 2008). The sensor-chips were then left at room temperature for 2 h.

The terminal phosphate group of the capture probe (ssDNA) were covalently coupled to either Pty-film *via* primary amine group or MCH-SAM *via* hydroxyl group, on their respective modified sensor-chip surfaces. The DNA phosphate group bound to primary amine and hydroxyl groups to form phosphoramidate and



phosphate ester bonds, respectively (Zhao et al., 1999). After immobilization, DNA modified sensor-chips were rinsed with ultrapure water, and finally the sensor-chips were immersed in 1-dodecanethiol (10 mM in ethanol) for 20 min in order to block pinholes on the affinity surface (Mahadhy et al., 2014a; Mahadhy et al., 2014b). The sensor-chips were stored at 4 °C until use.

Fig. 1a and 1b show schematically summarized modification procedures of the Pty-film- and MCH-SAM-modified sensor-chip surfaces, respectively.

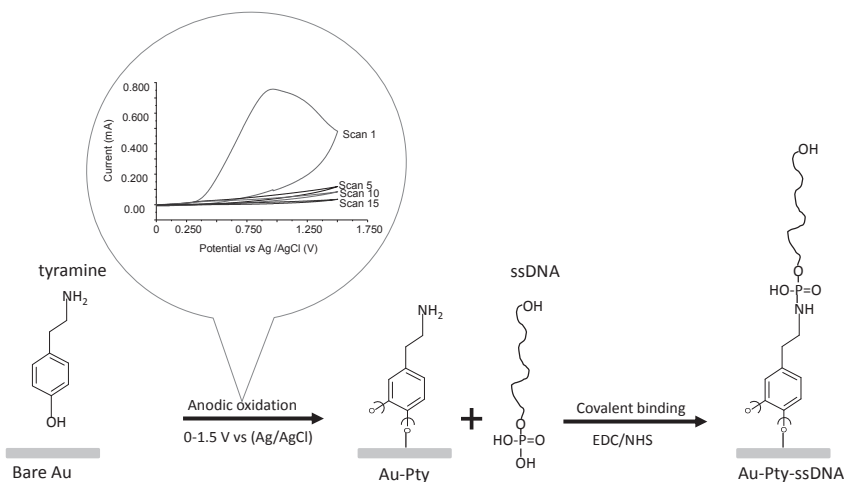


**Fig. 1a:** Sensor-chip surface was modified with Pty-film and followed by addition of ssDNA to form phosphoramidate ester bond. The inset shows the reduction in anodic peak current during electropolymerization of tyramine on the sensor-chip surface (scan numbers 1, 5, 10 and 15).

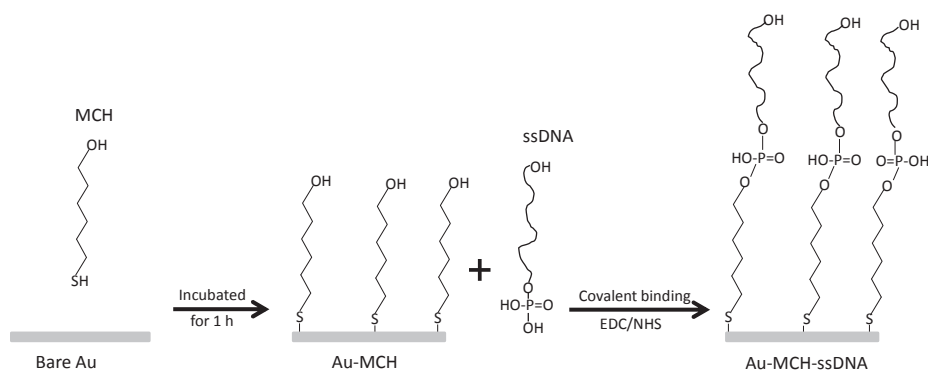


**Fig. 1b:** Sensor-chip surface was modified with MCH-SAM and followed by addition of ssDNA to form phosphate ester bond.

### 2.2.3 Electrochemical characterizations

The surfaces of the sensor-chips were electrochemically characterized, before and after chemical modifications, as well as after immobilization of ssDNA on the surfaces. The efficiency of the formation of modification layers on the sensor-chip surfaces can be described in terms of surface coverage, which can be estimated by either comparing the redox peaks between the modified- and bare-gold sensor-chips using CV in  $\text{Fe}(\text{CN})_6^{-3/-4}$  (Mahadhy et al., 2014a; Mahadhy et al., 2014b), or comparing the areas of the gold oxide (AuO) reduction peaks for the modified and bare gold sensor-chips using CV in 0.1 M  $\text{H}_2\text{SO}_4$  (Sabatani et al., 1987). Additionally, the sensor-chip surface coverage could be known by calculating the difference in the electric charges exchanged during the reduction of AuO for bare and modified- sensor-chip surfaces. The exchanged electric charges were calculated using General Purpose Electrochemistry System (GPES) software. The AuO reduction peaks for bare and modified gold sensor-chips were integrated, and the percentage coverage of a modified gold sensor-chip surface was determined as shown in Eq. 1.

$$\% \text{ Surface coverage} = \frac{Q_{\text{Bare}} - Q_{\text{Mod}}}{Q_{\text{Bare}}} \quad (1)$$

where  $Q_{\text{Bare}}$  and  $Q_{\text{Mod}}$  ( $\text{C cm}^{-2}$ ) are quantities of the exchanged electric charges in the reduction of AuO for bare and modified sensor-chip surfaces, respectively.

In the analytical step, higher temperatures are desirable to enhance the selectivity of the DNA-sensor. For that reason a predictable pattern describing the capacitance change due to temperature elevation for interface modified sensor-chip is essential. Therefore, the capacitances of the modified and bare sensor-chips were studied at room temperature (RT, 23 °C) and at elevated temperature (50 °C) for 30 min using the CapSense™ Biosystem.

### 2.2.4 Atomic force microscopy

The surface topography of the non-modified- and modified-sensor-chips in air was mapped by contact mode AFM at ambient temperature using a contact cantilever, PPP-CONSTCR (Park system, Suwon, Korea), with nominal resonance frequency of 23 kHz, thickness of 1  $\mu\text{m}$  and force constant of 0.2  $\text{N m}^{-1}$ . Imaged area for each sample was 5  $\mu\text{m}$  x 5  $\mu\text{m}$ . However, the surface topography of the modified sensor-chips that contained capture probe (ssDNA), was instead mapped by non-contact mode AFM, using a cantilever PPP-NHCR (Park system, Suwon, Korea), with thickness 4  $\mu\text{m}$ , resonance frequency in air of 330 kHz and force constant 42  $\text{N m}^{-1}$ . In non-contact mode AFM, the imaged area for each sample was 1  $\mu\text{m}$  x 1  $\mu\text{m}$ .

A comprehensive analysis of sample surface properties was made using principal amplitude parameters such as the average roughness ( $R_a$ ), ten-point mean height roughness ( $R_z$ ), root mean square roughness ( $R_q$ ) and peak to valley roughness

( $R_{pv}$ ). The mentioned parameters quantify the surface properties and provide valuable insight regarding quality of the layer on the surface (Raposo et al., 2007).

## 2.2.5 Capacitance measurements

### 2.2.5.1 Experimental set up

The current pulse-capacitance measurements were performed using an automated sequential injection flow system (CapSense™ Biosystem) (Fig. 2).

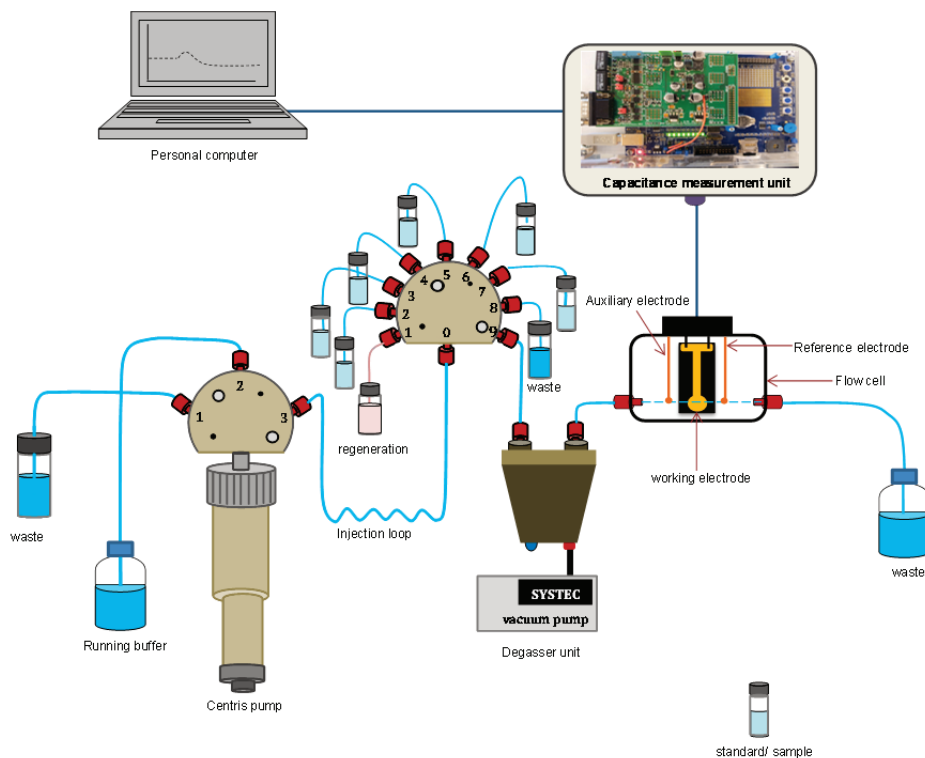


Fig. 2: Schematic drawing of a CapSense™ Biosystem coupled with a personal computer.

The CapSense™ Biosystem consists of a centris pump in built with a 3-port valve, which in turn is connected to a 9-port valve *via* an injection loop. It also consists of a degasser unit, a three-electrode-flow-cell, and a CapSense-capacitance measurement unit (Erlandsson et al., 2014). The port #1 of the 3- port valve is used to empty the waste in the initialization of the centris pump. Port #2 is connected to the working buffer (PB) solution in which the syringe plunger will suck and eject the PB solution. The 9-port valve is used to automatically and serially inject a 250  $\mu$ L of a standard/sample and regeneration solutions into the flow cell via a degasser unit. The working buffer is continuously supplied to the flow cell by the centris pump. The flow cell is connected to the CapSense-capacitance measurement unit, controlled by the software, and equipped with a

resistometer. The resistometer is connected between a potentiostat and the flow cell. Hence, an interrupted constant current pulse is supplied to the flow cell. The system has an inbuilt analog-to digital converter (ADC) unit. Therefore the capacitance across the sensor-chip/solution interface is automatically determined by the system from the slope of the potential curve (voltage *vs.* time) using Eq. 2, as described elsewhere (Erlandsson et al., 2014).

$$\text{Since, } C = \frac{Q}{V} = \frac{idt}{dV} = \frac{i}{u} \quad (2)$$

where  $C$ ,  $Q$  and  $V$  are the total capacitance, accumulated charge and built-in potential across the sensor-chip/solution interface, respectively;  $i$  is the electrical current supplied to the sensor-chip, and  $t$  is the current pulse period. A  $u$  is the slope of the linear curve,  $V$  plotted against  $t$ . The total capacitance,  $C$ , across the sensor-chip/solution interface is the sum of several capacitors in series Eq. 3 (Mahadhy et al., 2014a; Labib et al., 2009).

$$\frac{1}{C} = \frac{1}{C_{mat}} + \frac{1}{C_{cap}} + \frac{1}{C_{dl}} \quad (3)$$

where  $C_{mat}$  is the capacitance of the insulating layer on the sensor-chip surface,  $C_{cap}$  is the capture probe-capacitance and  $C_{dl}$  is the capacitance of the diffusion layer.

When buffer is continuously pumped into the system and the current pulse is intermittently applied after every 60 seconds, the system will register a constant capacitance  $C$ , a baseline. However, introduction of target probe on the sensor-chip hosting capture probe will lead to hybridization reaction, which in turn results in a decrease of  $C$ . This is due to the displacement of the counter ions from the electrode surface, as well as reduction of the capture probe layer-dielectric constant (Mahadhy et al., 2014a).

## 2.2.6 Analytical characterizations

### 2.2.6.1 Sensitivity and selectivity and re-usability studies

Samples of the target probe was prepared in PB at concentrations,  $10^{-13}$ ,  $10^{-12}$ ,  $10^{-11}$ ,  $10^{-10}$ ,  $10^{-9}$ ,  $10^{-8}$ , and  $10^{-7}$  M. Each concentration was applied on the Pty-ssDNA and MCH-ssDNA modified sensor-chips in triplicate. The linear ranges and the limit of detections (LODs) of the Pty-ssDNA and MCH-ssDNA sensor-chips were determined as described elsewhere (Buck and Lindner, 1994).

For the selectivity study, the above experiments were repeated by injecting  $10^{-8}$  M of non-target probe at 23 °C and 50 °C. The capture probe was used as non-target probe. The results were compared with those obtained from injecting the target probe.

The sensor-chips with different insulating layers were evaluated for re-usability by repetitively applying  $10^{-9}$  M of the target probe followed by regeneration step after each assay up to 15 cycles.

### 3. Results and discussion

#### 3.1 Effect of different experimental conditions

The factors affecting the deposition of the Pty and MCH immobilization layers on the sensor-chip surfaces were previously optimized in order to optimize the immobilization of the capture probe and hence, maximizing the sensitivity of the capacitive DNA-sensor. The cyclic voltammograms (CVs) recorded in 0.1 M  $\text{H}_2\text{SO}_4$  were used to determine % surface coverage by using Eq. 1 (results are not shown).

For sensor-chips covered with Pty-film, the effect of number of cycles during the CV for electropolymerization of tyramine was investigated for 5, 10, 15, 20, and 30 cycles. The insulation of the sensor-chip surface was found to get improved between, 5 to 15 cycles; however, there was no significant difference after 15 cycles. Thus, 15 cycles were taken as the optimal number of cycles for electropolymerization of Pty on the sensor-chip surface.

For sensor-chips covered with MCH-SAM, different concentrations of MCH, solvents and incubation time were investigated. The investigated concentrations were; 3.7, 10 and 40 mM, the deposition of MCH on the sensor-chip surface was found to increase with concentrations for 15 min incubation time. However, there was no difference in the surface coverage among the investigated concentrations at incubation times: 1, 3 and 15 h. Also, MCH prepared in ethanol showed better insulation property compared to that prepared in ultrapure water. Therefore, 3.7 mM MCH prepared in ethanol and 1 h incubation time were selected as the optimum conditions for insulation of sensor-chip surface with MCH-SAM.

#### 3.2 Surface coverage and capacitance-baseline

Table 1 shows the percentages of surface coverage and capacitance-baselines for Pty- and MCH-modified surfaces at their optimum experimental conditions, with and without ssDNA.

Pty-film covered the sensor-chip surface by 2.5 times more than the surface covered by MCH-SAM. Even after immobilization of ssDNA on the Pty and MCH modified surfaces, the Pty-film-ssDNA displayed the better insulating property with % surface coverage of 2.5 times larger than MCH-ssDNA.

Table 1: Pty-film and MCH-SAM modified sensor-chip surfaces with their % coverage and capacitances

Parameter (s)	Pty only	MCH only	Pty-ssDNA	MCH-ssDNA
% surface coverage	65 ± 2	26 ± 2	75 ± 3	30 ± 2
Capacitance/ baseline (nF cm <sup>-2</sup> )	10790	8510	11040	9140

The recorded capacitance-baseline of a bare gold sensor-chip surface at RT was 10420 nF cm<sup>-2</sup>. It was slightly increased to 10790 nF cm<sup>-2</sup> following adsorption of Pty-film on the sensor-chip surface, suggesting that the Pty-film, which is a non-conducting polymer layer, has increased the dielectric property of the sensor-chip surface. One possible explanation is that, the sensor-chip surface became more hydrophilic after adsorption of Pty-film due to the Pty-primary amine (-NH<sub>2</sub>) groups on the sensor-chip surface. Thus, the electrical double layer (EDL) at the surface-solution interface is pulled much closer to the sensor-chip surface for the Pty-film modified sensor-chip, resulting in increased capacitance (Mahadhy et al., 2014a).

On the other hand, when MCH was deposited on the bare surface of the sensor-chip, the capacitances decreased from 10420 to 8510 nF cm<sup>-2</sup>. The decrease in capacitance is most likely due to the low dielectric constant (Rivera-Gandia and Cabrera, 2007) and the hydrophobicity nature of the MCH-SAM (Ladik et al., 2010). The hydrophobicity of MCH-SAM modified surface is explained by the presence of the hydrophobic long hydrocarbon chains. Such hydrophobic layer drives the EDL away from surface of the sensor-chip, hence resulting in a decrease in the capacitance-baseline (Mahadhy et al., 2014a). Ladik and his co-workers used a contact-angle goniometry to investigate the hydrophobicity of MCH on the gold surface. Their results showed that when only MCH was added on the gold slide the surface became more hydrophobic (Ladik et al., 2010).

In all cases the capacitances were observed to increase after immobilization of ssDNA. This is in agreement with Ladik et al., (2010) that ssDNA is very hydrophilic, and as such its adsorption on the surface of the sensor-chip made the surface to be hydrophilic, hence attracting the EDL closer to the surface of the sensor-chip, which resulted in an increase in the capacitance-baseline.

When Pty and MCH modified sensor-chips were subjected at 50 °C, they showed different patterns of capacitance-baseline behaviour (Fig. 3). Initially, the registered capacitance-baselines of both sensor-chips were observed to rapidly increase. Then, Pty modified sensor-chip attained a stable baseline after 10 min. The baseline is notably higher (670.8 ± 0.2 nF) than the initial value (630 nF). Although, the capacitance-baseline of MCH modified sensor-chip reached a maximum capacitance-baseline after 8 min, it was then followed by a rapid

decline to even lower capacitance-baseline ( $526 \pm 0.5$  nF) than the initial value (530 nF); a stable baseline was attained after almost 18 min. The initial increases in capacitance-baselines that were observed in both sensor-chips could be due to temperature equilibration between the sensor-chips and electrolyte solution. The observed stabilization of the capacitance-baseline of Pty modified sensor-chip after the initial capacitance-baseline increase is in good agreement with the observation in the previous study (Mahadhy et al., 2014a).

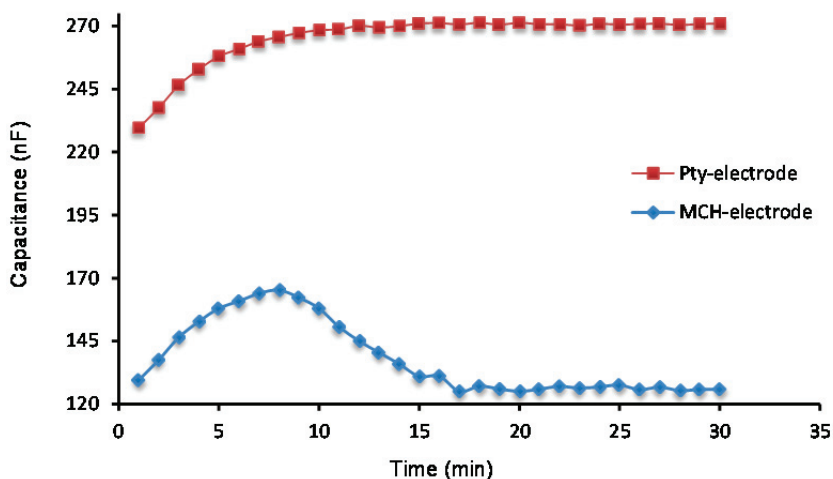


Fig. 3: Baselines for Pty and MCH modified sensor-chips at 50 °C for 30 min.

The possible explanation for the observed decrease in capacitance-baseline in MCH-modified sensor-chip after the initial capacitance-baseline increase could be the reorientation of the MCH-SAM at the collapsed sites of the sensor-chip (Bensebaa et al., 1998). The reorientation of the MCH-SAM resulted in an increase in the thickness of the MCH-SAM. As such, the sensor-chip surface getting more isolated against influence of the EDL, and therefore, the decrease of the capacitance was observed. Once the reorientation of the MCH-SAM has taken place, keeping the sensor-chip at the same temperature did not lead to further decrease of the capacitance.

### 3.3 Electrochemical properties

#### 3.3.1 Cyclic Voltammetry

The CVs for Pty-film and MCH-SAM modified sensor-chips with and without ssDNA are compared with a bare sensor-chip (Fig. 4 - 5b).

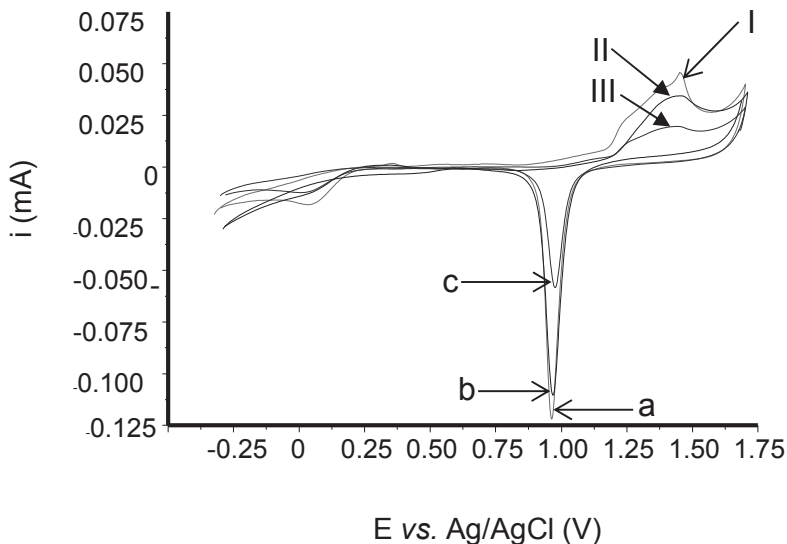


**Fig. 4:** Represents the reduction peaks of AuO for (a) bare- (b) MCH-modified- and (c) Pty-modified- sensor chips, with their Au oxidation peaks: I, II and III, respectively. The potential was swept in the range between, -0.3 to 1.7 V (*vs.* Ag/ AgCl) in 100 mM H<sub>2</sub>SO<sub>4</sub>, at a sweep rate of 0.1 V s<sup>-1</sup>.

Fig. 4 represents the CVs recorded in 0.1 M H<sub>2</sub>SO<sub>4</sub> for bare gold sensor chip, MCH-SAM- and Pty-film modified surfaces. The CVs used to compare the amount of electric charge exchanged during AuO reduction for the bare gold sensor-chip surface, MCH- and Pty- modified sensor-chip surfaces.

The bare sensor-chip surface displayed the highest AuO reduction peak of all (voltammogram, a). Following deposition of MCH-SAM (voltammogram, b) and Pty-film (voltammogram, c) on the sensor-chip surfaces brought about a decrease in the AuO reduction peaks. The observation indicates that, the presence of Pty/MCH layer on the gold electrode surface prevents the oxidation of gold electrode (see peaks I, II and III), resulting in a lower AuO reduction peak compared to the surface of the bare gold electrode. The magnitudes of the AuO reduction peaks followed the trend: bare- > MCH-SAM-modified- > Pty-film-modified- sensor-chip surface.

Fig. 5a and 5b represent the CVs for the redox process in Fe(CN)<sub>6</sub><sup>3-/4-</sup>, and Au oxidation/reduction process in 0.1 M H<sub>2</sub>SO<sub>4</sub>, respectively for the bare sensor-chip, the MCH-ssDNA- and Pty-ssDNA- modified sensor-chips. The significant decreases in redox peaks (Fig 5a) and AuO reduction peaks (Fig. 5b) were observed when the bare sensor-chip surfaces (voltammograms, a's) were compared with MCH-ssDNA (voltammograms, b's) and Pty-ssDNA (voltammograms, c's) modified sensor-chip surfaces in their respective figures.



The observed magnitudes of the redox and AuO reduction peaks followed the same trend as that observed in Fig. 4 when the sensor-chip surfaces were modified with MCH-SAM and Pty-film only i.e., bare- > MCH-ssDNA-modified- > Pty-ssDNA-modified-sensor-chip surface.

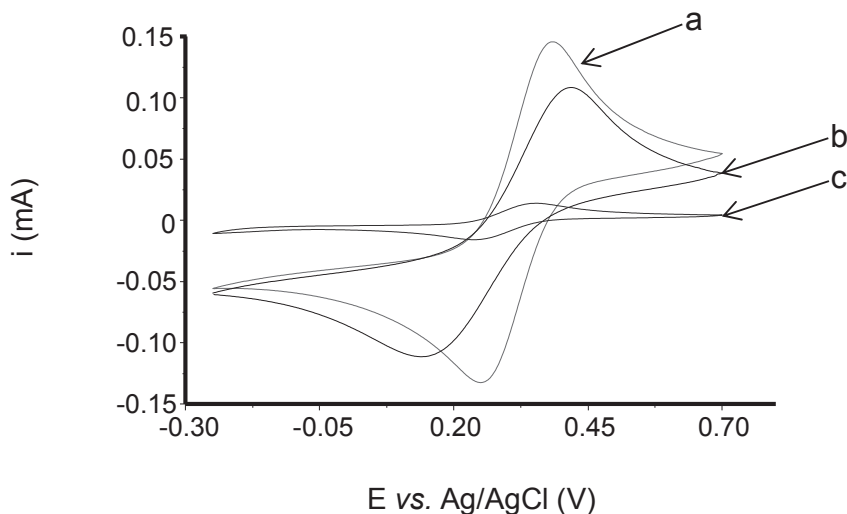


**Fig. 5a:** Cyclic voltammograms of (a) bare gold sensor-chip (b) gold sensor-chip modified with MCH-ssDNA (c) gold sensor-chip modified with Pty-ssDNA studied in 10 mM ( $K_3[Fe(CN)_6]$ ) in 100 mM KCl. The CV potential was swept at  $100\text{ mVs}^{-1}$  between a potential range of -300 to 700 mV (*vs.* Ag/AgCl).

The obtained electrochemical results demonstrate that, the Pty-film with or without ssDNA possess better insulating properties than MCH-SAM with or without ssDNA. This could be explained by the fact that electropolymerization of tyramine is not limited by the surface roughness (Strike et al., 1995); hence, it forms a strong adhering film on the surface (Losic et al., 2005). Unlike MCH-SAM whose adsorption and stability on the surface is critically dependent upon the preparation and cleanliness of the surface (Sabatani and Rubinstein, 1987). However, MCH offers advantages with respect to ease of preparation and analysis (Campuzano et al., 2006; Choi et al., 2004).

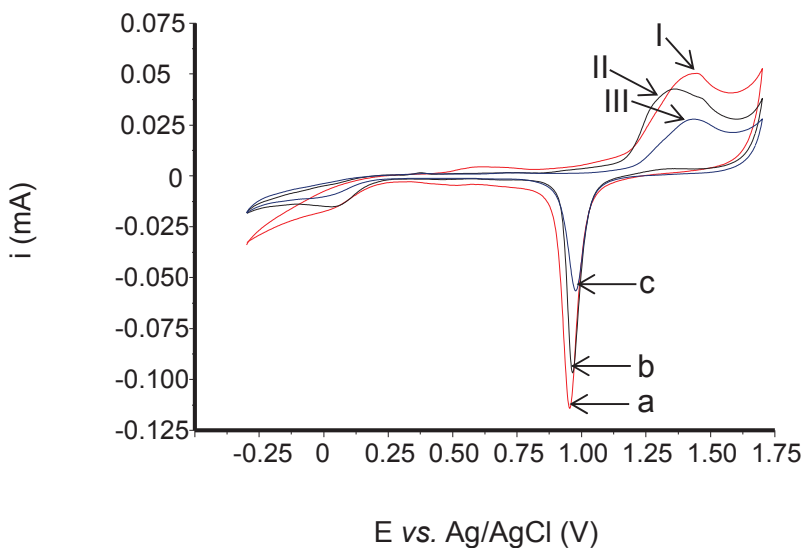


**Fig. 5b:** Represents the reduction peaks of AuO for (a) bare sensor-chip (b) sensor-chip modified with MCH-ssDNA and (c) sensor-chip modified with Pty-ssDNA with their Au oxidation peaks: I, II and III, respectively. The potential was swept in the range between, -300 to 1700 V (*vs.* Ag/AgCl) in 100mM H<sub>2</sub>SO<sub>4</sub>, at a sweep rate of 100 mV s<sup>-1</sup>.

### 3.4 Topographical analysis

The typical contact mode AFM images (scan size 5  $\mu\text{m}$  x 5  $\mu\text{m}$ ) for the bare, Pty-film and MCH-SAM gold sensor-chip surfaces with their peak profiles are shown in Fig. 6.

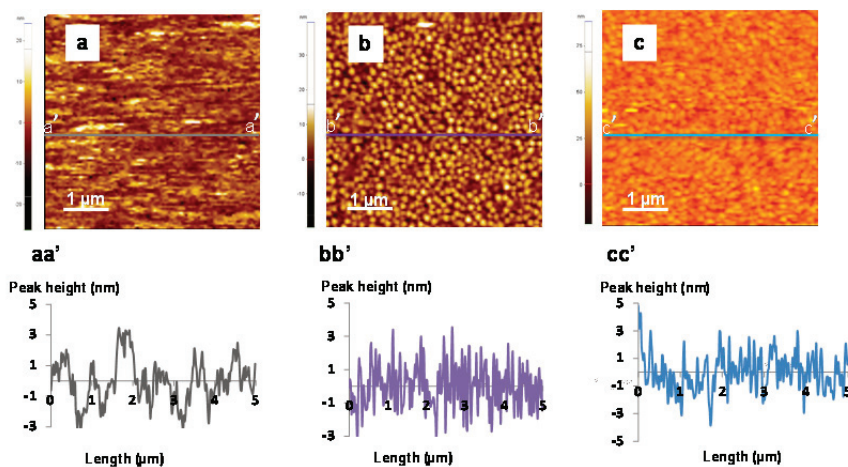


**Fig. 6:** The 5  $\mu\text{m}$  x 5  $\mu\text{m}$  AFM images tapped in contact mode: a) bare- (b) Pty-film-modified-, and (c) MCH SAM-modified- gold sensor-chips. The peak height profiles along the lines for (a), (b) and (c) are shown in the figures marked (aa'), (bb') and (cc'), respectively.

Topographic images showed the increase in roughness when sensor-chip surfaces were modified with Pty-film and MCH-SAM immobilization layers. The grain like features with white heads, and dark brown colour observed on the topographical images represent the peaks and depressions on the sensor-chip surfaces, respectively. Therefore, the bare gold sensor-chip surface is shown to be smoothest surface with the fewest peaks (Fig. 6a) of all three. Whilst, Pty-film modified sensor-chip surface (Fig. 6b), is said to be a rougher surface with more peaks than MCH modified sensor-chip surface (Fig. 6c).

The obtained information from topographical images is supported by the results obtained from peak height profiles analysis (Table 2).

**Table 2:** Roughness parameters of the sensor-chip surfaces

Surface	$R_a$ (nm)	$R_z$ (nm)	$R_q$ (nm)	$R_{pv}$ (nm)
Bare	2.90	14.50	3.35	16.00
Pty	3.60	20.40	4.60	25.10
MCH	3.10	17.50	3.85	21.70
Pty-ssDNA	3.80	14.00	4.60	18.30
MCH-ssDNA	2.50	11.30	3.20	15.70

Table 2 represents the surface peak profile analysis from Fig. 6. Variations of the surface roughness,  $R_a$ , and ten-point mean height roughness,  $R_z$ , values have same trend as the variations of root mean square roughness,  $R_q$  values for bare, Pty and MCH gold sensor-chip surfaces. The analysis showed the increase in roughness when the sensor-chip surface was modified with MCH-SAM and Pty-film, the  $R_a$  value increased from 2.90 for bare sensor-chip to 3.10 and 3.60 nm for MCH-SAM and Pty-film modified sensor-chip surfaces, respectively. The observed increase in the roughness for Pty-film modified sensor-chip agrees well with the results obtained in the taping mode (Sankoh et al., 2013; Teeeparuksapun et al., 2010). In addition, the  $R_q$  value for bare sensor-chip surface is relatively lower than that of MCH and Pty modified sensor-chip surfaces, which indicates that bare sensor-chip surface was the smoothest surfaces of all.

Peak to valley height,  $R_{pv}$  is also considered as a very important parameter since it gives a good description of the overall roughness of the surface. It may be simply defined as a vertical distance from the highest peak on the profile to the lowest valley over entire evaluation length of the profile (Vorburger, 2010). Table 2 also showed that, the  $R_{pv}$  values for the sensor-chip surfaces are in the following order: bare < MCH < Pty. For high  $R_{pv}$  value,  $R_z$  is also high due to the strong dependence of  $R_z$  on the peak heights and valley depths. Therefore, the  $R_z$  values

here indicated that MCH modified surface has less valley depths comparing to the Pty modified surface, but more than bare sensor-chip surface.

The results obtained from topographical images and peak height profile analysis prove the existence of self-organization nature of SAM molecules (MCH), which produce highly ordered smooth surface (Chaki et al., 2002). However, these findings suggest that Pty-film is not entirely self-limiting in growth as the electropolymerization of tyramine resulting into a rougher surface than that formed by MCH-SAM.

For Pty-ssDNA modified surface, there were more white spots observed on the surface (Fig. 7, A and A: 3D) than in MCH-ssDNA modified surface (Fig. 7, B and B: 3D).

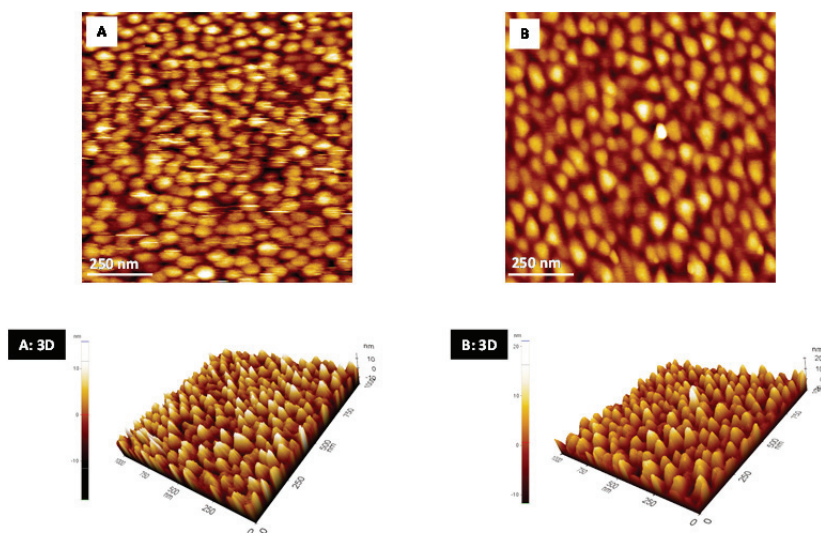


Fig 7: Non contact mode AFM images (scan size  $1\ \mu\text{m} \times 1\ \mu\text{m}$ ) of (A) gold sensor-chip surface after modified with Pty and coupled with ssDNA (B) gold sensor-chip surface after modified with MCH and coupled with ssDNA. The three dimensions (3D) images of (A) and (B) are shown in the figures marked (A: 3D) and (B: 3D), respectively.

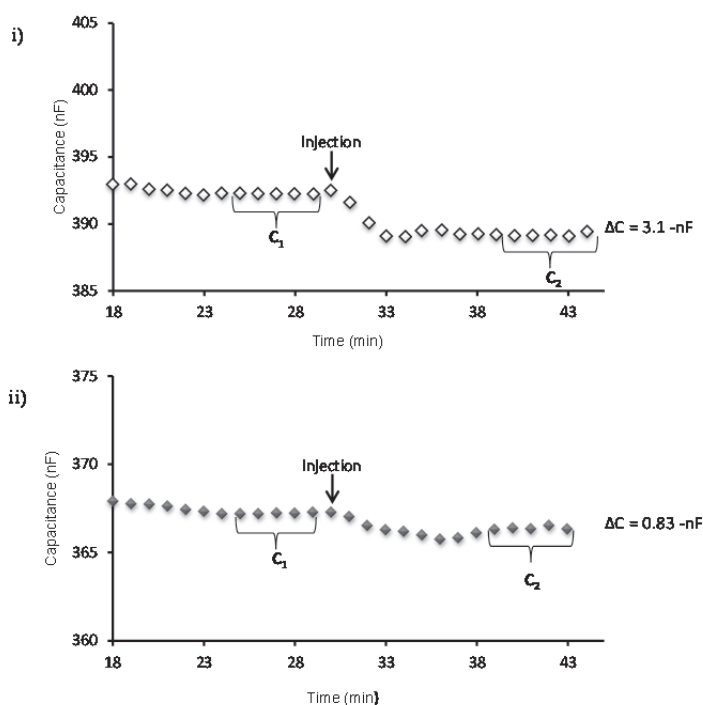
The white spots are believed to be ssDNA molecule peaks. Therefore Pty-ssDNA modified surface is said to be more densely packed with capture probe than the MCH-modified sensor-chip surface. Pty-film presents one reactive amine group per moiety, this group is easily protonated ( $-\text{NH}_3^+$ ). Such positively charged surface favours the immobilization of the negatively charged molecules like DNA. Hence, ssDNA molecules bearing negatively charged phosphate terminal functional groups were easily immobilized on the Pty-film, consequently a higher density of surface bond capture probe ssDNA (Tran et al., 2003). The observation was supported by the values of the roughness parameters obtained

from peak height profile analysis as shown on Table 2. The roughness factors of Pty modified sensor-chip increased after immobilization of capture probe ssDNA (Table 2). However, for MCH-modified sensor-chip, there was a decrease in surface roughness when capture probe ssDNA was immobilized onto it. One possible explanation could be that, the capture probe ssDNA was non-specifically adsorbed onto uncovered spaces of the MCH modified sensor-chip surface, resulting in a decrease in surface roughness. The defects on the MCH-SAM sensor-chip surface are mainly caused by a slow reorganization process. It usually requires some hours to maximize the molecules density and to reduce the defects on a sensor-chip surface (Chaki et al., 2002).

The AFM information indicate that, Pty-film offers a better sensor-chip surface coverage with a higher capture probe surface density than MCH-SAM.

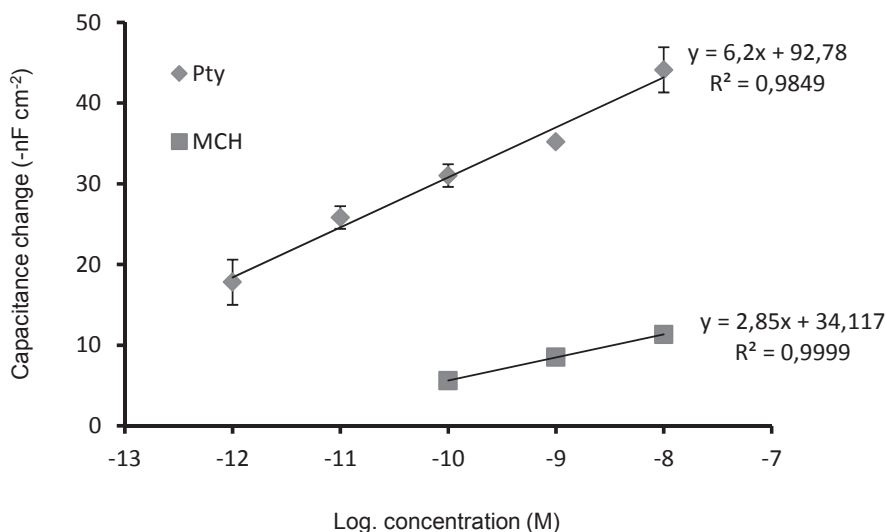
### 3.5 Sensitivity

Fig. 8a (i and ii) represents time-course graphs showing the capacitance changes (responses) from Pty- and MCH-ssDNA modified sensor-chips upon injection of 250  $\mu$ l of  $10^{-8}$  M target ssDNA at pH 7.2 (10 mM PB), respectively.



**Fig. 8a:** Time course graphs showing the responses from (i) Pty-ssDNA modified sensor-chip and (ii) MCH-ssDNA modified chip, to injection of 250  $\mu$ L of  $10^{-8}$  M target ssDNA.

The calibration curves of the capacitive DNA-sensor for Pty- and MCH-ssDNA modified sensor-chips in response to concentration of target ssDNA are depicted in Fig. 8b. The curves exhibited the linear patterns at log concentrations, equivalent to molar concentrations in the ranges of:  $10^{-8}$  to  $10^{-12}$  M for Pty modified surface and  $10^{-8}$  to  $10^{-10}$  M for MCH-modified surface, with LODs of  $4.0 \times 10^{-13}$  M and  $7.0 \times 10^{-11}$  M, respectively. The sensitivity and signal amplitude depend on the amount of the immobilized capture probe, ssDNA. Thus, these results complement the previously obtained results from electrochemical and topographical analyses, which suggested that Pty-film exhibited good insulating properties as well as provided much more spaces for immobilization of the capture probe that resulted in a higher capturing capacity. The higher capturing capacity led to the higher response signal and the lower LOD values, which are advantageous for capture assays involving small DNA molecules and for a sample with a very low concentration of target DNA molecules, respectively.



**Fig. 8b:** Calibration curves showing linearity range for target ssDNA hybridized with capture probe on the different sensor-chips modified with Pty- and MCH-ssDNA.

### 3.6 Selectivity

Fig. 9a shows the responses from Pty- and MCH-ssDNA sensor-chips to injection of equimolar concentrations of target and non-target samples at 23 °C (RT) hybridization temperature.

Although, a response from Pty-ssDNA modified sensor-chip to non-target ssDNA at 23 °C, was much higher ( $9.9 \pm 1.4$  - nF cm<sup>-2</sup>) than that obtained for

MCH-ssDNA modified sensor-chip ( $3.8 \pm 0.8$  - nF cm<sup>-2</sup>), still, this nontarget response is 25 % of a target response from the same sensor-chip, whilst, nontarget response from MCH-ssDNA sensor-chip accounts for 36 % of its target response. The Pty-film has favourable permselective properties (Yuqing et al., 2004), thus, preventing interfering species from approaching or contaminating the sensor-chip.

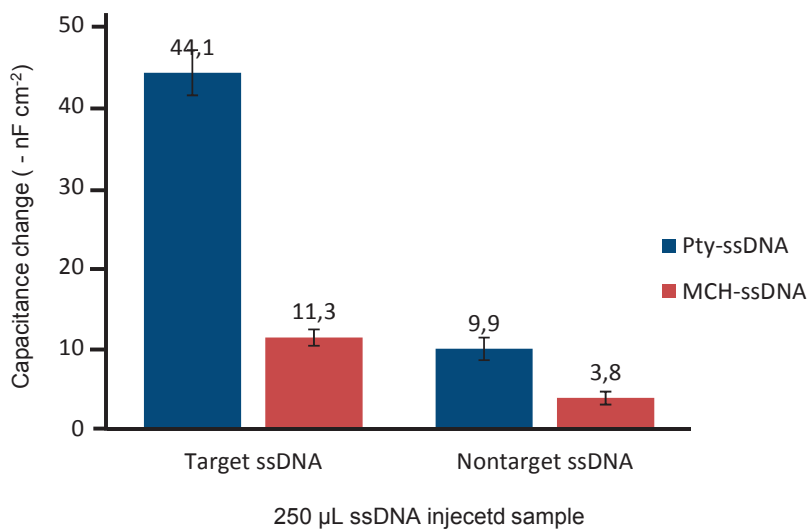
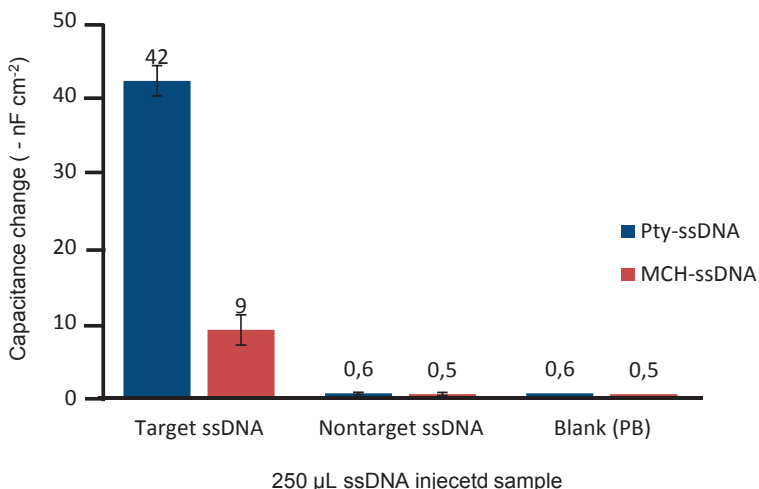


Fig. 9a: Amplitude of the responses from Pty- and MCH-ssDNA modified sensor-chips to injection of 250 µL of a 10<sup>-8</sup>M target and nontarget ssDNA each at 23 °C.

However, an effective selectivity for both MCH and Pty-ssDNA chip was obtained when the hybridization temperature was elevated to 50 °C (Fig. 9b).

The obtained response signals against non-target sample were  $0.6 \pm 0.1$  and  $0.5 \pm 0.2$  -nF cm<sup>-2</sup>, for Pty-ssDNA and MCH-ssDNA sensor-chips, respectively. These signals are regarded as false signals caused by a pressure drop (back-pressure) due to sample injection. The assumption was confirmed when the response signals obtained against blank (10 mM PB) samples corresponded with the signals against non-target samples. The obtained signals from blank samples were 0.6 and 0.5 -nF cm<sup>-2</sup> for Pty-ssDNA and MCH-ssDNA sensor-chips, respectively. The elevated temperature (50 °C) did not affect the signal amplitude from hybridization of the target probe on the Pty-ssDNA sensor-chip; however it did on the MCH-ssDNA sensor-chip. The signal amplitude was significantly reduced almost by 20 %, from 11 -nF cm<sup>-2</sup> at RT to 9 -nF cm<sup>-2</sup> at 50 °C. For the Pty-ssDNA modified sensor-chip, the reduced signal was less than 5 %, from 44 -nF cm<sup>-2</sup> at RT to 42 -nF cm<sup>-2</sup>.



**Fig. 9b:** Amplitude of the responses from Pty- and MCH-ssDNA modified sensor-chips to injection of 250  $\mu$ L of a  $10^{-8}$  M target and nontarget ssDNA each at 50  $^{\circ}$ C.

The observed lower signal amplitude on the MCH-ssDNA sensor-chip at 50  $^{\circ}$ C than at RT could be due to the pre-reorganisation of the MCH-ssDNA layer during a baseline stabilization prior to analysis. This led to the decrease of the capacitance-baseline in such a way that when the target probe was hybridized on the surface it could not produce the same signal response as that obtained at RT. On other hand, the obtained larger signal at RT was somewhat contributed with non-specific adsorption of target ssDNA.

### 3.7 Re-usability

High surface stability provides accuracy and precision, which allow repeated analysis on the same surface. Fig. 10 shows the percentage residual capacity of the Pty- and MCH-ssDNA sensors compared to number of injections.

For 15 cycles the binding capacity of Pty- and MCH-ssDNA retained about 90 % of the original capacitance change. Hence, both types of sensor-chips can be re-used with good reproducibility for more than 15 times, with relative standard deviation (% RSD) of 6 %, and 7 %, respectively. The low % RSD values suggest the high surface stability of strongly electrodeposited Pty-film (Zhou et al., 2009) and strongly chemisorbed MCH-SAM (Chaki et al., 2002) on the sensor-chip surfaces.



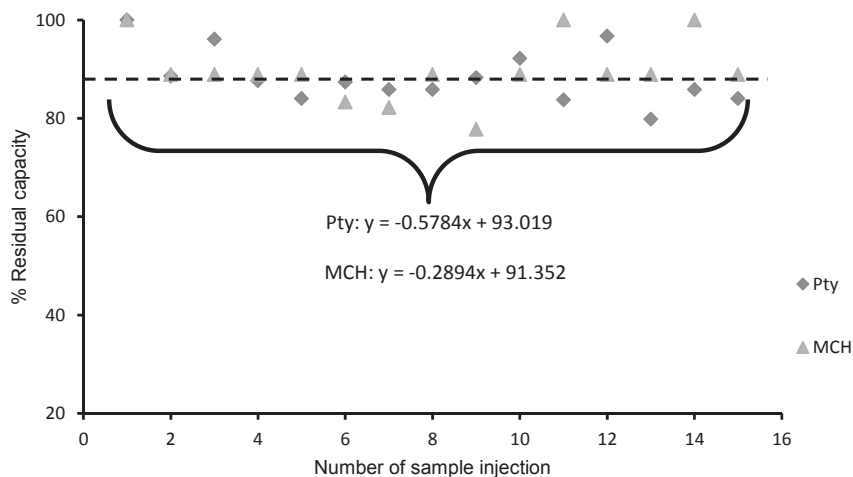


Fig. 10: Reusability of Pty- and MCH-ssDNA modified sensor-chips. 250  $\mu$ L of a  $10^{-9}$  M target ssDNA was repeatedly applied for 15 times on each sensor-chip with regeneration step between each individual assay.

#### 4. Conclusion

The study has demonstrated some of the physical, electrochemical and analytical characteristics of the Pty-film and MCH-SAM modified gold sensor-chips. The information obtained from CV and AFM from electrochemical and physical analyses, respectively, corresponded well with those obtained from CapSense™ Biosystem for analytical characterizations.

This study has enlightened that Pty-film is a more suitable immobilization layer than MCH-SAM on the gold sensor-chip surface that is intended to be used for capacitive DNA-sensor measurements. Pty-film has evidently shown good surface coverage giving fine insulating properties that resulted in a relatively high density of immobilized capture probe (ssDNA) and consequently, relatively high sensitivity and signal amplitude. Also, Pty-film surface was observed to be much more stable and thus, provides accuracy and precision and allows more than 15 repeated analyses on the same surface.

#### 5. Acknowledgements

Financial support from World Bank supported project titled ‘Capacity Building in Science, Technology and Higher education’ at University of Dar es Salaam, Tanzania, is gratefully acknowledged. Also, technical and logistical support from Higher education and Swedish Research Council is highly appreciated. Special thanks to Dr. Maria Wadsäter from Department of Physical Chemistry, Lund

University, Sweden, for her prompt assistance during AFM measurements and topographic analysis.

## 6. References

1. Ates M (2013). A review study of (bio) sensor systems based on conducting polymers. *Materials Science and Engineering C-Materials for Biological Applications*. 33, 1853–1859.
2. Bensebaa F, Ellis, TH, Badia A, Lennox, RB (1998). Thermal Treatment of n-Alkanethiolate Monolayers on gold, as observed by infrared spectroscopy, *Langmuir*. 14, 2361-2367.
3. Berggren C, Bjarnason B, Johansson G (1999). Instrumentation for Direct Capacitive Biosensors. *Instrumentation Science and Technology*. 27, 131-140.
4. Blasini DR, Tremont RJ, Batina N, Gonza'lez I, Cabrera CR (2003). Self-assembly of (3-mercaptopropyl)trimethoxysilane on iodine coated gold electrodes. *Electroanalytical Chemistry*. 540, 45-52.
5. Buck RP, Lindner E (1994). Recommendations for nomenclature of Ion-selective electrodes. *Pure Applied Chemistry*. 66, 2527-2536.
6. Campuzano S, Pedrero M, Montemayor C, Fatas E, Pingarron JM (2006). Characterization of alkanethiol-self-assembled monolayers-modified gold electrodes by electrochemical impedance spectroscopy. *Electroanalytical Chemistry*. 586, 112-121.
7. Chaki NK, Vijayamohan K (2002). Self-assembled monolayers as a tunable platform for biosensor applications, *Biosensors and Bioelectronics*. 17: 1–12
8. Choi J-W, Park K-S, Lee W, Oh B-K, Chun B-S, Pae S-H (2004). Regulation of anti-LDL immobilization on self-assembled protein G layer using CHAPS and its application to immunosensor. *Material Science and Engineering. C*. 24: 241–245.
9. Erlandsson D, Teeparuksapun K, Mattiasson B, Hedström M (2014). Automated flow-injection immunosensor based on current pulse capacitive measurements. *Sensors and Actuators, B*. 190:295– 304.
10. Fu Y, Yuan R, Xu L, Chai Y, Zhong X, Tang D (2005). Indicator free DNA hybridization detection via EIS based on self-assembled gold nanoparticles and bilayer two-dimensional 3-mercaptopropyltrimethoxysilane onto a gold substrate. *Biochemical Engineering*. 23: 37–44.
11. Kros A, Sommerdijk NAJM, Nolte RJM (2005). Poly(pyrrole) versus poly(3,4-ethylenedioxythiophene): implications for biosensor applications. *Sensors and Actuators, B*. 106: 289–295.
12. Labib M, Hedström M, Amin M, Mattiasson B (2009). A capacitive immunosensor for detection of cholera toxin. *Analytical Chimica Acta*. 634: 255–261.

13. Labib M, Hedström M, Amin M, Mattiasson B (2010). A novel competitive capacitive glucose biosensor based on concanavalin A-labeled nanogold colloids assembled on a polytyramine-modified gold electrode. *Analytical Chimica Acta*. 659, 194–200.
14. Ladik AV, Geiger FM, Walter, SR (2001). Immobilization of DNA onto gold and dehybridization of surface-bound DNA on glass. *Nanoscope*. 7, 19-23.
15. Lebogang L, Mattiasson B, Hedström M (2014). Capacitive sensing of microcystin variants of *Microcystis aeruginosa* using a gold immunosensor-chip modified with antibodies, gold nanoparticles and polytyramine. *Microchimica Acta*. 1-9.
16. Limbut W, Kanatharana P, Mattiasson B, Asawatreratanakul P, Thavarungkul P (2006). A comparative study of capacitive immunosensors based on self-assembled monolayers formed from thiourea, thioctic acid, and 3-mercaptopropionic acid. *Biosensors and Bioelectronics*. 22, 233–240.
17. Losic D, Cole M, Thissen H, Voelcker NH (2005). Ultrathin polytyramine films by electropolymerization on highly doped p-type silicon electrodes. *Journal of Surface Science*. 584, 245–257.
18. Mahadhy A, Ståhl-Wernersson E, Mattiasson B, Hedström M (2014a). Use of capacitive affinity biosensor for sensitive and selective detection and quantification of DNA -A model study. *Biotechnology Reports*. 3, 42-48.
19. Mahadhy A, Mamo G, Ståhl-Wernersson E, Mattiasson B, Hedström M (2014b). PRC-free ultrasensitive capacitive biosensor for selective detection and quantification of Enterobacteriaceae DNA. *Journal of Analytical and Bioanalytical Techniques*. 5, 210.
20. Malhotra, BD, Chaubey A, Singh SP (2006). Prospects of conducting polymers in biosensors. *Analytical Chimica Acta*. 578, 59–74.
21. Park S, Weaver MJ (2002). A versatile surface modification scheme for attaching metal nanoparticles onto gold: characterization by electrochemical infrared spectroscopy. *Journal of Physical Chemistry B*. 106, 8667-8670.
22. Peng H, Soeller C, Vigar N, Kilmartin PA, Cannell MB, Bowmaker GA, Cooney RP, Travas-Sejdic J (2005). Label-free electrochemical DNA sensor based on functionalised conducting copolymer. *Biosensors and Bioelectronics*. 20, 1821–1828.
23. Piwonski I, Grobelny J, Cichowski M, Celichowski G, Rogowski J (2005). Investigation of 3-mercaptopropyltrimethoxysilane self-assembled monolayers on Au(III) surface. *Applied Surface Science*. 242, 147–153.
24. Raposo M, Ferreira Q, Ribeiro PA. A guide for atomic force microscopy analysis of soft-condensed matter. In: Méndez-Vilas A, Díaz J (2007). *Modern research and educational topics in microscopy*. Formatex, Badajoz. pp 758- 769.
25. Rivera-Gandia J, Cabrera CR (2007). Self-assembled monolayers of 6-mercapto-1-hexanol and mercapto-*n*-hexyl-poly(dT)18-fluorescein on

- polycrystalline gold surfaces: an electrochemical impedance spectroscopy study. *Electroanalytical Chemistry*. 605, 145-150.
26. Sabatani E, Rubinstein I, Maoz R, Sagiv J (1987). Organized self-assembling monolayers on sensor-chips part I. Octadecyl derivatives on gold. *Electroanalytical Chemistry*. 219, 365-37.
  27. Sankoh S, Samanman S, Thipmanee O, Numnuam A, Limbut W, Kanatharana P, Vilaivan T, Thavarungkul P (2013). A comparative study of a label-free DNA capacitive sensor using a pyrrolidiny peptide nucleic acid probes immobilized through polyphenylenediamine and polytyramine non-conducting polymers. *Sensors Actuators, B*. 177, 543– 554.
  28. Strike DJ, Derooij NF, Koudelkahep M (1995). Electrochemical techniques for the modification of microelectrodes. *Biosensors and Bioelectronics*. 10, 61-66.
  29. Teeparuksapun K, Hedström M, Kanatharana P, Thavarungkul P, Mattiasson B (2012). Capacitive immunosensor for the detection of host cell proteins. *Journal of Biotechnology*. 157, 207-213.
  30. Teeparuksapun K, Hedström M, Wong EY, Tang S, Hewlett IK, Mattiasson B (2010). Ultrasensitive detection of HIV-1 p24 antigen using nanofunctionalized surfaces in a capacitive immunosensor. *Analytical Chemistry*. 82, 8406–841.
  31. Tichoniuk M, Ligaj M, Filipiak M (2008). Application of DNA hybridization biosensor as a screening method for the detection of genetically modified food components. *Sensors*. 8, 2118-2135.
  32. Vorburger TV. Methods for characterizing surface topography. In: Moore DT (2010). *Tutorial in optics*. Optical Society of America, Washington DC. pp 137-151.
  33. Yuqing M, Jianrong C, Xiaohua W (2004). Using electropolymerized non-conducting polymers to develop enzyme amperometric biosensors. *Journal of Trends in Biotechnology*. 22, 227-231.
  34. Zhao Y-D, Pang D-W, Hu S, Wang Z-L, Cheng J-K, Dai HP (1999). DNA-modified electrodes; part 4: optimization of covalent immobilization of DNA on self-assembled monolayers. *Talanta*. 49,751–756.
  35. Zhou L, Shang F, Pravda M., Glennon JD, Luong JHT (2009). Selective detection of dopamine using glassy carbon electrode modified by a combined electropolymerized permselective film of polytyramine and polypyrrole-1-propionic acid. *Electroanalysis*. 21, 797-803.



## Paper IV



# Rapid Detection of the *mecA* gene for Diagnosis of Methicillin-Resistant *Staphylococcus aureus* by a Novel, Label-free Real-time Biosensor

Ally Mahadhy<sup>1</sup>, Eva StåhlWernersson<sup>1</sup>, Bo Mattiasson<sup>1,2</sup>, Martin Hedström<sup>1,2\*</sup>

<sup>1</sup>Department of Biotechnology, Lund University, P.O. Box 124, SE-22100 Lund, Sweden.

<sup>2</sup>CapSenze HB, Medicon Village, SE-22838 Lund, Sweden.

\*Corresponding author. Tel.: +46 46-222 75 78; fax: +46 46-222 47 13. E-mail address: Martin.Hedstrom@biotek.lu.se

## Abstract

This work presents a rapid, selective and sensitive automated sequential injection flow capacitive biosensor technique for detection of the *mecA* gene, which is associated with methicillin-resistant *Staphylococcus aureus*. A DNA-based capture probe was immobilized on the gold electrode surface and the electrode was integrated in the capacitive sensor system. A constant current pulse was applied and the resulting capacitance was detected. Injection of the target DNA sample to the sensor surface induced hybridization to occur on the electrode surface, which resulted in a shift in the measured capacitance ( $\Delta C$ ). The  $\Delta C$  was directly proportional to the concentrations of the applied target probe with linearity ranging from  $10^{-12}$  to  $10^{-7}$  moles *per* litre. The biosensor displayed a noticeable sensitivity with a detection limit of  $6.0 \times 10^{-13}$  moles *per* litre and a recovery of 95 % of the *mecA* gene spiked in human saliva. Moreover, the biosensor presented a promising selectivity. It could clearly discriminate single-base, two-base and twelve-base mismatch probes with a decrease in the signal strength by 13 %, 26 %, and 89 %, respectively relative to the signal strength of the complementary target probe. There was no significant signal observed for the non-complementary probe. The biosensor-chip could be re-used for more than 15 cycles with residual capacity of  $93 \pm 6$  % and a RSD of 6 % by regenerating the biosensor-chip with a solution of 50 mM NaOH.

**Keywords:** CapSenze, Real-time biosensor; Automated sequential injection; *mecA*-gene; Methicillin-resistant *Staphylococcus aureus*; Complex biological matrix.



# 1. Introduction

*Staphylococcus aureus* is an important pathogen to humanity, responsible for various community-acquired and nosocomial infections, including impetigo, cellulitis, necrotizing fasciitis, abscess, osteomyelitis, pneumonia and sepsis [1]. Patients undertaking haemodialysis or suffering from diabetes are more vulnerable to *S. aureus* infections [2,3]. The evolution towards methicillin-resistance poses *S. aureus* as one of the most deadly bacteria present today [4]. Hence, as methicillin-resistant *S. aureus* (MRSA) is insensitive to standard antibiotics, the resulting chronic infection and high rate of mortality contribute to a significant increase in the health care expenses. A risk of dying from bacterial infection is 64 % for patients with an MRSA-infection compared to those with other ordinary forms of bacterial infections [5].

MRSA is resistant to all  $\beta$ -lactam antibiotics, including penicillin, cephalosporins cloxacillin and methicillin. The targets for  $\beta$ -lactam antibiotics are cell wall-synthesizing enzymes known as penicillin-binding proteins (PBPs). MRSA produces a new version of penicillin-binding protein 2a (PBP2a) with a reduced affinity to  $\beta$ -lactam antibiotics. Hence, it takes over the high-binding-affinity proteins (PBPs) [6]. The gene that encodes PBP2a, *mecA*, is located on the MRSA chromosome and is widely distributed among *S. aureus* [7].

Laboratory screening for MRSA faces a serious challenge with regard to the currently available screening methods. Hence, there is a clear disproportion between sensitivity, turnaround time, selectivity and cost of the existing methods. Currently, MRSA screening methods are categorized into culture- and molecular-based methods. The former is employed for phenotypic test, while the latter is for genotypic assays. The culture-based methods comprise broth-, plate- and chromogenic- media tests, which determine the  $\beta$ -lactam antibiotics bacteriostatic or bacteriocidal effect to *S. aureus* [8]. Such methods are laborious and time-consuming, including up to 3 days incubation time [9]. The most common molecular methods that are used for MRSA analysis are a polymerase chain reaction (PCR) and microarray technologies [4,8,10]. These methods are indeed sensitive and quick [10], but also significantly expensive, hence unaffordable for many health care, educational and research institutions, mainly in the third-world countries.

Considering the background outlined above, priority in clinical researches must be set towards the development of faster and cheaper tools for MRSA diagnosis. In this work, a novel, rapid and sensitive technique, i.e. a capacitive DNA-sensor, is presented for the detection of the *mecA* gene in spiked human saliva. The capacitive DNA-sensor utilizes hybridization of the target sequence of *mecA* gene to the capture DNA probe that is immobilized on the sensor-chip. The instrumentation, CapSense™ Biosystem employs a constant current pulse that is applied to the sensor electrode from which the registered capacitance is recorded.

The principle and applications of capacitive transduction in DNA-sensors have previously been reported elsewhere [11,12]. The hybridization of the target *mecA* gene to the capture probe results in a decrease in the registered capacitance that is proportionally related to the concentrations of the analyte.

## 2. Materials and Methods

### 2.1 Materials

The 25-mer *mecA* gene probes were constructed based on the *S. aureus* subsp. *aureus* MRSA252 *mecA* gene sequence available at the National Center for Biotechnology Information (NCBI) [13] as shown in Table 1. The probes were purchased from Integrated DNA Technologies, Inc. (Leuven, Belgium). Human saliva was collected from one of the authors of this work. Absolute ethanol and sodium hydroxide were purchased from VWR international (Radnor, USA). Acetone, tyramine (99 %), *N*-(3-dimethylaminopropyl) *N*-ethylcarbodiimide hydrochloride (EDC), *N*-hydroxysuccinimide (NHS), 1-dodecane thiol and 6-mercaptohexanol (MCH) were obtained from Sigma-Aldrich (Steinheim, Germany). All other chemicals used were of analytical grade. All buffers and regeneration solutions were prepared in ultrapure water (Millipore purification system, Massachusetts, USA). All solutions were filtered through a membrane (pore size 0.22  $\mu\text{m}$ ) and degassed prior to use.

Table 1: DNA probes used in this study

Name of the probe	Sequence (5'→3') (25-mer)
Capture probe (CP)	GCTCAGGTACTGCTATCCACCCTCA
Complementary target probe (TP)	TGAGGGTGGATAGCAGTACCTGAGC
Single-base mismatched probe (SMT)	TGAGGGTGGAT <u>T</u> G CAGTACCTGAGC
Two-base mismatched probe(TMT)	TGAGGGTGGAT <u>TG</u> CAGTAC <u>CT</u> GAGC
Twelve-base mismatched probe (12MT)	<u>T</u> <u>C</u> <u>A</u> <u>C</u> <u>G</u> <u>C</u> <u>T</u> <u>C</u> <u>G</u> <u>T</u> <u>T</u> <u>T</u> <u>G</u> <u>G</u> <u>A</u> <u>G</u> <u>A</u> <u>A</u> <u>G</u> <u>C</u> <u>A</u> <u>G</u> <u>T</u> <u>G</u>
Non-complementary probe (NC)	ACTCCCACCTATCGTCATGGACTCG

### 2.2 Methods

#### 2.2.1 Fabrication of electrode surface.

A custom-made disposable thin film gold electrode with a diameter of 3 mm and a purity of 99.99 % (Academic workshop, Linköping University, Sweden) was used as sensor-chip in this study. The fabrication process started by cleaning an

electrode in acetone while sonicated for 5 min, then it was rinsed with ultrapure water before sonicated again in ethanol for another 5 min. The electrode was lastly cleaned in piranha solution (mixture of 3 parts of concentrated H<sub>2</sub>SO<sub>4</sub> and 1 part of 30 % H<sub>2</sub>O<sub>2</sub>) for 5 min as well. Thereafter, the cleaned electrode was coated with a polytramine (Pty) film by electropolymerization of tyramine on the electrode surface using cyclic voltammetry (CV), as explained elsewhere [14,15]. The electrode was then coated with the capture probe, where the electrode surface was flooded with a 10  $\mu$ L solution mixture: 10  $\mu$ M capture probe, 8 mM NHS and 5 mM EDC in 0.01 M potassium phosphate buffer (PB), pH 7.2 [14]. The electrode was left at room temperature for 2 h in a container which was previously purged with a nitrogen gas stream. Thereafter, the electrode was directly dried in an oven at 50 °C for 10 min. After immobilization, the electrode was dipped in 10 mM 1-dodecanethiol (in ethanol) for 20 min in order to cover pinholes on the active surface [11,12], and finally kept at 4 °C until use. It should be noted that the electrode (the sensor-chip) was rinsed with ultrapure water and dried with nitrogen gas stream after each modification step.

### 2.2.2 Experimental set up and current pulse for capacitance measurements

In this study, the principle of detection is based on the electrical double layer (EDL) theory, which is described in detailed elsewhere [11,12]. A software-controlled-automated-sequential-injection system (Fig. 1) was used for all capacitance measurements. This system was developed by CapSenze (Lund, Sweden). It consists of a centris pump, which is supplied with 3-port valve and a 5 ml syringe pump. Port #1 is used to remove the waste during start-up of the system while, the syringe plunger sucks buffer from a container through port #2, and dispenses to an injection loop *via* a port #3. The injection loop from the port #3 is linked with the inlet to a 9-port valve. Ports #1 to #7 of the 9-port valve were used for either regeneration or standard/sample solution infusion, while port #8 is for draining the waste. Port #9 is extended to a degasser unit, which in turn is connected to a three electrode-flow cell [17]. A fixed volume of 250  $\mu$ L of the regeneration and standard/sample solutions were sequentially and automatically introduced to the three electrode-flow cell. The three-electrode flow-cell is electrically connected to the capacitance measurement unit. The capacitance measurement unit is equipped with an analog-to digital converter (ADC) unit and in the end is controlled by the in-house made software. A constant current pulse is automatically sent to the sensor-chip, and the system automatically computes the total capacitance ( $C_{TOT}$ ) over the sensor-chip /solution interface. The  $C_{TOT}$ , also known as the EDL capacitance calculated by Eq. 1 [17].

$$V = i(R_s + \frac{t}{C_{TOT}}) \quad (1)$$

where  $V$  is the over-all potential registered in the system when applying the current  $i$  during time  $t$  in the solution with the ohmic resistance,  $R_s$ .

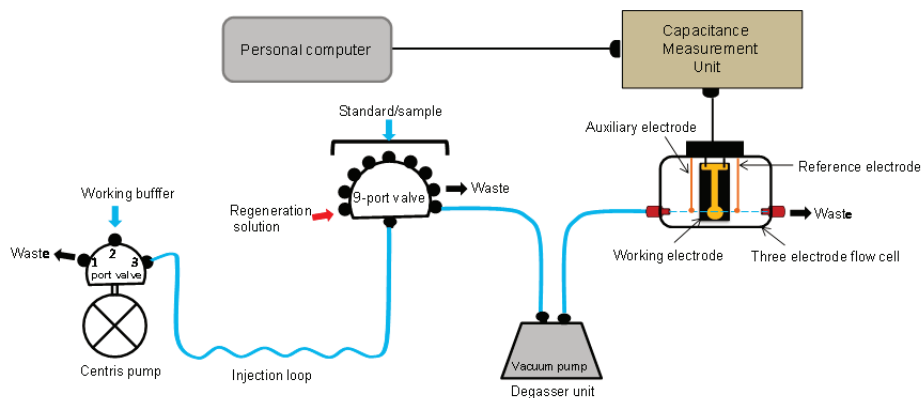


Fig. 1: Schematic illustration of an automated sequential injection flow system.

By plotting  $V$  vs.  $t$ , the linear curve is established, with  $V$ -intercept ( $V_0$ ) =  $iR_s$ . Then  $C_{TOT}$  can be determined from the slope ( $u$ ) of the linear curve.

$$\text{Since, } C_{TOT} = \frac{dQ}{dV_C} = \frac{idt}{dV_C} = \frac{i}{u} \quad (2)$$

where  $Q$  and  $V_C$  are the charge accumulated and the built-in potential across the EDL, respectively and  $u$  is the slope of the linear curve.

### 2.2.3 Establishment of a calibration curve

Samples of the target complementary probe were prepared in PB, pH 7.2 at a concentration ranging from  $10^{-6}$  to  $10^{-14}$  M having a dilution factor of 10. The standard samples were placed in connection to the injection ports of the CapSense system for analysis. Each sample was analysed in triplicate, and the mean of the three signal values with its standard deviation for each sample was reported.

### 2.2.4 Re-usability of the sensor-chip hosting the capture probe

Reusability of the sensor-chip was determined by repeatedly injecting  $10^{-9}$  M of the standard target probe with intermittent regeneration steps for 20 cycles, visualized in terms of the relative standard deviation (% RSD). The study was performed under the same conditions as that described for the establishment of the calibration curve.

### 2.2.5 Detection of base-mismatches

A concentration of  $10^{-8}$  M of single-, two-, and twelve-base mismatches, as well as non-complementary probes in PB with 30 % formamide were applied to the capacitive sensor system. The obtained signals for each probe was compared with that obtained for the standard target complementary probe after subtraction the effect of PB with 30 % formamide.

### 2.2.6 Determination of matrix effects on the *mecA* gene

The 25-mer *mecA* gene standard samples in PB were spiked to 900  $\mu\text{l}$  human saliva to make concentrations of  $10^3$ ,  $10^1$ , and  $10^0$  nmol L<sup>-1</sup>. The samples were then diluted by a factor of  $10^5$ ,  $10^3$ , and  $10^2$  in the same buffer, respectively, so as to achieve the same final concentration of the *mecA* gene in all dilutions, for analytical and comparative purposes. Each dilution was injected to the capacitive DNA-sensor, and the % recovery of the *mecA* gene from each dilution of saliva was determined according to Eq. 3.

$$\% \text{ Recovery} = \frac{\Delta C_1 - \Delta C_2}{\Delta C_3} \times 100 \quad (3)$$

where  $\Delta C_1$  is the signal of the *mecA* spiked- and  $\Delta C_2$  is the signal of non-spiked saliva samples, both at equal dilution;  $\Delta C_3$  is the signal registered off the calibration curve for  $10^{-11}$  M *mecA* gene in PB.

A non-specific response of the capacitive DNA-sensor due to saliva effects were studied too. Different dilutions ( $10^2$ ,  $10^3$  and  $10^5$ ) of non-spiked saliva samples (in PB) were introduced in to the system and the registered signals were determined.

Furthermore, so as to comprehend the salivary microbiological complexity, the diluted samples of non-spiked saliva were cultured on Luria-Bertani (LB) agar plates, and incubated at 37 °C for 24 h, the bacterial colonies on the plates were visualized with the naked eye, and enumerated by using the plate count technique [12].

## 3. Results and Discussion

### 3.1 Calibration and operational characteristics

Injection of the standard complementary target 25-mer *mecA* gene sample into the capacitive DNA-sensor system induced the hybridization reaction between the injected *mecA* gene and capture probe on the sensor-chip, which resulted in a capacitance change ( $\Delta C$ ) as shown on Fig. 2.

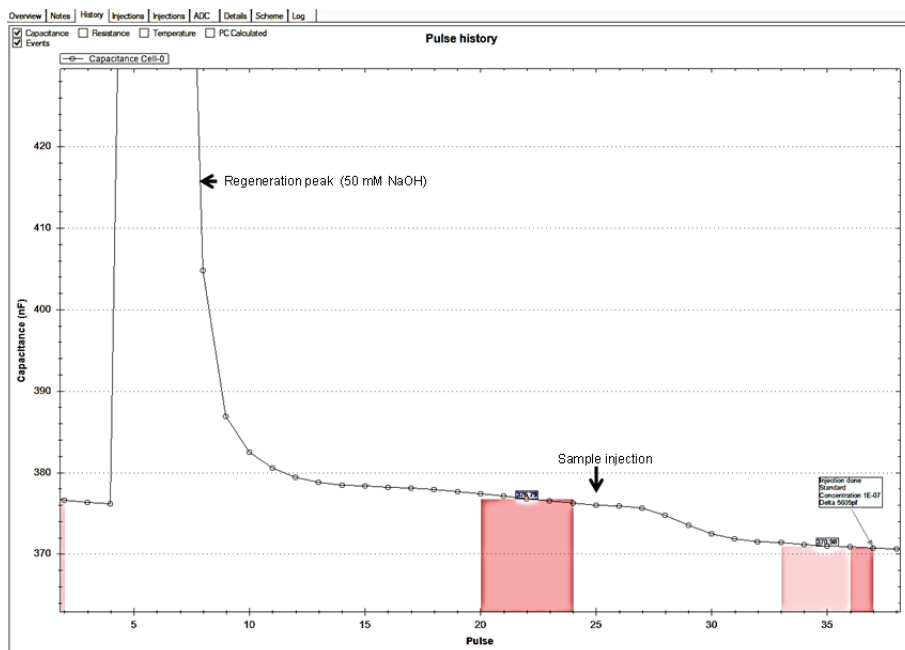


Fig. 2: Time course graph showing a signal ( $\Delta C$ ) after injection of target sample into the CapSense™ Biosystem. The analysis took 10 minutes.

The  $\Delta C$  was directly proportionally to the concentration of the injected target *mecA* gene sample. The curve of applied concentrations *vs.*  $\Delta C$  is represented in Fig. 3. A linear relationship was observed from  $1.0 \times 10^{-12}$  to  $1.0 \times 10^{-7}$  M, and the detection limit that was calculated according to Buck and Lindner [18], was found to be  $6.0 \times 10^{-13}$  M (0.6 pM). To the best of our knowledge this is the lowest reported LOD for label-free techniques. The achieved LOD for the capacitive DNA-sensor was 38 and 17 times lower than the electrochemical biosensors reported by Liu et al., [19] and Watanabe et al., [20], respectively. Liu et al., reported a LOD of 23 pM for the detection of the *mecA* gene, utilizing the sandwich hybridization assay with the dual labelling technique, involving gold nanoparticles and alkaline phosphatase, while Watanabe et al., were successfully detecting down to 10 pM of the *mecA* gene using modified gold nanoparticles probes. In this study, the EDL thickness presumed to be less than 0.01  $\mu\text{m}$ , since the concentration of PB in these measurements was 10 mM [21]. This implies that the electrode surface was in close proximity to the EDL [11,12], hence, making the proposed capacitive DNA-sensor to respond to extremely low concentration of the analyte.

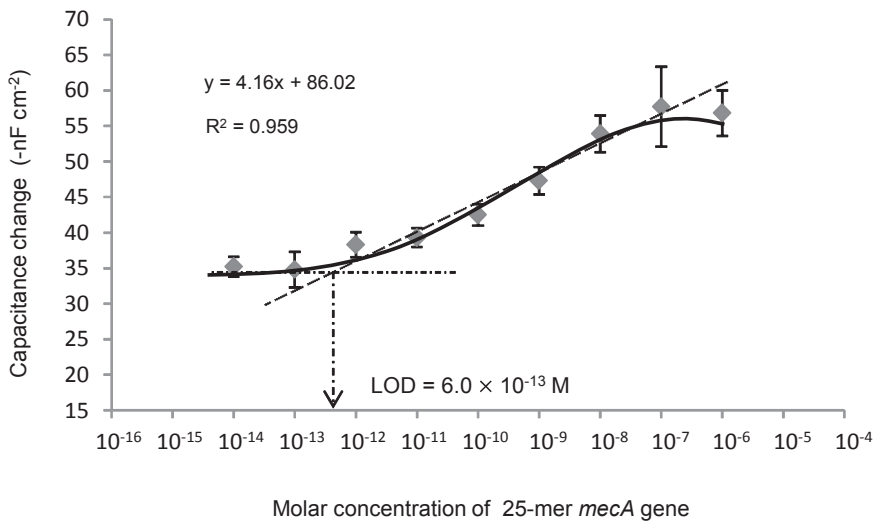


Fig. 3: The established calibration curve of the capacitive DNA-sensor showing a linearity range and LOD for 25-mer *mecA* gene sample in PB. The curve was established at 23 °C.

The electrode was regenerated with pulses of 50 mM NaOH and could be used for more than 15 cycles with residual capacity of  $93 \pm 6\%$ , and RSD value of 6% as shown in Fig. 4.

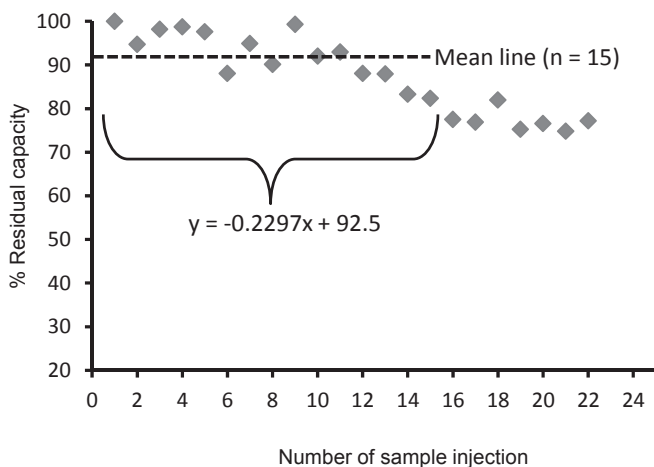
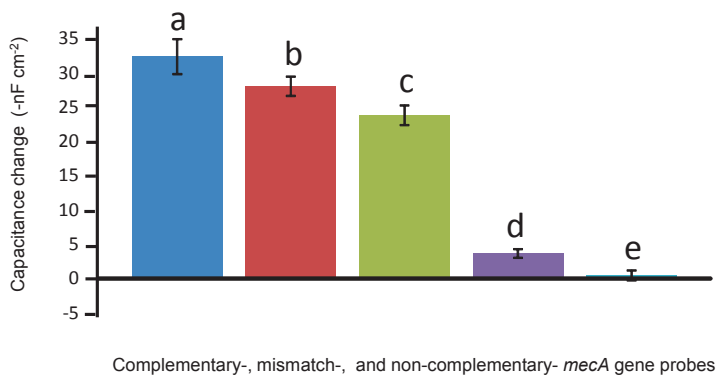


Fig. 4: Reusability of the sensor-chip. A volume of 250  $\mu\text{L}$  of a  $10^{-9}$  M target *mecA* gene was repeatedly applied on the sensor-chip up to 22 times with regeneration step between each individual assay.

### 3.2 Detection of base-mismatches

The ability of the developed capacitive DNA-sensor to detect different base-mismatches was investigated. Equal molar concentrations of target *mecA* gene samples, containing different base-mismatches were hybridized on the capture probe, and  $\Delta C$  response was recorded. A significant difference in signal ( $\Delta C$ ) between complementary target, single-base-mismatch, two-base-mismatch, and twelve-base-mismatch probes was observed (Fig. 5).



**Fig. 5:** Comparison of recorded signal upon hybridization of (a) complementary target (b) single-base-mismatch probe (c) two-base-mismatch probe (d) 12-base-mismatch probe and (e) non-complementary probe to capture probe.

The signal strength was found to decline by 13 %, 26 %, and 89 % for single-base, two-base, and twelve-base mismatches, respectively, comparative to the complementary probe signal. The observed reduction in signal for mismatches probes is an effect of the base-pair break of the *mecA*-capture probe/*mecA* target duplex. It reveals the ability of the capacitive DNA-sensor to distinguish between complementary and other targets with base-mismatches. Insignificant  $\Delta C$  was noticed for a non-complementary probe.

### 3.3 Determination of the sample matrix effects

#### 3.3.1 The effect of human saliva (matrix) on the sensor signal.

In order to differentiate between the matrix-borne electrochemical signal and its specific target *mecA* gene-mediated hybridization response, non-spiked human saliva, at dilution factors the same as that for spiked-human saliva, was injected into the capacitive DNA-sensor system and the response was followed as shown in Fig. 6. Low dilutions of non-spiked human saliva samples produced non-specific signals when were applied to the capacitive DNA-sensor (Fig. 6a, 6b). Infact typical human saliva contains about  $1.8 \times 10^9$  bacteria ml<sup>-1</sup> saliva, mostly originated from other mouth surfaces [22,23]. In this study, the salivary bacteria



in the diluted non-spiked human saliva ( $10^2$ ,  $10^3$  and  $10^5$  dilution factors), cultured on LB-agar plates (Fig. 7), were found to contain about  $10^7$ ,  $10^6$  and  $10^4$  Cfu ml<sup>-1</sup>, respectively. Therefore, the observed non-specific signal can be explained by the non-specific-hydrophobic interactions between the electrode surface-capture-probe-aromatic rings and bacterial cell surface and/or other protein contents in the saliva. Such increase in hydrophobicity on the electrode surface pushes the EDL away from the surface, which in turn results in the observed non-specific signal,  $\Delta C$ . However, its amplitude was significantly decreased as a result when increasing the dilution factor of the injected sample (Fig. 6c).

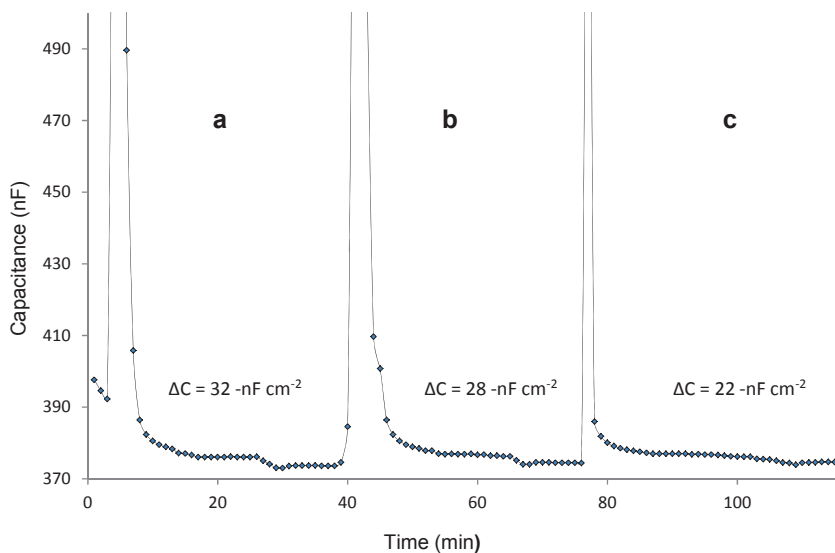


Fig. 6: Showing the observed matrix-borne signals resulted from injecting different dilutions of unspiked human saliva samples in to the capacitive DNA-sensor (a)  $10^2$  times diluted (b)  $10^3$  times diluted and (c)  $10^5$  times diluted.

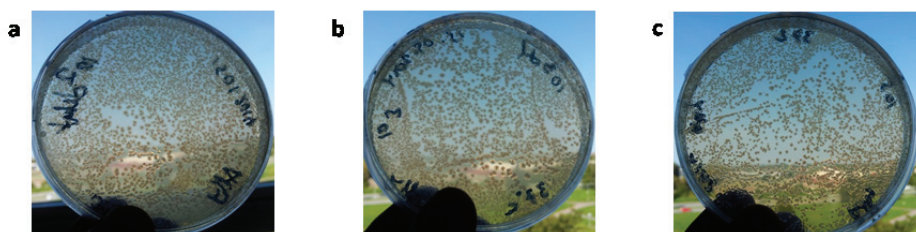


Fig. 7: Salivary bacteria grown from (a)  $10^2$  (b)  $10^3$  and (c)  $10^5$  times diluted human saliva samples.

### 3.3.2 Recovery of the *mecA* gene from human saliva

The *mecA*-spiked samples were analysed in triplicate and the average signal were used to calculate the percentage recovery of the target gene from human saliva. The results from the study are shown in Table 2. The highest percentage recovery with the lowest uncertainty was obtained in the most diluted sample, suggesting that further sample dilution decreases the effects of the matrix. However, the system needs to be optimized since too much sample dilution will lead to loss of signal. It should be noted that in this study the concentration of the analyte was kept constant while diluting the matrix.

Table 2: Biosensing of spiked *mecA* gene in human saliva

Sample dilution	Final concentration (nmol L <sup>-1</sup> )	Calculated concentration (nmol L <sup>-1</sup> )	% Recovery	% RSD (n = 3)
10 <sup>2</sup>	0.01	0.0071	71	9.0
10 <sup>3</sup>	0.01	0.0076	76	6.5
10 <sup>5</sup>	0.01	0.0095	95	3.5

## 4. Conclusion

This work has described a novel, automated, selectivity and sensitive fast biosensor technique for diagnosis of methicillin-resistant *S. aureus* based on the detection of the *mecA* gene. The developed biosensor could, with high sensitivity detect the *mecA* gene from the complex human saliva with a recovery of 95 %. The biosensor showed a remarked selectivity, with the possibility to clearly discriminate the complementary probe, from single-base, two-base, twelve-base mismatch and non-complementary probes. This work provides a foundation to extend the study towards the analysis of real MRSA-*mecA* gene in clinical samples.

## 5. Acknowledgements

Financial support from World Bank supported project titled “Capacity Building in Science, Technology and Higher education” at University of Dar es Salaam, Tanzania, is gratefully acknowledged. Also, technical and logistical support from Higher education and Swedish Research Council is highly appreciated.

## 6. References

1. Long, C.B., Madan, R.P., Herold, B.C., 2010. Diagnosis and management of community-associated MRSA infections in children. *Expert Review of Anti-infective Therapy*. 8, 183-195.
2. Lowy, F.D., 1998. *Staphylococcus aureus* Infections. *New England Journal of Medicine*. 339, 520-532.
3. Shlaes, D.M., Gerding, D., John Jr, J.F., 1997. Infectious diseases society of america joint committee on the prevention of antimicrobial resistance: guidelines for the prevention of antimicrobial resistance in hospitals. *Clinical Infectious Diseases*. 25, 584-599.
4. Malhotra-Kumar, S., Haccuria, K., Michiels, M., Ieven, M., Poyart, C., Hryniewicz, W., Goossens, H., 2008. Current trends in rapid diagnostics for methicillin-resistant *Staphylococcus aureus* and glycopeptide-resistant enterococcus species. *Journal of clinical microbiology*. 46, 1577-1587.
5. W.H.O., 2014. Antimicrobial resistance: global report on surveillance. Geneva.
6. Lim, D., Strynadka, N.C., 2002. Structural basis for the  $\beta$  lactam resistance of PBP2a from methicillin-resistant *Staphylococcus aureus*. *Nature Structural & Molecular Biology*. 9, 870-876.
7. Severin, A., Tabei, K., Tenover, F., Chung, M., Clarke, N., Tomasz, A., 2004. High level oxacillin and vancomycin resistance and altered cell wall composition in *Staphylococcus aureus* carrying the staphylococcal *mecA* and the enterococcal *vanA* gene complex. *Journal of Biological Chemistry*. 279, 3398-3407.
8. Calfee, D.P., Salgado, C.D., Classen, D., Arias, K.M., Podgorny, K., Anderson, D.J., Burstin, H., Coffin, S.E., Dubberke, E.R., Fraser, V., (2008). Strategies to prevent transmission of methicillin-resistant *Staphylococcus aureus* in acute care hospitals. *Strategies*. 29, S62-S80.
9. Cleven, B.E., Palka-Santini, M., Gielen, J., Meembor, S., Krönke, M., Krut, O., 2006. Identification and characterization of bacterial pathogens causing bloodstream infections by DNA microarray. *Journal of clinical microbiology*. 44, 2389-2397.
10. Towner, K., Talbot, D., Curran, R., Webster, C., Humphreys, H., 1998. Development and evaluation of a PCR-based immunoassay for the rapid detection of methicillin-resistant *Staphylococcus aureus*. *Journal of medical microbiology*. 47, 607-613.
11. Mahadhy, A., Ståhl-Wernersson, E., Mattiasson, B., Hedström, M., 2014. Use of a capacitive affinity biosensor for sensitive and selective detection and quantification of DNA- A model study. *Biotechnology Reports*. 3, 42-48.
12. Mahadhy, A., Mamo, G., Ståhl-Wernersson, E., Mattiasson, B., Hedström, M., 2014. PRC-free ultrasensitive capacitive biosensor for selective detection

- and quantification of Enterobacteriaceae DNA. *Journal of Analytical and Bioanalytical Techniques*. 5, 210.
13. Holden, M.T., Feil, E.J., Lindsay, J.A., Peacock, S.J., Day, N.P., Enright, M.C., Foster, T.J., Moore, C.E., Hurst, L., Atkin, R., 2004. Complete genomes of two clinical *Staphylococcus aureus* strains: evidence for the rapid evolution of virulence and drug resistance. *Proceedings of the National Academy of Sciences of the United States of America*. 101, 9786-9791.
  14. Teeparuksapun, K., Hedstrom, M., Wong, E.Y., Tang, S.X., Hewlett, I.K., Mattiasson, B., 2010. Ultrasensitive detection of HIV-1 p24 antigen using nanofunctionalized surfaces in a capacitive immunosensor. *Analytical Chemistry*. 82, 8406-8411.
  15. Labib, M., Hedstrom, M., Amin, M., Mattiasson, B., 2010. A novel competitive capacitive glucose biosensor based on concanavalin A-labeled nanogold colloids assembled on a polytyramine-modified gold electrode. *Analytica Chimica Acta*. 659, 194-200.
  16. Tichoniuk, M., Ligaj, M., Filipiak, M., 2008. Application of DNA hybridization biosensor as a screening method for the detection of genetically modified food components. *Sensors*. 8, 2118-2135.
  17. Erlandsson, D., Teeparuksapun, K., Mattiasson, B., Hedström, M., 2014. Automated flow-injection immunosensor based on current pulse capacitive measurements. *Sensors and Actuators B-Chemical*. 190, 295-304.
  18. Buck, R.P., Lindner, E., 1994. Recommendations for nomenclature of ion-selective electrodes -Iupac Recommendations 1994. *Pure and Applied Chemistry*. 66, 2527-2536.
  19. Liu, M., Xiang, H., Hua, E., Wang, L., Jing, X., Cao, X., Sheng, S., Xie, G., 2014. Ultrasensitive electrochemical biosensor for the detection of the *mecA* gene sequence in methicillin resistant strains of *Staphylococcus aureus* employing gold nanoparticles. *Analytical Letters*. 47, 579-591.
  20. Watanabe, K., Kuwata, N., Sakamoto, H., Amano, Y., Satomura, T., Suye, S.-i., 2014. A smart DNA sensing system for detecting methicillin-resistant *Staphylococcus aureus* using modified nanoparticle probes, *Biosensors and Bioelectronics*. (In press).
  21. Bard, A.J., Faulkner, L.R., 2001. *Electrochemical methods: fundamentals and applications*. Second edition. John Wiley & Sons, Inc. New York.
  22. Madigan, M.T., Martinko, J.M., Stahl, D.A., Clark, D.P., 2012. *Brock, Biology of microorganisms*. Pearson Education, Inc. San Francisco.
  23. Kort, R., Caspers, M., van de Graaf, A., van Egmond, W., Keijsers, B., Roeselers, G., 2014. Shaping the oral microbiota through intimate kissing. *Microbiome*. 2, 41.



